

Active Filters and Oscillators Using Current Feedback Operational Amplifiers

by

Saad Mohammad Al-Shahrani

A Thesis Presented to the

FACULTY OF THE COLLEGE OF GRADUATE STUDIES
KING FAHD UNIVERSITY OF PETROLEUM & MINERALS
DHAHRAN, SAUDI ARABIA

In Partial Fulfillment of the
Requirements for the Degree of

MASTER OF SCIENCE

In

ELECTRICAL ENGINEERING

October, 1995

INFORMATION TO USERS

This manuscript has been reproduced from the microfilm master. UMI films the text directly from the original or copy submitted. Thus, some thesis and dissertation copies are in typewriter face, while others may be from any type of computer printer.

The quality of this reproduction is dependent upon the quality of the copy submitted. Broken or indistinct print, colored or poor quality illustrations and photographs, print bleedthrough, substandard margins, and improper alignment can adversely affect reproduction.

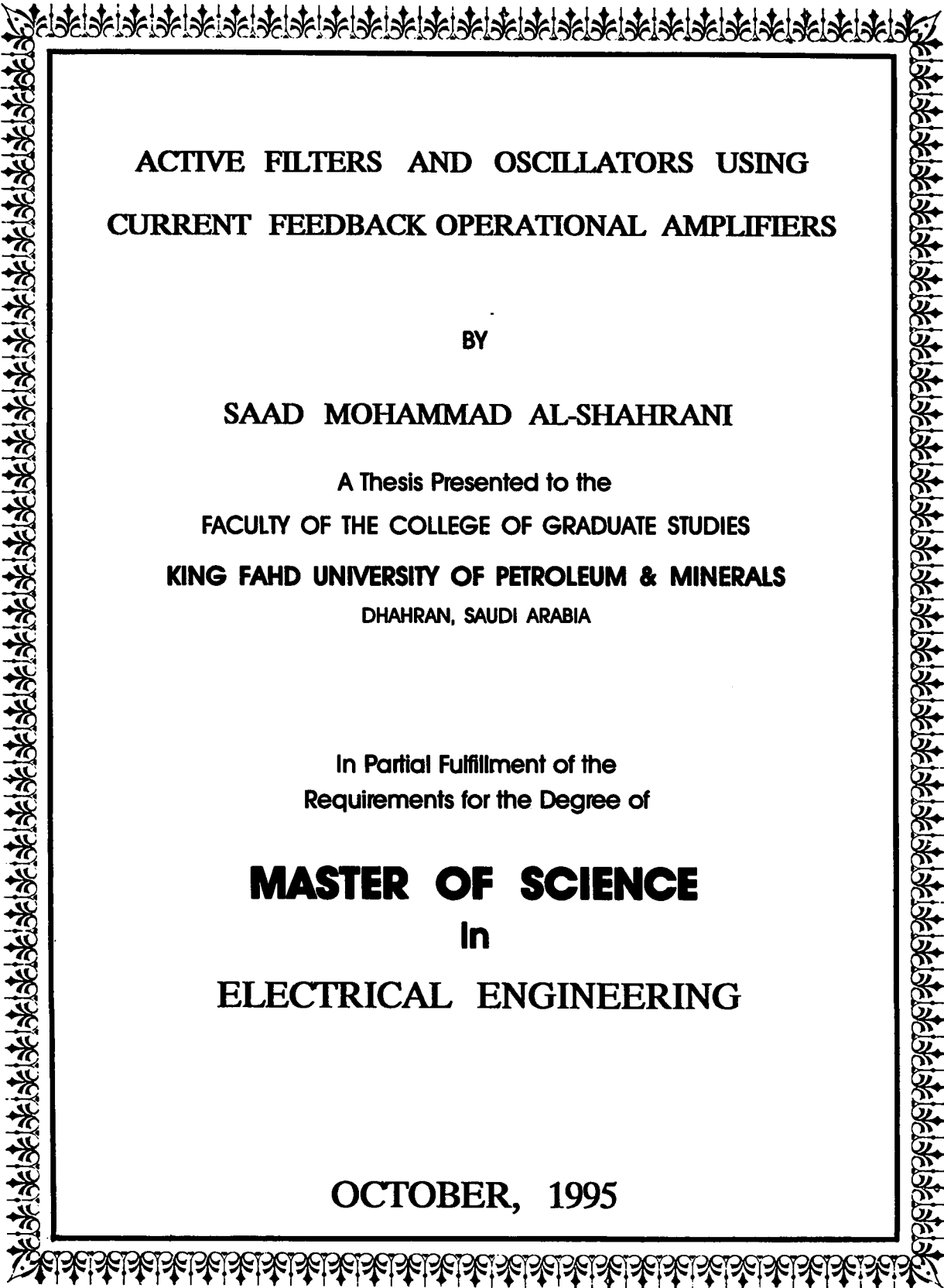
In the unlikely event that the author did not send UMI a complete manuscript and there are missing pages, these will be noted. Also, if unauthorized copyright material had to be removed, a note will indicate the deletion.

Oversize materials (e.g., maps, drawings, charts) are reproduced by sectioning the original, beginning at the upper left-hand corner and continuing from left to right in equal sections with small overlaps. Each original is also photographed in one exposure and is included in reduced form at the back of the book.

Photographs included in the original manuscript have been reproduced xerographically in this copy. Higher quality 6" x 9" black and white photographic prints are available for any photographs or illustrations appearing in this copy for an additional charge. Contact UMI directly to order.

UMI

A Bell & Howell Information Company
300 North Zeeb Road, Ann Arbor, MI 48106-1346 USA
313/761-4700 800/521-0600



**ACTIVE FILTERS AND OSCILLATORS USING
CURRENT FEEDBACK OPERATIONAL AMPLIFIERS**

BY

SAAD MOHAMMAD AL-SHAHRANI

A Thesis Presented to the
FACULTY OF THE COLLEGE OF GRADUATE STUDIES
KING FAHD UNIVERSITY OF PETROLEUM & MINERALS
DHAHRAN, SAUDI ARABIA

In Partial Fulfillment of the
Requirements for the Degree of

MASTER OF SCIENCE
In
ELECTRICAL ENGINEERING

OCTOBER, 1995

UMI Number: 1376963

**UMI Microform 1376963
Copyright 1996, by UMI Company. All rights reserved.**

**This microform edition is protected against unauthorized
copying under Title 17, United States Code.**

UMI

**300 North Zeeb Road
Ann Arbor, MI 48103**

**KING FAHD UNIVERSITY OF PETROLEUM & MINERALS
DHAHRAN, SAUDI ARABIA**

This these, written by

Saad Mohammad Al-Shahrani

*under the direction of his Thesis Advisor, and approved by his Thesis committee, has
been presented to and accepted by the Dean, College Graduate studies, in partial
fulfillment of the requirements for the degree of*

MASTER OF SCIENCE IN ELECTRICAL ENGINEERING

Thesis Committee:




Dr. M. T. Abuelma'atti (Chairman)



Dr. A. R. K. Al-Ali (Member)



Dr. M. A. Koussa (Member)




Dr. Z. J. Saati (Member)



Dr. Samir Al-Baiyat

Department Chairman



Dr. Ala. H. Rabeh
Dean, College of Graduate Studies

Date: 30-10-95



To

My Father, My Mother,

My uncle Meraai

and

My wife

For their patience, moral support and encouragement

Acknowledgment

First and foremost all praise to Almighty Allah Who gave me the courage and patience to carry out this work successfully.

Acknowledgment is due to King Fahd University of Petroleum and Minerals for providing support to this work.

My deep appreciation goes to my major thesis advisor Dr. M. T. Abuelma'atti for his constant help, guidance and the countless hours of attention he devoted throughout the course of this work. He was always kind, understanding and sympathetic towards me. Working with him was indeed a wonderful and learning experience which I thoroughly enjoyed.

Thanks are due to my committee members Dr. Al-Ali, Dr. Saati and Dr. Kousa for thier interest and cooperation.

TABLE OF CONTENTS

Acknowledgment	i
Contents	ii
List of Figures	v
List of Tables	ix
Abstract (English)	x
Abstract (Arabic)	xi
CHAPTER I	
INTRODUCTION	1
1.1 The Current Feedback Operational Amplifier	1
1.2 Literature Review for the CFOA Application	12
1.3 Problem Definition	13
1.4 Thesis Organization	14
CHAPTER II	
ACTIVE FILTERS	15
2.1 Introduction	15
2.2 How to Evaluate an Active Filter?	16
2.3 Universal Second-order Filters	18
2.3.1 Universal Voltage-mode Multiple Inputs Single Output Filter	18

2.3.2 Universal Voltage-mode Single Input Multiple Output Filter	30
2.3.3 Universal Current-mode Multiple Inputs Single Output Filters	36
CHAPTER III	
OSCILLATORS AND SIGNAL GENERATORS	49
3.1 Introduction	49
3.2 How to Evaluate an Oscillator?	50
3.3 Sinusoidal Oscillators	51
3.3.1 Sinusoidal Oscillators Exploiting the pole of the CFOA	52
3.3.2 Sinusoidal Oscillator Based on Ideal CFOA	70
3.4 Square, Triangular and Ramp Waveforms Generator	81
CHAPTER IV	
EFFECT OF CFOA NON-IDEALITIES	93
4.1 Introduction	93
4.2 Effect of the Non-idealities on the Active Filter Circuits	96
4.3 Effect of the Non-idealities on the Oscillator Circuits	106
CHAPTER V	
CONCLUSION AND FUTURE WORK	112
5.1 Introduction	112
5.2 Conclusions	113

5.3 Directions for Future work	115
APPENDIX	116
Appendix A	117
Appendix B	121
Appendix C	124
REFERENCES	127

LIST OF FIGURES

1.1a VOA equivalent	3
1.1b Closed-Loop noninverting amplifier	3
1.2 Simplified circuit diagram of a current feedback amplifier	4
1.3 Model for the CFOA	6
1.4 Closed-Loop noninverting CFOA	6
1.5 Alternative four-transistor input buffer	11
1.6 Eight-transistor input buffer	11
2.1 Universal voltage-mode filter [15]	19
2.2 Proposed universal voltage-mode filter (I)	19
2.3 Measured frequency response of the BP, HP, and AP filters	24
2.4 Proposed universal voltage-mode filter (II)	25
2.5a Measured frequency response of the BR filter	29
2.5b Measured frequency response of the LP filter	29
2.6 Proposed universal voltage-mode single input multiple output filter (III)	31
2.7 Comparison between theoretical and experimental results for the HP, AP filter	35
2.8 Proposed universal current-mode filter (I)	37
2.9 Voltage to current converter	37
2.10 Comparisons between theoretical and experimental results for the BP and LP filters	42

2.11 Proposed current-mode universal filter (II)	43
2.12 Comparison between the theoretical and experimental results for the PB and LP filters	47
3.1 Proposed oscillator structure	57
3.2 Equivalent circuit of the oscillator structure of Fig. 3.1	57
3.3 Five oscillator circuits derived from Fig. 3.1	58
3.4 Variation of the frequency of oscillation of Figs. 3.3a, b, d, and e	69
3.5 Comparisons between theoretical and experimental results for Figs. 3.3d and e	60
3.6 Proposed sinusoidal oscillator with single resistor control and all capacitor grounded (II)	62
3.7a Proposed oscillator structure (III)	65
3.7b Sinusoidal oscillator circuit derived from Fig.3.7a	65
3.8 Comparisons between theoretical and experimental results of Fig. 3.6	68
3.9 Comparisons between theoretical and experimental results of Fig. 3.7	68
3.10 configuration for synthesizing sinusoidal oscillators using a CFOA (IV)	71
3.11 Proposed Sinusoidal oscillator	71
3.12 Configuration for synthesizing sinusoidal oscillators using a CFOA (V)	75
3.13 Proposed sinusoidal oscillator derived from Fig.3.12	78
3.14 Proposed sinusoidal oscillator with single resistor control and all capacitors grounded	78
3.15 Comparisons between theoretical and experimental results of Fig. 3.11	79

3.16 Comparisons between theoretical and experimental results of Fig. 3.14	79
3.17 Proposed signals generator	82
3.18 The output waveforms of Fig. 3.17	84
3.19 Comparisons between theoretical and experimental results of Fig. 3.17	86
3.20 Schmitt trigger with a CFOA	90
3.21 Proposed square waveform generator	90
3.22 Comparisons between theoretical and experimental results of Fig. 3.21	91
4.1 Svaboda-model of non-ideal CFOA (AD844)	94
4.2 Bruun model	95
4.3 Modified Bruun model	95
4.4 The proposed universal voltage-mode filter of Fig.2.1	96
4.5 Equivalent circuit of the active filter of Fig. 4.4 using Svabodda model	97
4.6 Comparison between experimental and calculated results for the BP and HP filters of the universal active filter shown in Fig. 4.4	100
4.7 Comparison between experimental and calculated results for the BP filter of the universal filter shown in Fig. 2.7	101
4.8 The proposed universal voltage-mode filter of Fig. 2.4	102
4.9 Equivalent circuit of Fig. 4.8 using Svoboda model	103
4.10 Comparison between experimental and calculated results for the BR and LP filters of the universal active filter shown in Fig. 4.8	105
4.11 The proposed oscillator circuit of Fig 3.14	106
4.12 Equivalent circuit of the oscillator circuit of Fig. 4.8 using Svoboda model	107

4.13 Comparison between experimental and calculated results for the frequency of oscillation of Fig. 4.11	109
4.14 Comparison between experimental and calculated results for the frequency of oscillation of Fig.3.3(d)	110
4.15 Comparison between experimental and calculated results for the frequency of oscillation of Fig. 3.3(e)	110
4.16 Comparison between experimental and calculated results for the frequency of oscillation of Fig. 3.6	111

List of Tables

3.1 Frequency and condition of oscillation of the circuits of Fig. 3.4	55
3.2 Frequency of oscillation and its sensitivities to active elements of the circuits of Fig. 3.4	56
3.3 Remaining sinusoidal oscillators derived from Fig. 3.10	72
4.1 Comparison of measured and calculated values of the frequency of oscillation of Fig. 4.11	108

Abstract

Name: Saad Mohammad Al-Shahrani
Title: Active Filters and Oscillators Using Current Feedback
Operational amplifiers
Major Field: Electrical Engineering
Date of Degree: October, 1995

In this thesis, New current feedback operational amplifier (CFOA)-based filter, oscillator and signal generator circuits were proposed. In order to be compatible with integration requirements, these circuits use minimum number of active elements and enjoy independent control of the critical circuit parameters. The effects of parasitics, voltage and current tracking errors of the CFOA on the circuit parameters were discussed. Reasonable agreement between theory and measurements was obtained in all circuits.

Master of Science Degree

King Fahd University of Petroleum and Minerals

Dhahran, Saudi Arabia

October, 1995

خلاصة الرسالة

الاسم / سعد محمد سعد الشهراني

عنوان الرسالة / مولدات ذبذبة ومرشحات باستخدام مكبر العمليات ذو التغذية التيارية
الراجعة .

التخصص / الهندسة الكهربائية

تاريخ الشهادة / أكتوبر ١٩٩٥م

في هذه الأطروحة تمّ استنباط وعرض عدد من الدوائر الإلكترونية باستخدام مكبر مثالي للعمليات ذو التغذية التيارية الراجعة للحصول على مولدات للذبذبة وكذلك مرشحات . من أجل تحقيق المتطلبات اللازمة لتصنيع هذه الدوائر على صورة دوائر متكاملة فقد روعي تحقيق الشروط الآتية في الدوائر المقترحة وهي : استخدام أقل عدد من المقاومات والمكثفات كذلك عدم إعتداد الخصائص الأساسية للدوائر على بعضها البعض بحيث يمكن تغيير أحدها بدون أن يتأثر الآخر . تمت أيضاً مناقشة تأثير الخصائص غير المثالية لمكبر العمليات ذو التغذية التيارية الراجعة على الدوائر المقترحة ولوحظ أنّ هذا التأثير يكون كبيراً عند الترددات العالية ، وباستخدام ثلاثة نماذج غير مثالية لمكبر العمليات ذو التغذية التيارية الراجعة أمكن الحصول على نتائج أفضل .

درجة الماجستير في العلوم

جامعة الملك فهد للبترول والمعادن

الظهران - المملكة العربية السعودية

أكتوبر ١٩٩٥م

Chapter 1

Introduction

1.1 The Current Feedback Operational Amplifier

The voltage op amp (VOA) is used extensively throughout the electronic industry, as it is a cheap, easy to use, analogue building block. Fig.1.1(a) shows a model for the VOA where A is the frequency dependent open loop voltage gain and r_i is the input resistance of op amp. Assuming that the open loop gain of the VOA can be expressed by:

$$A(s) = \frac{A_o \omega_1}{(s + \omega_1)} \quad (1.1)$$

where A_o is the open loop dc gain and ω_1 is the pole of the VOA, then, by routine analysis we can get the closed loop gain of the non inverting amplifier shown in Fig.1.1(b). It will be given by

$$\frac{V_o}{V_i} = \frac{A_o \omega_1}{s + \omega_1 (1 + A_o / G)} \quad (1.2)$$

where

$$G = R_1 / (R_1 + R_2) \quad (1.3)$$

From equation (1.2) one can see that the closed loop bandwidth is inversely proportional to G . Thus any attempt to change the gain will affect the bandwidth. This is the major disadvantage of the VOA-based circuit [2]. In addition to this, VOAs also suffer from limited slew rate characteristic because of its inherent nonlinearity [1]. Where the slew rate is defined as the maximum rate of change of the output voltage.

Because of the poor performance of VOA, many researchers have looked for a new device with better performance. This new device, the current feed back operational amplifier (CFOA), was originated by Comlinear in 1980.

To appreciate the inner workings of the CFOA, it is instructive to examine the simplified circuit diagram of Figure 1.2.

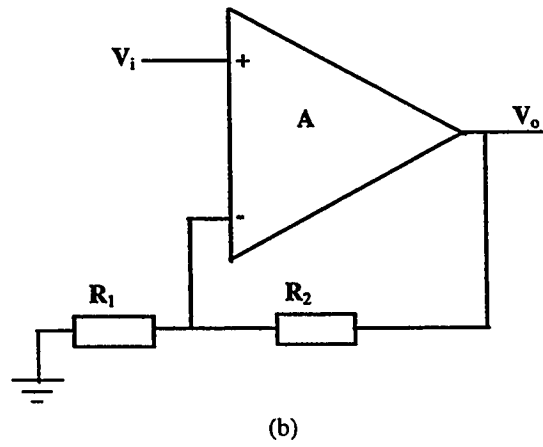
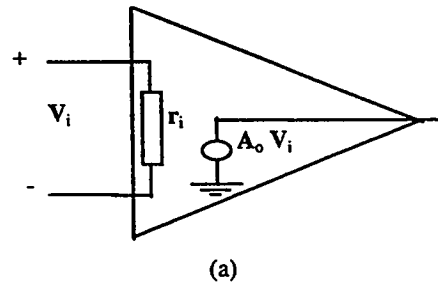


Fig.1.1: a- VOA equivalent b- Closed-loop noninverting amplifier

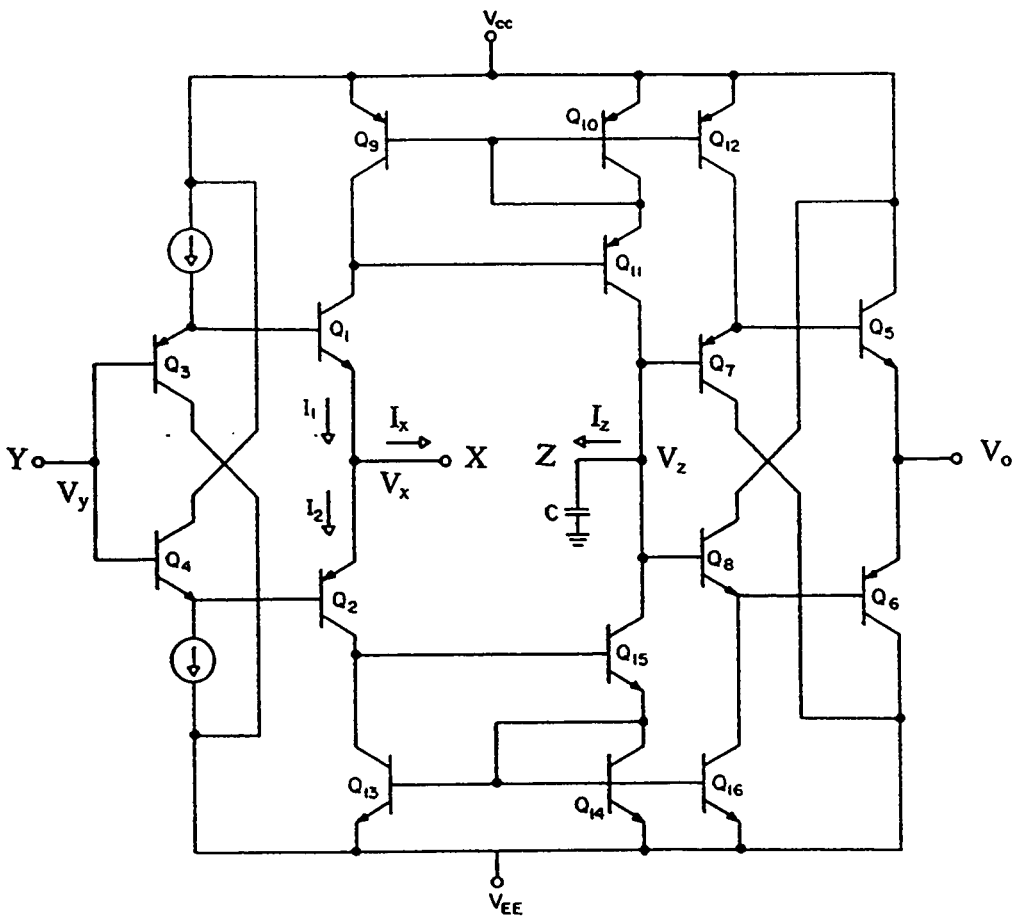


Fig.1.2: Simplified circuit diagram of a current feedback amplifier

The input buffer consists of transistors Q_1 through Q_4 . While Q_1 and Q_2 form a low output-impedance push-pull stage, Q_3 and Q_4 do three jobs at the same time. First, they form emitter followers, thus providing the circuit with high input resistance. Second, Q_3 and Q_4 provide V_{be} compensation for Q_1 and Q_2 respectively in a way to have $V_x = V_y$. And finally, V_{beQ3} and V_{beQ4} generate the bias voltage required for the complementary transistors Q_1 and Q_2 to eliminate the crossover distortion.

Summing currents at the inverting node yields $I_1 - I_2 = I_x = I_{inv}$, where I_1 and I_2 are the push-pull transistor currents. A pair of Wilson current mirrors, consisting of transistors $Q_9 - Q_{10} - Q_{11}$ and $Q_{13} - Q_{14} - Q_{15}$, reflect these currents and recombine them at a common node, whose equivalent capacitance to ground is denoted as C . By mirror action, the current through this capacitance is $I_z = I_1 - I_2$.

The voltage developed by C in response to this current is then conveyed to the output via a second buffer, made up of Q_5 through Q_8 . When the feedback loop is closed as in Fig.1.4, and whenever an external signal tries to unbalance the two inputs, the input buffer will begin sourcing (or sinking) an unbalance current I_{inv} to the external resistance's. This imbalance I_{inv} is then conveyed by the Wilson mirrors to the capacitor C , causing V_o to swing in the positive (or negative) direction until the original imbalance is neutralized via the negative feedback loop [3].

An ideal CFOA can therefore be described by $I_x = I_z$, $V_x = V_y$, $V_o = V_z$ and $I_y = 0$. The CFOA can be represented by the model shown in Fig.1.3. The CFOA consists of two main parts: the input buffer and the transimpedance amplifier. The buffer is connected between the inverting and the non inverting terminals. As a result of this buffer, the non inverting terminal has high input impedance and the inverting terminal has low input impedance. The transimpedance amplifier senses the current I_{inv} following inward or outward the inverting terminal and produces output voltage. Equation (1.4) indicates the relation between I_{inv} and the output voltage where $A(s)$ is the transimpedance amplifier gain.

$$V_o = A(s)I_{inv} \quad (1.4)$$

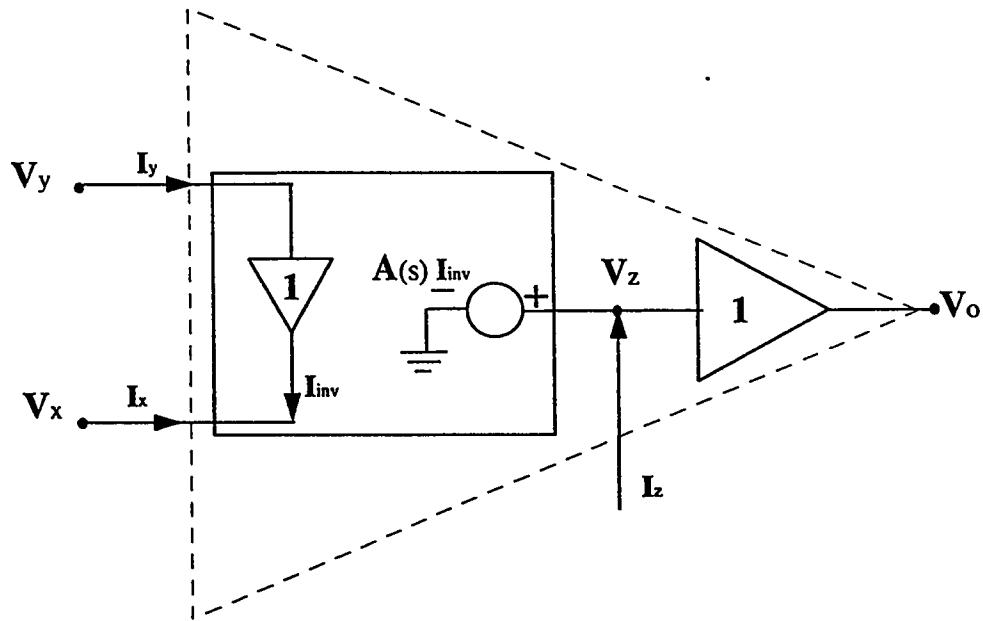


Fig.1.3 : Model for the CFOA

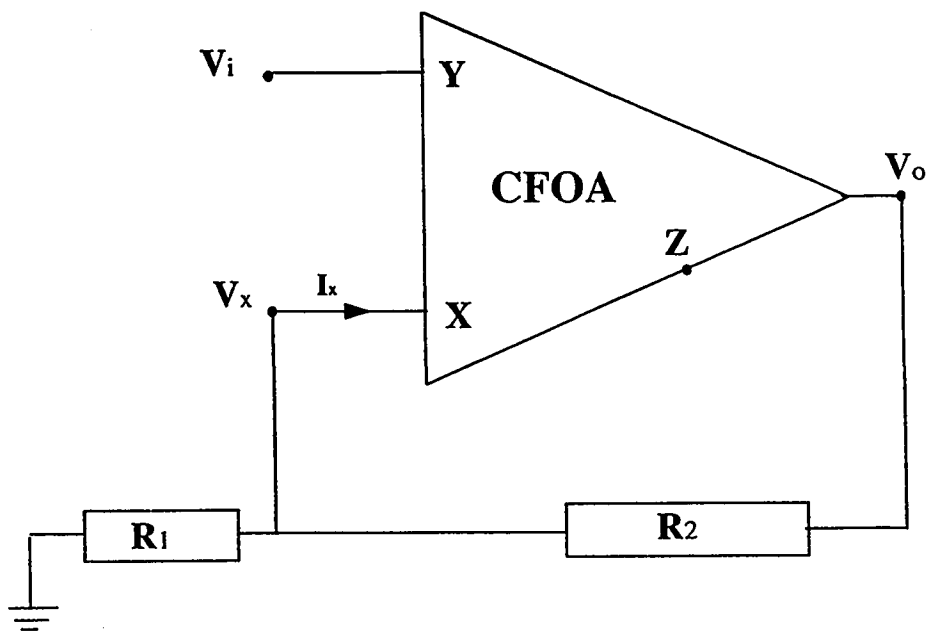


Fig.1.4: Closed-loop noninverting CFOA

Now consider the CFOA-based noninverting amplifier of Fig 1.4. By routine analysis using the model of Fig 1.3. we can get the closed loop gain of the CFOA circuit shown in Fig 1.4. Assuming that the open loop gain of the CFOA can be expressed by:

$$A(s) = A_o\omega_1/(s + \omega_1) \quad (1.5)$$

where A_o is the open loop *dc* gain and ω_1 is the pole of the CFOA, then,

$$\frac{V_o}{V_i} = \frac{A_o\omega_1(1/R_1 + 1/R_2)}{s + \omega_1(1 + A_o/R_2)} \quad (1.6)$$

From equation (1.6) the pole and the *dc* gain of the closed loop noninverting CFOA are $\omega_1(1 + A_o/R_2)$ and $A_o(1/R_1 + 1/R_2) / (1 + A_o/R_2)$, respectively. Thus it is clear that we can adjust the bandwidth by changing R_2 and after that the gain can be controlled via R_1 without affecting the bandwidth.

The slew rate of the CFOA is defined as the maximum rate of change of the output voltage. Since the output voltage is proportional to I_{inv} as shown in equation (1.4) and there is no upper limit to I_{inv} then there is no slew rate limiting in CFOAs. The absence of the slew rate limiting allows for faster settling times [2], where the settling time is defined as the amount of time t_s it takes for the output to reach steady state.

Although ideal analysis of the CFOA indicates that the closed loop gain can be controlled via R_1 without affecting the dynamics of the CFOA, due to non-zero output impedance of the input buffer it is affected. Though there is dependency between the

closed loop gain and the bandwidth, it is not as drastically as with the VOA. Denoting the output impedance of the input buffer R_o , Equation (1.7) shows the effect of R_o on the closed loop gain of the CFOA[3].

$$\frac{V_o}{V_i} = \left(1 + \frac{R_2}{R_1}\right) \frac{\frac{A_o \omega_1}{Z_2}}{s + \omega_1(1 + A_o/Z_2)} \quad (1.7)$$

where

$$Z_2 = R_2 \left(1 + \frac{R_o}{R_1 // R_2}\right) \quad (1.8)$$

From equations (1.7) and (1.8) one can see that, because of the finite value of the output resistance R_o , the gain and the bandwidth can no longer be independently adjusted. Thus it is preferable to have R_o as close to zero as possible.

Despite its advantages, the CFOA suffers from some disadvantages. The CFOA is unstable with capacitive feedback. To study the stability of the CFOA with capacitive feedback Equation (1.7) can be written in terms of the loop gain as shown in Equation (1.9) where R_2 in equation (1.8) is replaced with $R_2 // (1/sC_2)$ in order to take the effect of the feedback capacitor into consideration.

$$\frac{V_o}{V_i} = \left(1 + \frac{R_2}{R_1}\right) \frac{1}{1 + (1/T(s))} \quad (1.9)$$

where

$$T(s) = \frac{A(s)}{Z_2} \quad (1.10)$$

Equation (1.11) expresses the effect of the feedback capacitor on the loop gain.

$$T(s) = \frac{A(s)(1 + sR_2C_2)}{R_2R_1 + R_0R_1 + R_0R_2 + R_0R_1R_2sC_2} \quad (1.11)$$

If the overall shift of the loop gain reaches -180° at the crossover frequency due to high-order poles of $A(s)$, the loop gain will become $T = -1$, making the closed loop gain infinite, by equation (1.9). Where the crossover frequency is the frequency at which the magnitude of the loop gain is equal to unity. When this condition is met, the circuit will oscillate. Even if the phase shift fails to reach 180° , the closed loop response might be unstable [3].

In addition, the CFOA has low overall gain. This resulted from single gain stages which produces low overall gain. Furthermore, input stage characteristics are generally dependent on the matching of integrated PNP transistors to those NPN types, further exorbitant DC mismatches such as offset voltages, CMRR and to some extent PSRR [4]. Where the power supply rejection ratio PSRR is the ratio of the change the input offset voltage to the corresponding change in one power-supply voltage, with all remaining power voltages held constant.

Although it is possible to overcome these drawbacks with additional circuitry, the price to be paid is the distortion of the AC advantages. To minimize the offset voltages other types of input stage can be used. Fig.1.5 shows a four transistor input stage with two diodes and two transistors. These diodes and transistor are connected in a way such that like-types are matched with like. Using this type of the input stage a great improvement in the offset voltage V_{os} can be achieved. Unfortunately, this input

stage has a disadvantage of a low noninverting input impedance and a high noninverting input bias current and noise. Another type of the input stage is the eight-transistor buffer shown in Fig.1.6. This input stage offers the advantages of high noninverting input impedance, low noninverting input bias current and matching like transistors with like. On the other hand, its inverting input impedance is greater than the previous types [5]. This disadvantage increase the dependency between the closed loop gain and the bandwidth as shown in Equation 1.7.

The input stages can be also cascaded to improve V_{os} , but this may result in serious input stage slew rate limitations. The CFOA has worse noise performance than VOA. In fact, this is due to the high value of the input current to the CFOA's inverting input [5].

From the above discussion we note that the CFOA has some attractive advantages ; higher slew rate and bandwidths independent of gain. These advantages can be exploited in many applications to get better performance than the VOA-based designs. It is worth mentioning here that whatever the measures taken to improve the performance of CFOA's , commercially available CFOAs suffer from three major sources of error ; namely, *the current tracking error* defined by $I_z = \alpha I_x$ where $\alpha = 1 - \delta_i$, $|\delta_i| \ll 1$, *the output voltage tracking error* defined by $V_o = \gamma V_z$ and *the input voltage tracking error* defined by $V_x = \beta V_y$ where $\gamma = 1 - \delta_o$, $|\delta_o| \ll 1$ and $\beta = 1 - \delta_v$, $|\delta_v| \ll 1$. These current and voltage tracking errors are due mainly to the mismatches in the transistors as well as the nonideal current transfer ratios of the current mirrors used.

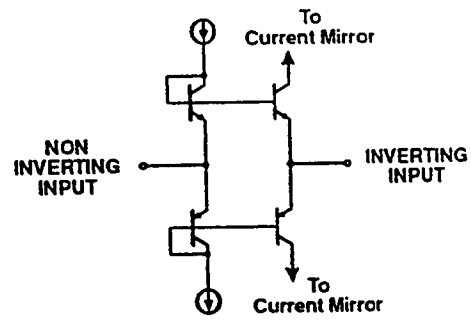


Fig.1.5: Alternative Four-Transistor Input Buffer

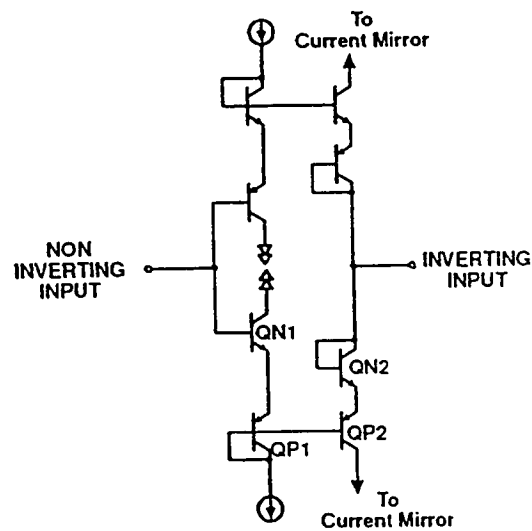


Fig.1.6: Eight-Transistor Input Buffer

1.2 Literature Review for the CFOA Application

Over the last decade researchers have looked for implementation of known applications using the CFOA. Fabre proposed in [6] the implementation of bandpass, lowpass and highpass filters using a single commercial available transimpedance operational amplifier; the AD844. Then, he concluded that using CFOA, including a compensation pin, to implement second-order filters will give better performance than using VOA. One configuration realizing series resistor-inductor and series capacitor-frequency-dependent negative resistance using CFOA is reported in [7]. The same configuration is used to implement second order lowpass, highpass and bandpass filters. Fabre in [8] proposed a new configuration for a gyrator where two CFOA are used. Highpass and bandpass filters are implemented from this gyrator. In [9] Celma, Pedro and Carlosena proposed a new sinusoidal oscillator using the CFOA. Then, they concluded that the sinusoidal oscillator built around the CFOA exhibits superior features with respect to those built around the VOA in terms of higher frequencies of operation, lower distortion and increased frequency accuracy. A multiphase sinusoidal oscillator using the parasitic poles of the CFOA is presented in [10]. The oscillator can generate n signals which are equal in amplitude and equally spaced in phase. The effects caused by the nonlinearity of the CFOA on the oscillation frequency and condition have been analyzed. A voltage mode notch, lowpass and bandpass filters are implemented using current-feedback amplifiers in [11]. New analogue divider circuits using the CFOAs are presented in [12]. Basically, they consist of two CFOAs, two MOS transistors biased in the triode region, and a resistor. In [13], new sinusoidal oscillators with single element control has been realized using a CFOA. Shen and Cheng have shown in [14] three new sinusoidal oscillators using the current feedback

amplifier pole. Two of the proposed oscillators consist of CFOA's and resistors only and the third one consists of one CFOA, three resistors and a capacitor. A current feedback amplifier (CFOA)- based universal filter deduced from a Mason graph is presented in [15].

1.3 Problem Definition

From the literature review it appears that the use of the CFOA in designing various analog circuits is not widely studied by researchers in the field. It is the major intention of this thesis to evaluate some of the recently proposed linear analog signal processing circuits for example, filters and oscillators, using CFOA. The advantages and disadvantages of these circuits are studied, and an effort is made to improve their performance based on certain criteria. In specific, the following issues are addressed.

1. New applications will be developed using CFOA particularly current-mode active filters and square, triangular and ramp waveforms generator.
2. Modified applications will be developed using the CFOA particularly voltage-mode active filters and oscillators.
3. These applications will be tested experimentally. Then a comparison between the experimental and calculated results will be done.
4. The effect of the CFOA nonidealities on the performance of the proposed circuits will be discussed.

1.4 Thesis organization

The thesis work is presented as follows. In Chapter 2 active filters using the CFOA's are discussed. Chapter 3 deals with oscillators circuits using CFOA's. Chapter 4 discusses the non ideality effects on the CFOA's application (active filters and oscillators).The conclusions and suggestions for future work are discussed in Chapter 5.

Chapter 2

Active Filters

2.1 Introduction

The filter is an important building block in communication systems. A filter is a frequency-selective device that is used to limit the spectrum of a signal to some specified band of frequencies. Its frequency response is characterized by a passband and a stopband. The frequencies inside the passband are transmitted with little or no linear distortion, whereas those in the stop-band are rejected or highly attenuated. The filter may be of the low-pass (LP), high-pass (HP), band-pass (BP), band-reject(BR) or all-pass (AL) type, depending on whether it transmits low, high, intermediate, all but not intermediate, or all frequencies, respectively.

There are two main types of filters: active-RC filters and switched-capacitor filters, Active-RC filters utilize opamps together with resistors and capacitors. The switched-capacitor filter technique is based on the realization of a resistor by switching a capacitor between two circuit nodes at a sufficiently high rate. This is equivalent to a resistor connecting these two nodes.

2.2 How To Evaluate an Active Filter?

There are many factors to be taken into consideration to evaluate an active filter in order to get an optimum one.

1. Independent control of the basic parameters of the filter for example the center frequency ω_0 and the bandwidth ω_0/Q_0 where Q_0 is the quality factor.
2. To overcome the effect of the stray capacitance all capacitor should be grounded and minimum possible number of resistors should be floating.
3. It will be of great advantage if ω_0 especially and (ω_0/Q_0) can be controlled via grounded resistors. This situation will help to get a programmable filter by replacing these resistors by programmable resistors, for example a JFET transistor.
4. The filter is efficient from economic point of view (in terms of area and power consumption) if it has few number of active and passive components.
5. The sensitivity of the filter parameters $(\omega_0, \omega_0/Q_0)$ to passive components should be as low as possible and it shouldn't exceed 1.

Because of the tolerance in component values and because of the finite CFOA gain, the response of the actual filter will deviate from the ideal response. As a mean for predicting such deviations, the filter designer employs the concept of sensitivity. These sensitivities can be quantified using the classical sensitivity function S_x^y , defined as

$$S_x^y = \lim_{\Delta X \rightarrow 0} \frac{\Delta Y/Y}{\Delta X/X} \quad (2.1)$$

$$S_x^y = \frac{\partial Y}{\partial X} \frac{X}{Y} \quad (2.2)$$

where X denotes the value of a component (a resistor, or a capacitor) and Y denotes a circuit parameter of interest (ω_0 or ω_0/Q_0).

These factors were adopted with potential manufacturing of the proposed circuits in IC form. For such purpose it is necessary to reduce to the minimum the required silicon area, To make all the passive components grounded as this makes it easy to take into account the effect of stray capacitances as well as paving the way to implement on the chip tuning circuits. This is why we try to use minimum number of active and passive components. Also the independent control of the center frequency and bandwidth makes the implementation of tuning on the chip an easy task.

2.3 Universal Second-order Filters

A universal filter is the filter which can realize different functions (LP, HP, BP, BR and AL filters). There are two types of universal filters: single input multiple outputs and multiple inputs single output. The first one can realize different functions simultaneously at different points, where, in the second one different functions can be realized one at a time by controlling the inputs.

2.3.1 Universal Voltage-mode Multiple Inputs Single

Output Filter

A current feedback amplifier (CFOA)-based universal filter deduced from a Mason graph is shown in Fig.2.1 [15]. This filter has the following merits:

- (i) Very low output impedance which makes the voltage-mode circuit cascadable.
- (ii) ω_0 can be adjusted without affecting Q_0 .
- (iii) The sensitivities of ω_0 and Q_0 to passive and active components are small.
- (iv) There are no requirements for critical component matching conditions to realize the five filter types.

Since nothing is perfect, here are some demerits for this filter. It has four floating components one of them is a capacitor and the rest are resistors. Moreover, Q_0 cannot be adjusted without affecting ω_0 .

A new universal filter is proposed in this section which has some advantages over the available universal filter [15]. This filter employs three CFOAs, four capacitors and two resistors as shown in Fig.2.2.

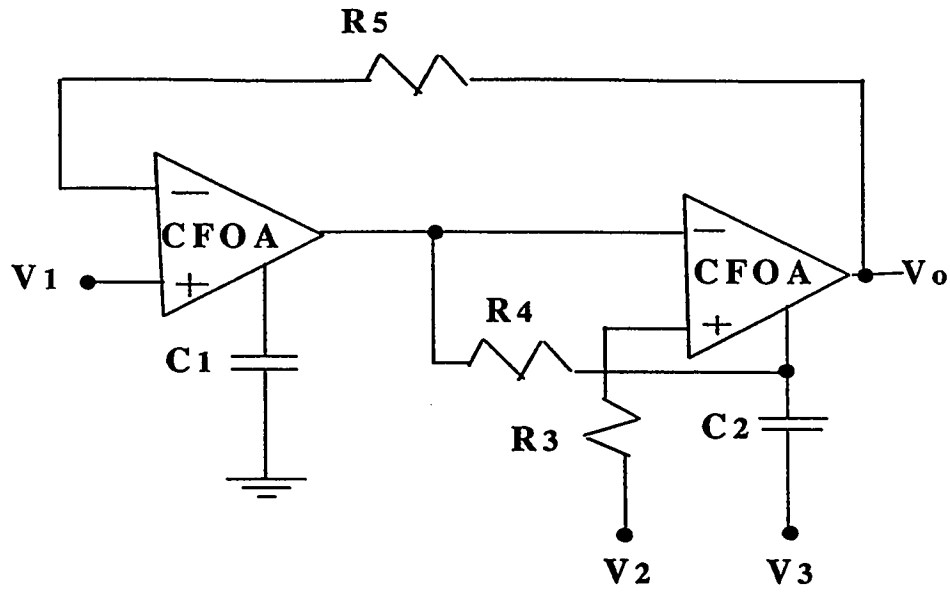


Fig.2.1. *Universal voltage-mode filter [15]*

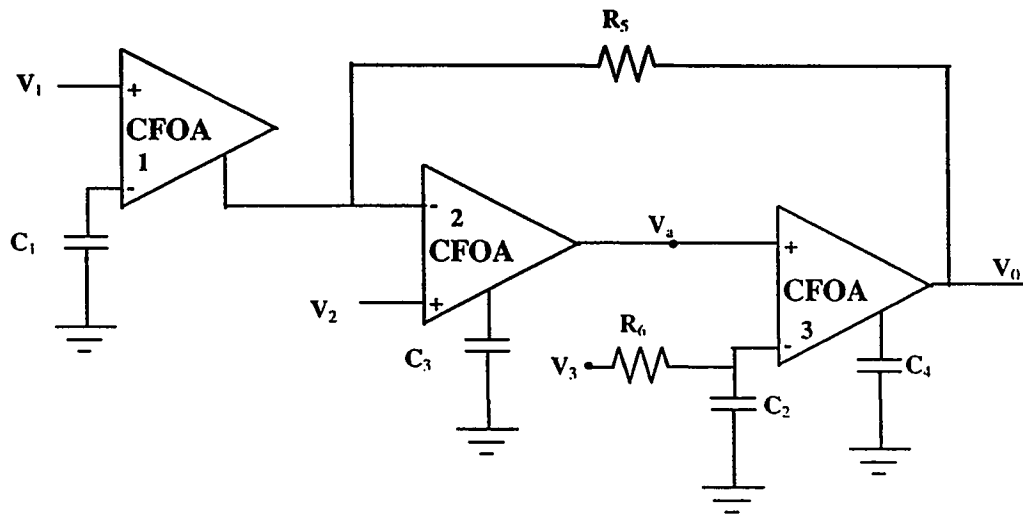


Fig.2.2: *Proposed universal voltage-mode filter (I)*

Referring to figure 2.2 and using the CFOA model of Fig.1.3 , voltage V_a can be expressed as

$$V_a = -\frac{sC_1}{sC_3}V_1 + \frac{G_5}{sC_3}V_2 - \frac{G_5}{sC_3}V_o \quad (2.3)$$

and the voltage V_o can be expressed as

$$V_o = \frac{(sC_2 + G_6)}{sC_4}V_a - \frac{G_6}{sC_4}V_3 \quad (2.4)$$

Combining equations (2.3) and (2.4) gives,

$$V_o = \left(\frac{sC_2 + G_6}{sC_4} \right) \left(\frac{-sC_1}{sC_3} \right) V_1 + \left(\frac{sC_2 + G_6}{sC_4} \right) \left(\frac{G_5}{sC_3} \right) (V_2 - V_o) - \left(\frac{G_6}{sC_4} \right) V_3 \quad (2.5)$$

or

$$V_o = \frac{-(s^2C_1C_2 + G_6sC_1)V_1 + (G_5sC_2 + G_5G_6)V_2 - (G_6sC_3)V_3}{s^2C_3C_4 + G_5sC_2 + G_5G_6} \quad (2.6)$$

Specialization of the numerator in equation (2.6) result in the following filter function:

$$\text{If } G_5C_2 = G_6C_3$$

$$C_3 = C_1$$

$$C_2 = C_4$$

(i) Lowpass:

$$V_1 = 0, V_2 = V_3 = \text{input voltage signal.}$$

(ii) Highpass:

$$V_2 = 0, -V_1 = V_3 = \text{input voltage signal}$$

(iii) Bandpass:

$$V_1 = V_2 = 0, V_3 = \text{input voltage signal}$$

(iv) Band-notch:

$$V_2 = -V_1 = -(1/2) V_3 = \text{input voltage signal}$$

(v) Allpass:

$$-V_1 = V_2 = V_3 = \text{input voltage signal}$$

From equation (2.6) the center frequency ω_o and bandwidth ω_o/Q_o are given by

$$\omega_o = \left(\frac{G_5 G_6}{C_3 C_4} \right)^{1/2} \quad (2.7)$$

$$\frac{\omega_o}{Q_o} = \left(\frac{C_2 G_5}{C_4 C_3} \right) \quad (2.8)$$

So, the sensitivities of ω_o and ω_o/Q_o to passive components are

$$S_{G_5}^{\omega_o} = S_{G_6}^{\omega_o} = 1/2, \quad S_{C_3}^{\omega_o} = S_{C_4}^{\omega_o} = -1/2$$

$$S_{C_2}^{\frac{\omega_o}{Q_o}} = S_{G_5}^{\frac{\omega_o}{Q_o}} = -S_{C_4}^{\frac{\omega_o}{Q_o}} = -S_{C_3}^{\frac{\omega_o}{Q_o}} = 1$$

all of which are small.

Taking into account the nonidealities of a CFOA, namely, $i_z = \alpha i_x$, $v_x = \beta v_y$ and $v_o =$

γv_z where $\alpha = 1 - \delta_i$ and $|\delta_i| \ll 1$, denotes the current tracking error, $\beta = 1 - \delta_v$ and

$|\delta_v| \ll 1$ denotes the input voltage tracking error and $\gamma = 1 - \delta_o$ and $\gamma = 1 - \delta_o$ and

$|\delta_o| \ll 1$ denotes the output voltage tracking error, equation (2.6) becomes

$$V_o = \frac{-(s^2 C_1 C_2 + s G_6 C_1) \beta_1 \alpha_1 V_1 + (s C_2 G_5 + G_5 G_6) \beta_2 V_2 - s \frac{G_6 C_3}{\alpha_2 \gamma_2} V_3}{s^2 \frac{C_4 C_3}{\alpha_2 \alpha_3 \gamma_1 \gamma_3} + s C_2 G_5 + G_5 G_6} \quad (2.9)$$

From equation (2.9) the center frequency ω_o and the bandwidth ω_o/Q_o are given by:

$$\omega_o = \left(\frac{G_5 G_6}{C_4 C_3} \right)^{\frac{1}{2}} (\alpha_2 \alpha_3 \gamma_1 \gamma_3)^{\frac{1}{2}} \quad (2.10)$$

$$\frac{\omega_o}{Q_o} = \left(\frac{C_2 G_5}{C_3 C_4} \right) (\alpha_2 \alpha_3 \gamma_1 \gamma_3) \quad (2.11)$$

So, the sensitivities of ω_o and ω_o/Q_o to active components are

$$S_{\alpha_2}^{\omega_o} = S_{\alpha_3}^{\omega_o} = S_{\gamma_1}^{\omega_o} = S_{\gamma_3}^{\omega_o} = 1/2$$

$$S_{\alpha_2}^{\frac{\omega_o}{Q_o}} = S_{\alpha_3}^{\frac{\omega_o}{Q_o}} = S_{\gamma_1}^{\frac{\omega_o}{Q_o}} = S_{\gamma_3}^{\frac{\omega_o}{Q_o}} = 1$$

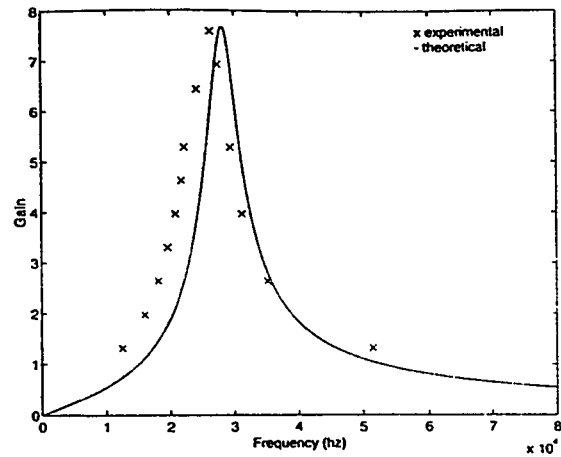
all of which are small.

This filter offers the following advantageous features:

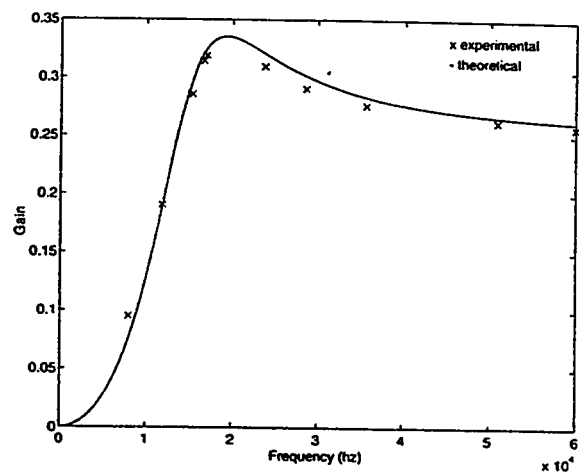
- (i) Very low output impedance which makes the voltage-mode circuit cascadable.
- (ii) Orthogonal adjustment of ω_o and (ω_o/Q_o) can be done easily via R_6 or C_2 . That is to say ω_o and (ω_o/Q_o) can be controlled independently.
- (iii) The sensitivities of ω_o and ω_o/Q_o to passive and active components are small.
- (iv) All capacitors are grounded.
- (v) Only two resistors are floating.

Despite the advantages of the proposed circuit, the main drawback is the requirements for matching conditions between passive elements.

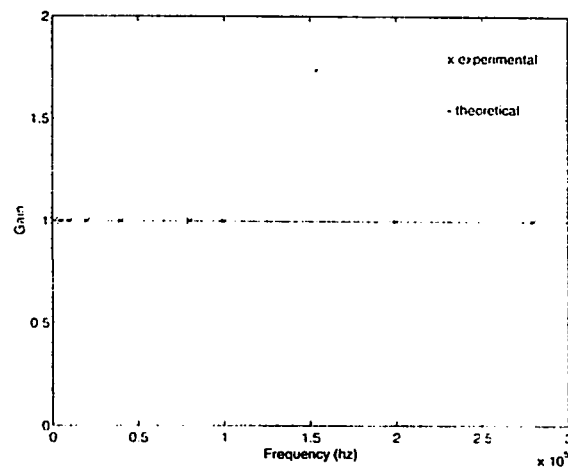
To demonstrate the theoretical behaviour of the proposed network, BP, HP and AP filter prototypes have been realized with discrete components. The measured frequency responses of these filters, using the CFOA AD844, shown in Fig. 2.3 agree with theory.



(a)



(b)



(c)

Fig.2.3: Measured frequency response of the BP,HP, and AP filter.

a)BP: $R_6=2K\Omega$, $R_5=8K\Omega$, $C_1=C_3=1nF$, $C_7=0.5nF$ and $C_4=2nF$

b)HP: $R_6=8.24K\Omega$, $R_5=3.09K\Omega$, $C_1=C_3=C_7=1nF$ and $C_4=4nF$

c)AP: $R_6=R_5=5K\Omega$, $C_1=C_3=C_7=C_4=1nF$

In an attempt to overcome the disadvantage of the proposed universal filter of Fig.2.2 and [15], another universal voltage-mode filter has been developed and is shown in Fig.2.4.

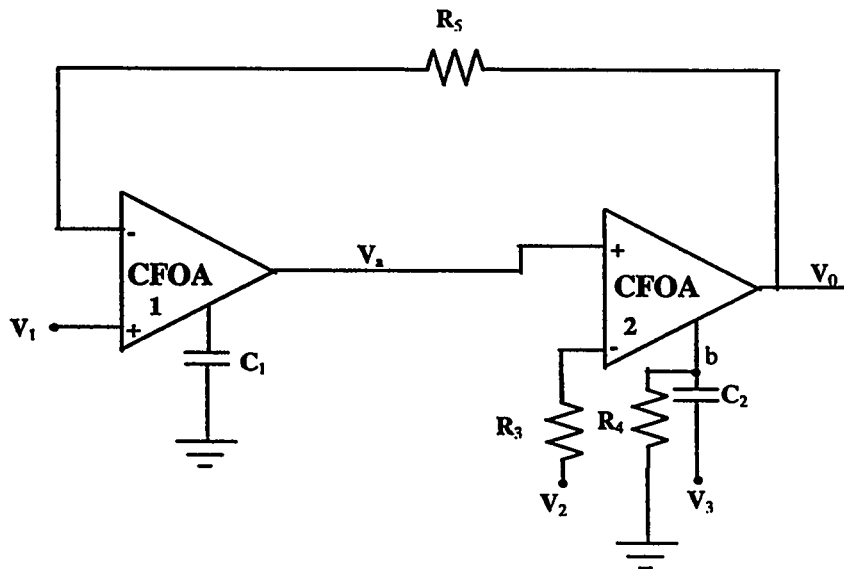


Fig.2.4 Proposed universal voltage-mode filter (II)

A simple analysis for this circuit using the CFOA model of Fig.1.3 gives

$$V_o = \frac{s^2 C_2 C_1 V_3 - s G_3 C_1 V_2 + G_3 G_5 V_1}{s^2 C_1 C_2 + s G_4 C_1 + G_3 G_5} \quad (2.12)$$

Specialization of the numerator in equation (2.12) result in the following functions:

(i) Lowpass:

$$V_2 = V_3 = 0, V_1 = \text{input voltage signal.}$$

(ii) Highpass:

$$V_1 = V_2 = 0, V_3 = \text{input voltage signal}$$

(iii) Bandpass:

$$V_3 = V_1 = 0, V_2 = \text{input voltage signal}$$

(iv) Band-notch:

$$V_2 = 0, V_1 = V_3 = \text{input voltage signal}$$

(v) Allpass:

$$R_3 = R_4$$

$$V_1 = V_2 = V_3 = \text{input voltage signal}$$

From equation (2.12) the center frequency ω_o and the bandwidth ω_o/Q_o are given by

$$\omega_o = \left(\frac{G_3 G_5}{C_1 C_2} \right)^{1/2} \quad (2.13)$$

and

$$\frac{\omega_o}{Q_o} = \left(\frac{G_4}{C_2} \right) \quad (2.14)$$

The sensitivities of ω_o and ω_o/Q_o for passive components are given by

$$S_{G_3}^{\omega_o} = S_{G_5}^{\omega_o} = 1/2; \quad S_{C_1}^{\omega_o} = S_{C_2}^{\omega_o} = 1/2$$

$$S_{G_4}^{\frac{\omega_o}{Q_o}} = -S_{C_2}^{\frac{\omega_o}{Q_o}} = 1$$

Thus, the sensitivities of ω_o and ω_o/Q_o to passive components are small.

Taking into account the voltage tracking error and the current tracking error the output voltage can be given by

$$V_o = \frac{\alpha_1 \alpha_2 \beta_1 \beta_2 \gamma_1 G_5 G_3 V_1 - s C_1 G_3 \alpha_2 V_2 - s^2 C_2 C_1 V_3}{s^2 \frac{C_1 C_2}{\gamma_2} + s \frac{G_4 C_1}{\gamma_2} + \alpha_1 \alpha_2 \beta_2 \gamma_1 G_3 G_5} \quad (2.15)$$

From equation (2.15) the center frequency ω_o and the bandwidth ω_o/Q_o are given by:

$$\omega_o = \left(\frac{G_3 G_5}{C_1 C_2} \right)^{\frac{1}{2}} (\alpha_1 \alpha_2 \beta_2 \gamma_1 \gamma_2)^{\frac{1}{2}} \quad (2.16)$$

$$\frac{\omega_o}{Q_o} = \left(\frac{G_4}{C_2} \right) \quad (2.17)$$

So, the sensitivities of ω_o and ω_o/Q_o to active components are

$$S_{\alpha_1}^{\omega_o} = S_{\alpha_2}^{\omega_o} = S_{\beta_2}^{\omega_o} = S_{\gamma_1}^{\omega_o} = S_{\gamma_2}^{\omega_o} = 1/2$$

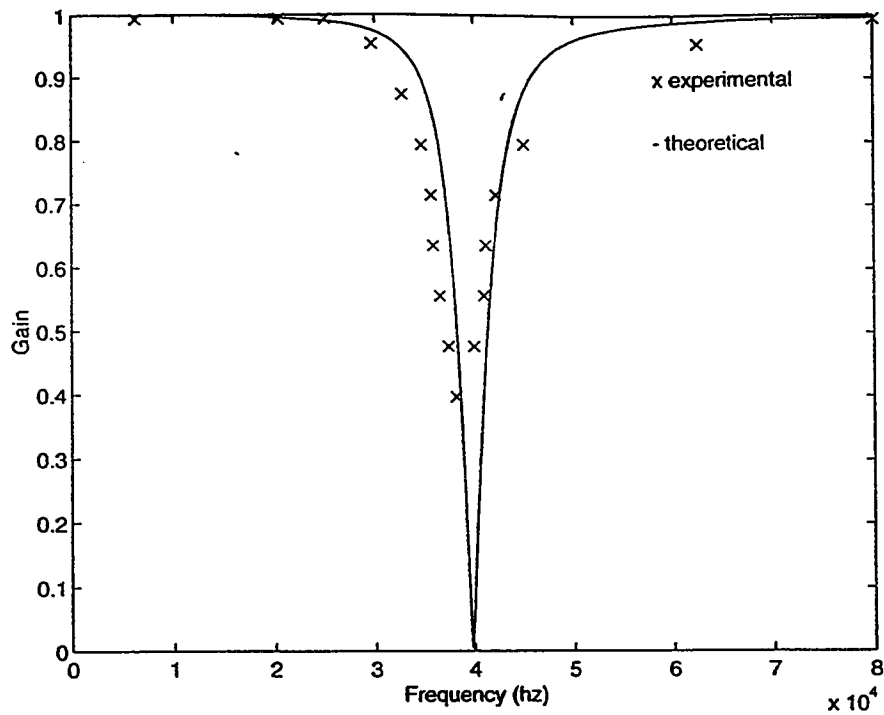
$$S_{\alpha_1}^{\frac{\omega_o}{Q_o}} = S_{\alpha_2}^{\frac{\omega_o}{Q_o}} = S_{\beta_2}^{\frac{\omega_o}{Q_o}} = S_{\gamma_1}^{\frac{\omega_o}{Q_o}} = S_{\gamma_2}^{\frac{\omega_o}{Q_o}} = 0$$

all of which are small.

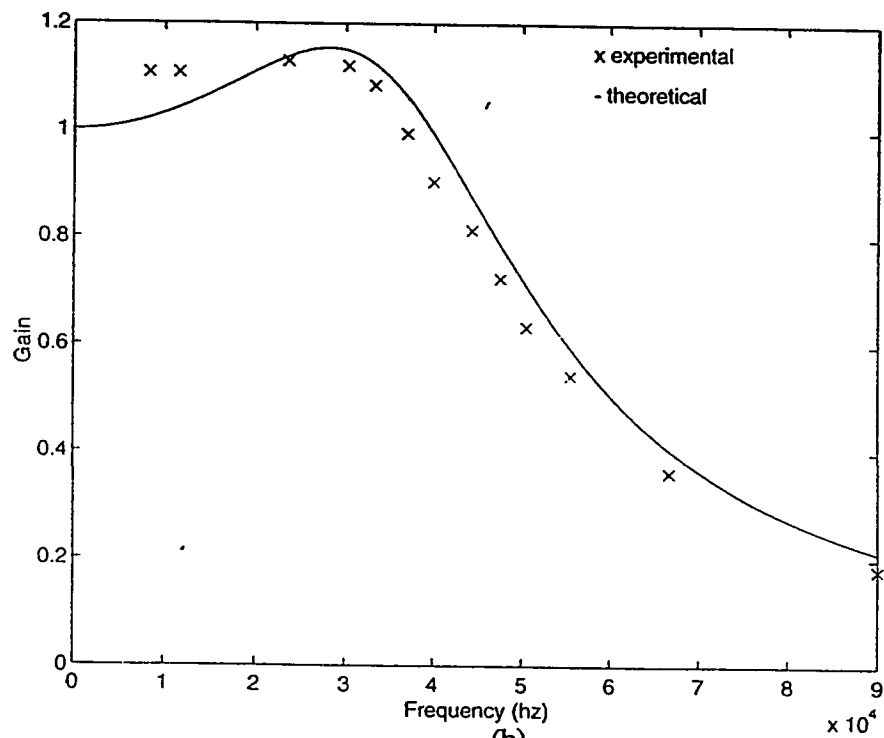
This filter has the following merits:

- (i) There are no requirements for critical component matching conditions to realize the five filter types.
- (ii) Orthogonal adjustment of ω_0 and ω_0/Q_0 can be achieved via R_3 , R_5 , C_1 or R_4 .
- (iii) It has less number of active components.
- (iv) The sensitivities of ω_0 and ω_0/Q_0 to passive and active components are small.
- (v) Very low output impedance which makes the voltage-mode circuit cascadable.
- (vi) It has a few number of floating elements (two resistors and one capacitor).

To demonstrate the practical behavior of the proposed circuit relative to the theoretical response, the circuit of Fig. 2.3 is examined as BR filter with $R_3=R_5=2K\Omega$, $R_4=15K\Omega$ and $C_1=C_2=2nF$ and as LP filter with $R_3=R_4=R_5=2K\Omega$, and $C_1=C_2=2nF$. The experiment result obtained using the CFOA AD844 and theoretical response are shown in Fig. 2.5.



(a)



(b)

Fig.2.5: Measured frequency response of :

(a) the BR filter

(b) the LP filter

2.3.2 Universal Voltage-mode Single Input Multiple Output Filter

Chang, Hwang and Tu have presented a voltage-mode universal filter in [11]. This filter offers the following advantages:

- (i) There are no requirements for component matching conditions.
- (ii) Orthogonal control of ω_0 and (ω_0/Q_0) can be done easily. That is to say ω_0 and (ω_0/Q_0) can be controlled independently.
- (iii) All the used capacitors are grounded.
- (iv) The sensitivities of ω_0 and ω_0/Q_0 to passive and active components are small.
- (v) Very low output impedance which makes the voltage-mode circuit cascadable.
- (vi) It realize three functions at the same time.

Despite these advantages, this filter has some disadvantages. It has floating resistors. Though ω_0 can be controlled without affecting ω_0/Q_0 , it is controlled by a capacitor. An extension work for this circuit is shown in Fig.2.6, where two more filters are realized. The price paid for realizing more functions here is the increase in the number of the active elements (CFOA).

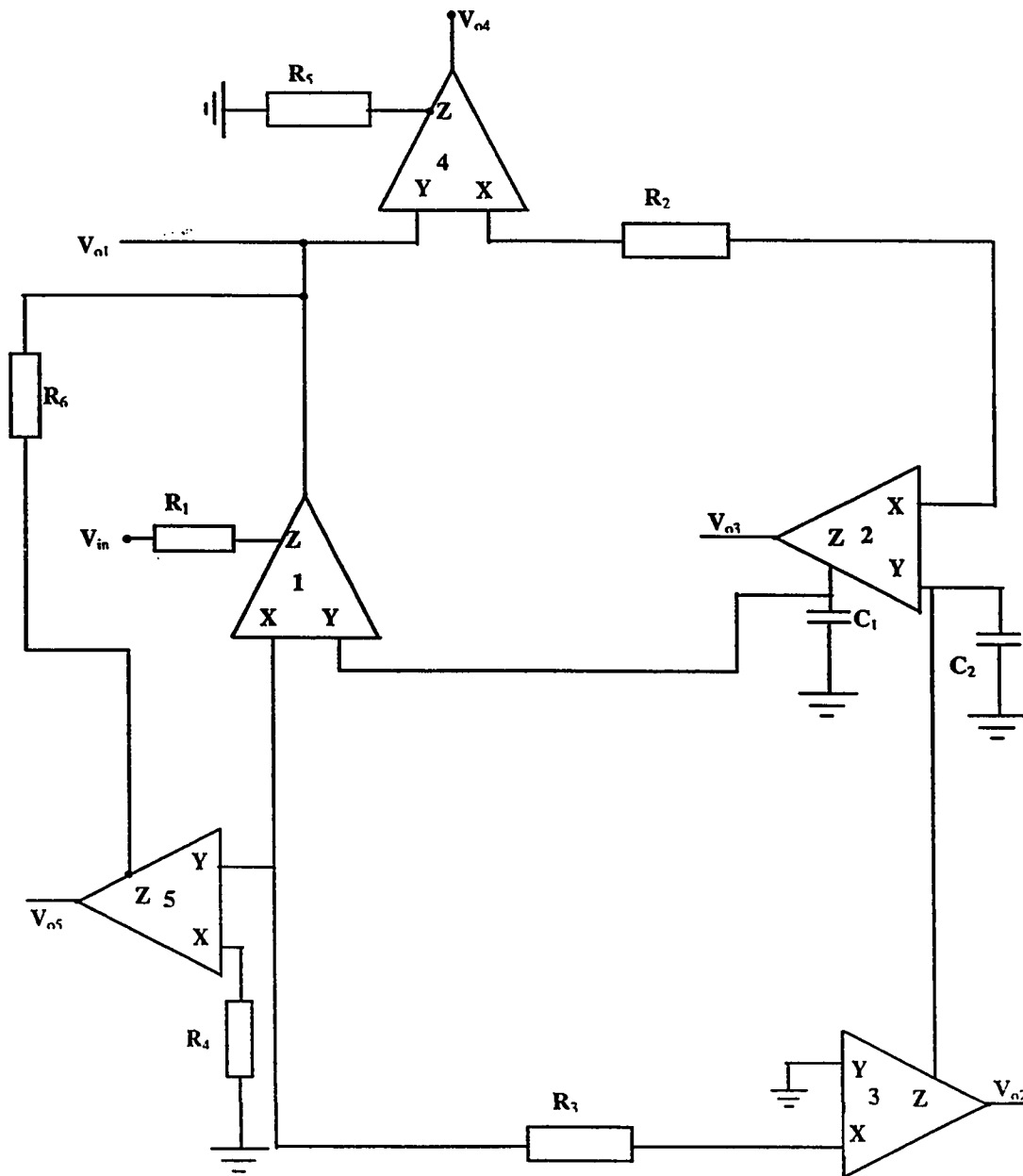


Fig. 2.6: Proposed universal voltage-mode filter (III)

A simple analysis for this circuit using the CFOA model of Fig.1.3 gives

$$\frac{V_{o1}}{V_{in}} = \frac{s^2 C_1 C_2 G_1 + G_1 G_2 G_3}{s^2 C_1 C_2 G_1 + s C_2 G_2 G_3 + G_1 G_2 G_3} \quad (2.18)$$

$$\frac{V_{o2}}{V_{in}} = \frac{G_1 G_2 G_3}{s^2 C_1 C_2 G_1 + s C_2 G_2 G_3 + G_1 G_2 G_3} \quad (2.19)$$

$$\frac{V_{o3}}{V_{in}} = \frac{-s G_2 G_3 C_2}{s^2 C_1 C_2 G_1 + s C_2 G_2 G_3 + G_1 G_2 G_3} \quad (2.20)$$

$$\frac{V_{o4}}{V_{in}} = \frac{s^2 C_1 C_2 G_3 G_2 G_5}{s^2 C_1 C_2 G_1 + s C_2 G_2 G_3 + G_1 G_2 G_3} \quad (2.21)$$

$$\frac{V_{o5}}{V_{in}} = \frac{s^2 C_1 C_2 G_1 - \frac{R_6}{R_4} s C_2 G_2 G_3 + G_1 G_2 G_3}{s^2 C_1 C_2 G_1 + s C_2 G_2 G_3 + G_1 G_2 G_3} \quad (2.22)$$

Where equations (2.18-22) represent the BR, LP, BP, HP and AP filters respectively.

R_6 should be equal to R_4 to realize the AP filter.

The center frequency ω_0 and the bandwidth ω_0/Q_0 are given by

$$\omega_0 = \left(\frac{G_2 G_3}{C_1 C_2} \right)^{1/2} \quad (2.23)$$

$$\frac{\omega_0}{Q_0} = \left(\frac{G_2 G_3}{C_1 G_1} \right) \quad (2.24)$$

The sensitivities of ω_o and ω_o/Q_o to passive components are

$$S_{G_2}^{\omega_o} = S_{G_3}^{\omega_o} = -S_{C_1}^{\omega_o} = -S_{C_2}^{\omega_o} = 1/2$$

$$S_{G_3}^{\frac{\omega_o}{Q_o}} = S_{G_2}^{\frac{\omega_o}{Q_o}} = -S_{C_1}^{\frac{\omega_o}{Q_o}} = -S_{C_2}^{\frac{\omega_o}{Q_o}} = 1$$

all of which are small.

Taking into account the voltage tracking error and the current tracking error the output voltage can be given by:

$$V_{oi} = \frac{\frac{\gamma_3}{\alpha_1 \alpha_2 \beta_1 \beta_2} s^2 C_1 C_2 G_1 + \frac{\gamma_3 \alpha_3}{\alpha_1 \gamma_1} G_1 G_2 G_3}{\frac{\gamma_3}{\alpha_1 \alpha_2 \gamma_1 \beta_1 \beta_2} s^2 G_1 C_1 C_2 + \frac{\gamma_3}{\beta_2} s C_2 G_2 G_3 + \frac{\gamma_3 \alpha_3}{\alpha_1 \gamma_1} G_1 G_2 G_3} \quad (2.25)$$

The center frequency ω_o and the bandwidth ω_o/Q_o are given by:

$$\omega_o = \left(\frac{G_2 G_3}{C_1 C_2} \right)^{\frac{1}{2}} (\alpha_2 \alpha_3 \beta_1 \beta_2)^{\frac{1}{2}} \quad (2.26)$$

$$\frac{\omega_o}{Q_o} = \left(\frac{G_2 G_3}{C_1 G_1} \right) (\alpha_1 \alpha_2 \gamma_1 \beta_1) \quad (2.27)$$

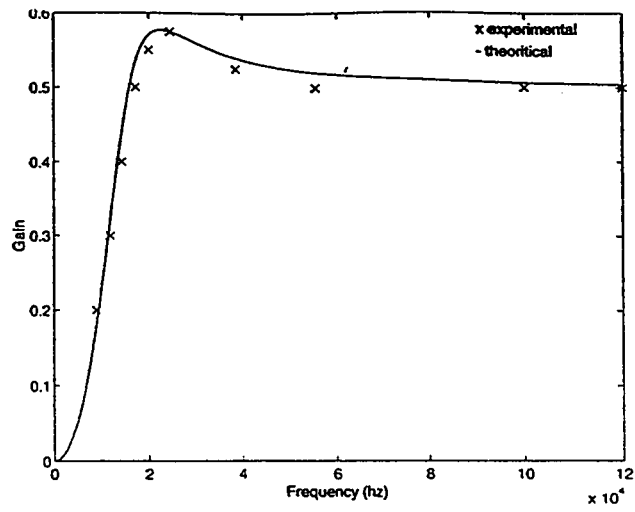
So, the sensitivities of ω_o and ω_o/Q_o to active components are

$$S_{\alpha_2}^{\omega_o} = S_{\alpha_3}^{\omega_o} = S_{\beta_1}^{\omega_o} = S_{\beta_2}^{\omega_o} = 1/2$$

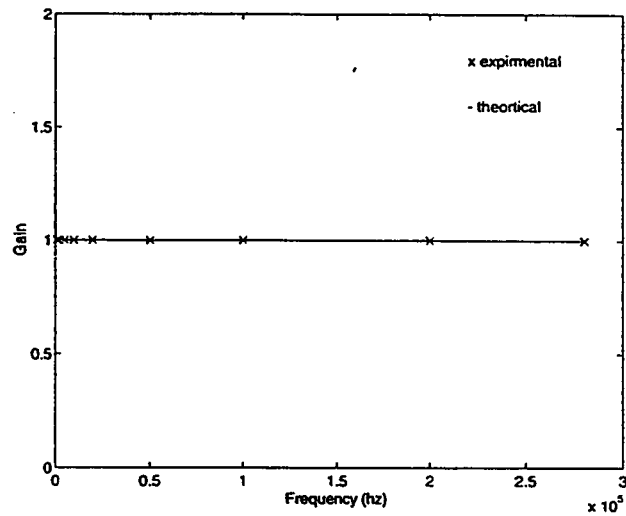
$$S_{\alpha_1}^{\frac{\omega_o}{Q_o}} = S_{\gamma_1}^{\frac{\omega_o}{Q_o}} = -S_{\alpha_2}^{\frac{\omega_o}{Q_o}} = -S_{\beta_1}^{\frac{\omega_o}{Q_o}} = 1$$

all of which are small.

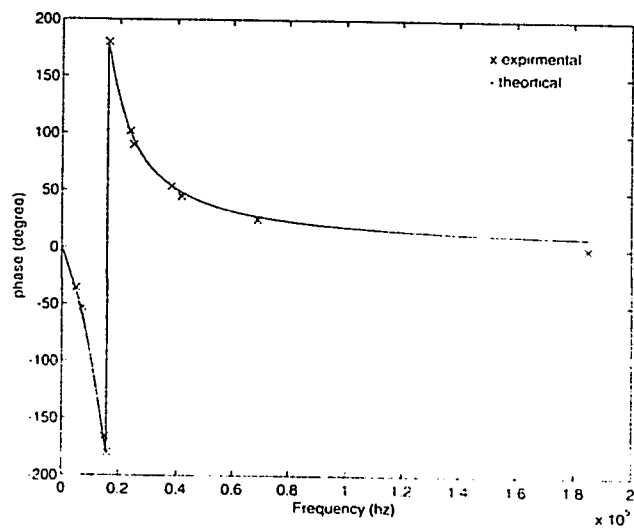
This filter has the same advantages and disadvantages of the universal filter in [11]. Fig 2.7 shows a comparison between the theoretical and the practical behaviors of the filter of Fig 2.6. The experimental results were obtained using the CFOA AD844 with $R_1=R_2=R_3=10\text{K}\Omega$, $C_1=C_2=1\text{nF}$, $R_5=5\text{K}\Omega$, and $R_4=R_6=4.6\text{K}\Omega$.



(a)



(b)



(c)

Fig.2.7: Comparison between theoretical and experimental results for
 (a) The HP filter
 (b) The magnitude of the AP filter
 (c) The phase of the AP filter

2.3.3. Universal Current-mode Multiple Inputs Single Output Filter

There is a growing interest in designing analogue current-mode signal processing circuits nowadays. In these circuits the current rather than the voltage is used as the active variable either throughout the whole circuit or only in certain critical areas. The use of current as the active parameter can result in circuits operating with higher signal bandwidths, greater linearity and larger dynamic range than voltage mode circuits.[16]

It is usual to realize a high-order filter by cascading the first-and second-order filters. One of the obvious advantages of the current-mode approach is that it can easily cascade the current- mode filters without additional matching circuits. There are many circuits that can realize universal current-mode filter using VOA or current conveyer.

A new universal current-mode filter employing only two CFOA is shown in Fig 2.8. Fig.2.9 shows how a current source can be generated from a voltage source.

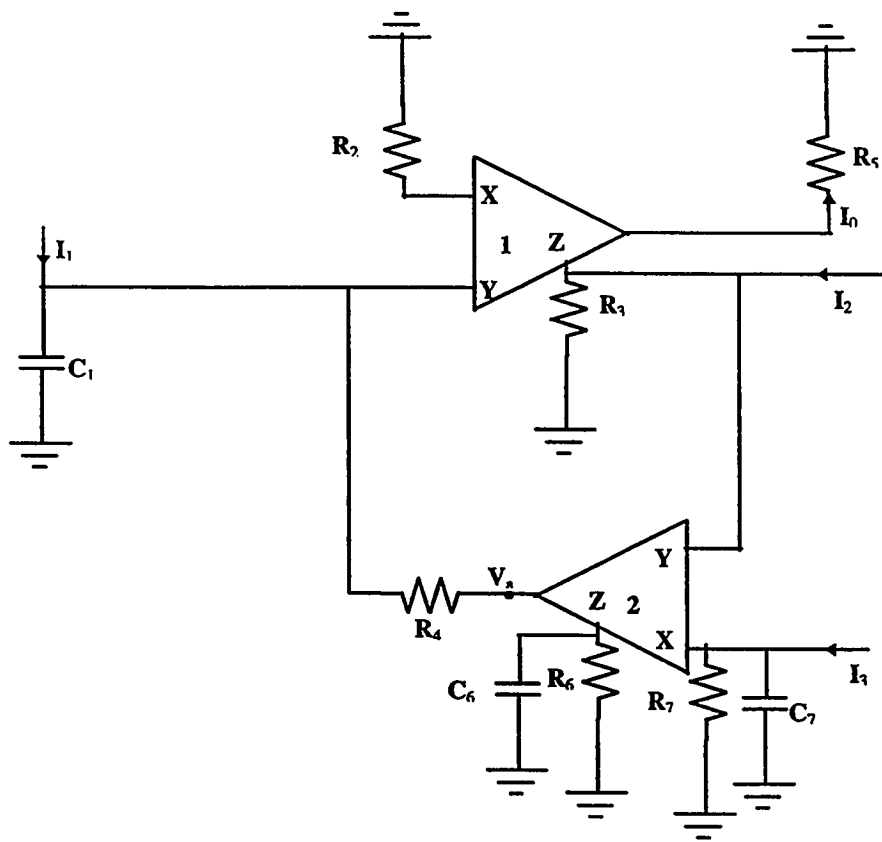


Fig.2.8: Proposed universal current -mode filter (I)

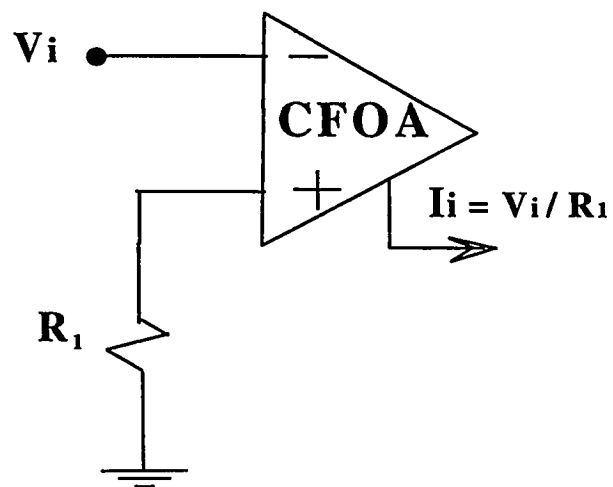


Fig.2.9. Voltage to current converter

Using the CFOA model of Fig.1.3, routine analysis for Fig.2.8 yields

$$I_0 = \frac{I_2[s^2 G_5 C_1 C_6 + s(G_6 G_5 C_1 + G_4 G_5 C_6) + G_4 G_5 G_6] - I_3[G_4 G_5 G_2] + I_1[s G_5 G_2 C_6 + G_5 G_2 G_6]}{s^2(G_3 C_6 C_1) + s(G_3 G_6 C_1 + G_3 G_4 C_6 - G_4 G_2 C_7) + (G_3 G_6 G_4 - G_4 G_2 G_7)} \quad (2.28)$$

Specializations of the numerator in equation (2.28) result in the following filter functions.

$$\text{For } G_2 = 2 G_4 = 2 G_6$$

$$\text{and } C_6 = C_1$$

(i) Lowpass:

$$I_2 = I_1 = 0, I_3 = \text{input current signal.}$$

(ii) Highpass:

$$-I_1 = I_2 = -1/2 I_3 = \text{input current signal}$$

(iii) Bandpass:

$$I_3 = I_1 = \text{input current signal}$$

(iv) Band reject:

$$-I_1 = I_3 = I_2 = \text{input current signal}$$

(v) Allpass:

$$-I_1 = I_2 = \text{input current signal}$$

But, it needs additional conditions:

$$G_5 = G_3 = G_4, G_7 = G_6 \text{ and } C_7 = C_6$$

From equation (2.28) the center frequency ω_0 and the bandwidth ω_0/Q_0 are given by

$$\omega_0 = \left(\frac{G_3 G_6 G_4 - G_4 G_2 G_7}{G_3 C_6 C_1} \right)^{1/2} \quad (2.29)$$

$$\frac{\omega_0}{Q_0} = \frac{G_3 G_6 C_1 + G_3 G_4 C_6 - G_4 G_2 C_7}{G_3 G_6 C_1} \quad (2.30)$$

From equations (2.29) and (2.30) it is obvious that ω_0 can be adjusted by changing R_7 without disturbing the parameter ω_0/Q_0 .

So, the sensitivities of ω_0 and ω_0/Q_0 to passive components are

$$S_{C_6}^{\omega_0} = S_{C_1}^{\omega_0} = -S_{G_4}^{\omega_0} = -\frac{1}{2}$$

$$S_{G_6}^{\omega_0} = -S_{G_2}^{\omega_0} = \frac{1}{2} \frac{G_2 G_7}{G_3 G_6 - G_2 G_7}, \quad S_{G_6}^{\omega_0} = \frac{1}{2} \frac{G_6 G_3}{G_3 G_6 - G_2 G_7}$$

$$S_{C_1}^{\frac{\omega_0}{Q_0}} = \frac{-G_3 G_4 C_6 + G_4 G_2 C_7}{G_3 G_6 C_1 + G_3 G_4 C_6 - G_4 G_2 C_7}$$

$$S_{G_6}^{\frac{\omega_0}{Q_0}} = \frac{G_6 G_3 C_1}{G_3 G_6 C_1 + G_3 G_4 C_6 - G_4 G_2 C_7}$$

$$S_{G_3}^{\frac{\omega_0}{Q_0}} = \frac{G_4 G_2 C_7}{G_3 G_6 C_1 + G_3 G_4 C_6 - G_4 G_2 C_7}$$

$$S_{G_4}^{\frac{\omega_0}{Q_0}} = \frac{G_4 G_3 C_6 - G_2 G_4 C_7}{G_3 G_6 C_1 + G_3 G_4 C_6 - G_4 G_2 C_7}$$

$$S_G^{\frac{\omega_0}{Q_0}} = \frac{-G_4 G_2 C_7}{G_3 G_6 C_1 + G_3 G_4 C_6 - G_4 G_2 C_7}$$

$$S_{C_6}^{\frac{\omega_0}{Q_0}} = \frac{-G_6 G_3 C_1 + G_4 G_2 C_7}{G_3 G_6 C_1 + G_3 G_4 C_6 - G_4 G_2 C_7}$$

For $G_3 \geq 4G_7$

and

$$G_3C_6 \geq 2G_2C_7$$

the sensitivities of ω_0 and ω_0/Q_0 to passive components are small (≤ 1).

Taking into account the voltage tracking error and the current tracking error the output

current of equation (2.28) can be expressed by

$$I_0 = \frac{I_2[s^2G_5C_1C_6 + s(G_6G_5C_1 + G_4G_5G_6) + G_4G_5G_6] \frac{1}{\alpha_1\beta_1} - I_3[G_4G_5G_2]\gamma_2\alpha_2 - I_1[sG_5G_2C_6 + G_5G_2G_6]}{s^2 \frac{(G_3C_6C_1)}{(\gamma_1\alpha_1\beta_1)} + s \left[\frac{(G_3G_6C_1 + G_3G_4C_6)}{\gamma_1\alpha_1\beta_1} - \frac{(G_4G_2C_7)(\gamma_2\beta_2\alpha_2)}{\gamma_1} \right] + \left[\frac{(G_3G_6G_4)}{\gamma_1\alpha_1\beta_1} - \frac{(G_4G_2C_7)(\gamma_2\beta_2\alpha_2)}{\gamma_1} \right]}$$

(2.31)

From equation (2.31) the center frequency ω_0 and ω_0/Q_0 are given by

$$\omega_0 = \left(\frac{(G_3G_6G_4) - (G_4G_2G_7)(\alpha_1\alpha_2\gamma_2\beta_1\beta_2)}{G_3C_6C_1} \right)^{1/2} \quad (2.32)$$

$$\frac{\omega_0}{Q_0} = \frac{(G_3G_6C_1 + G_3G_4C_6) - (G_4G_2C_7)(\alpha_1\alpha_2\gamma_2\beta_1\beta_2)}{G_3C_6C_1} \quad (2.33)$$

So, the sensitivities of ω_0 and ω_0/Q_0 to active components are

$$S_{\alpha_1}^{\omega_0} = S_{\alpha_2}^{\omega_0} = S_{\gamma_2}^{\omega_0} = S_{\beta_1}^{\omega_0} = S_{\beta_2}^{\omega_0} = -\frac{1}{2} \frac{(G_4G_2G_7)(\alpha_1\alpha_2\gamma_2\beta_1\beta_2)}{(G_3G_6G_4) - (G_4G_2G_7)(\alpha_1\alpha_2\gamma_2\beta_1\beta_2)}$$

$$S_{\alpha_1}^{\omega_o} = S_{\alpha_2}^{\omega_o} = S_{\gamma_2}^{\omega_o} = S_{\beta_1}^{\omega_o} = S_{\beta_2}^{\omega_o} = \frac{-(G_4 G_2 G_7)(\alpha_1 \alpha_2 \gamma_2 \beta_1 \beta_2)}{(G_3 G_6 G_4) - (G_4 G_2 G_7)(\alpha_1 \alpha_2 \gamma_2 \beta_1 \beta_2)}$$

For $(G_4 G_2 G_7)(\alpha_1 \alpha_2 \gamma_2 \beta_1 \beta_2) \gg G_3 G_6 G_4$

the sensitivities of ω_o and ω_o/Q_o to active components are small

This filter has many advantages.

- (i). Orthogonal adjustment of ω_o and ω_o/Q_o can be done via C_7 and R_7 .
- (ii). It has a low number of active components.
- (iii). All used capacitor are grounded.
- (iv). It has a few number of floating elements.

However, the major disadvantage of this circuit is requiring matching conditions to realize the different filter functions. Also it employs nine passive elements.

To verify the theoretical prediction of the proposed network, LP and BP filter prototypes have been realized. The calculated and measured frequency response using the CFOA AD844 of the LP and BP filters are shown in Fig.2.10.

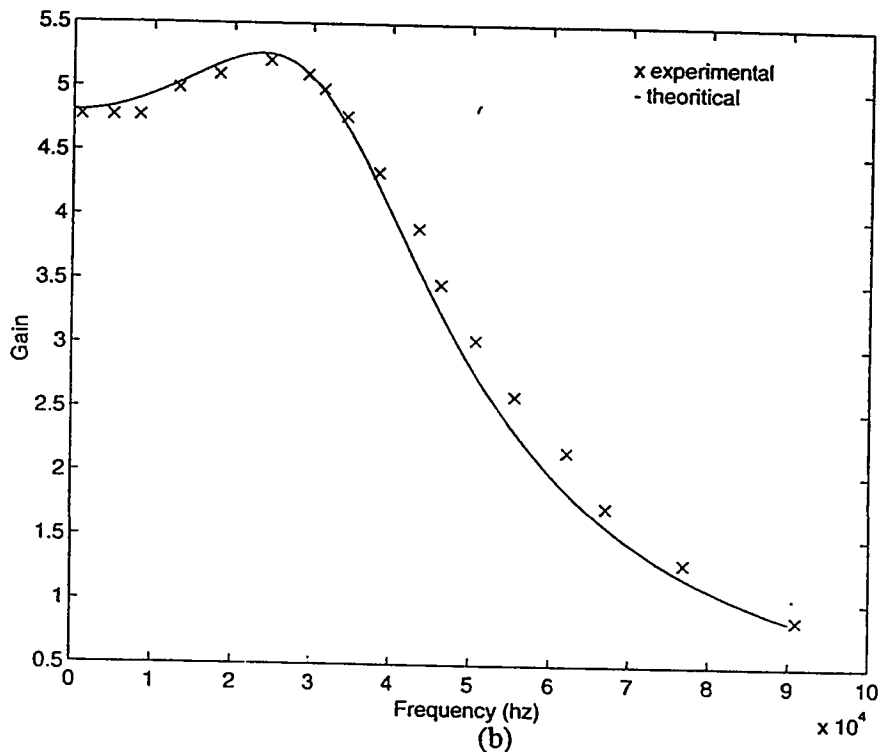
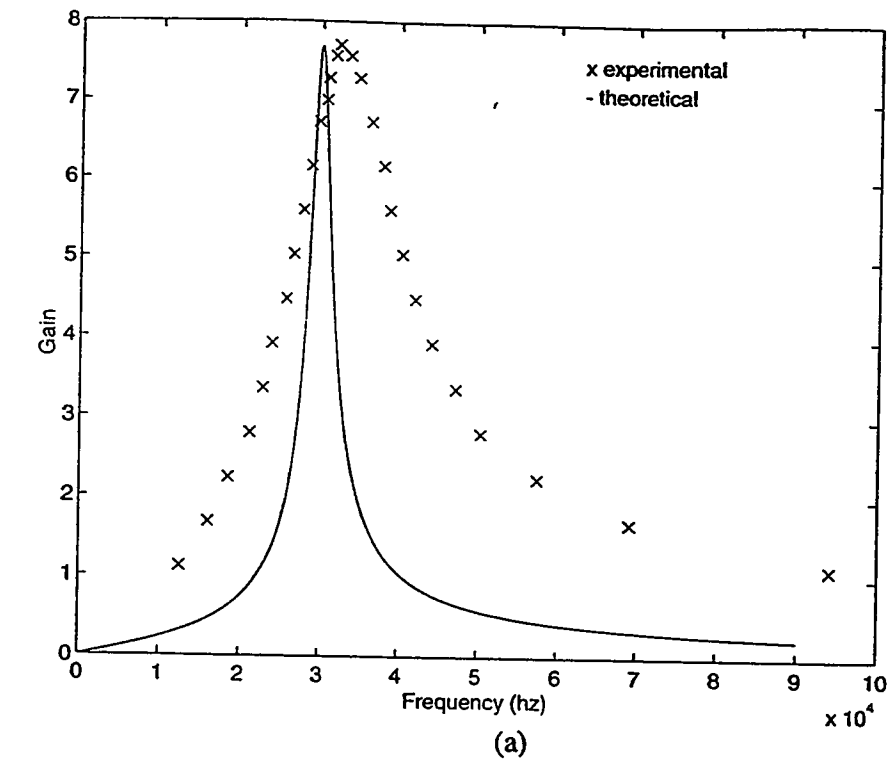


Fig.2.10: Comparisons between theoretical and experimental results for the BP and LP filter

a)BP: $R_2=1500\Omega$, $R_3=R_4=R_6=1970\Omega$, $R_5=1964\Omega$, $R_7=3000\Omega$, $C_1=C_6=1nF$, $C_7=1.5nF$

b)LP: $R_2=1968\Omega$, $R_3=1970\Omega$, $R_4=1967\Omega$, $R_5=1964\Omega$,
 $R_6=1970\Omega$, $R_7=2493\Omega$, $C_1=C_6=1nF$, $C_7=1.5nF$

Specializations of the numerator in equation (2.34) result in the following filter function:

(i) Lowpass:

$$I_2 = I_1 = 0, I_3 = \text{input current signal.}$$

(ii) Highpass:

$$\begin{aligned} & \text{If } G_4 = G_2 \\ I_2 = I_1 &= \text{input current signal} \\ I_3 &= 0 \end{aligned}$$

(iii) Bandpass:

$$\begin{aligned} I_3 = I_2 &= 0 \\ I_1 &= \text{input current signal} \end{aligned}$$

(iv) Band-notch:

$$\begin{aligned} & \text{If } G_4 = G_2 \\ I_1 = I_2 = I_3 &= \text{input current signal} \end{aligned}$$

(v) Allpass:

$$\begin{aligned} & \text{If } G_5 = G_3 = G_4 = G_7 \\ & C_7 = C_6 \\ -I_1 = I_2 = I_3 &= \text{input current signal} \end{aligned}$$

From equation (2.34) the center frequency ω_o and the bandwidth (ω_o/Q_o) are given by

$$\omega_o = \left(\frac{G_4 G_2 G_7}{G_3 C_6 C_1} \right)^{1/2} \quad (2.35)$$

$$\frac{\omega_o}{Q_o} = \left(\frac{G_3 G_4 C_6 + G_4 G_2 C_7}{G_3 C_6 C_1} \right) \quad (2.36)$$

So, the sensitivities of ω_o and (ω_o/Q_o) for passive components are

$$S_{G_4}^{\omega_o} = S_{G_2}^{\omega_o} = S_{G_7}^{\omega_o} = -S_{G_3}^{\omega_o} = -S_{C_6}^{\omega_o} = -S_{C_1}^{\omega_o} = \frac{1}{2}$$

$$S_{G_4}^{\frac{\omega_o}{Q_o}} = -S_{C_1}^{\frac{\omega_o}{Q_o}} = 1$$

$$S_{G_2}^{\frac{\omega_o}{Q_o}} = S_{C_7}^{\frac{\omega_o}{Q_o}} = -S_{G_3}^{\frac{\omega_o}{Q_o}} = -S_{C_6}^{\frac{\omega_o}{Q_o}} = \frac{G_4 G_2 C_7}{G_2 G_4 C_6 + G_4 G_2 C_7}$$

all of which are small.

Taking into account the voltage tracking error and the current tracking error equation

(2.34) reduces to:

$$I_o = \frac{I_2 \gamma_1 \beta_2 (s^2 G_5 C_1 C_6 + s G_4 G_5 C_6) + I_3 \alpha_1 \alpha_2 \alpha_3 \gamma_1 \beta_2 [G_4 G_5 G_2] - I_1 \alpha_1 \alpha_2 \gamma_1 \beta_2 [s G_5 G_2 C_6]}{s^2 G_3 C_6 C_1 + s (G_3 G_4 C_6 + G_4 G_2 C_7 \alpha_1 \alpha_2 \alpha_3 \beta_2 \beta_3) + G_4 G_2 G_7 \alpha_1 \alpha_2 \alpha_3 \beta_2 \beta_3} \quad (2.37)$$

From equation (2.37) the center frequency ω_o and the bandwidth (ω_o/Q_o) are given by

$$\omega_o = \left(\frac{G_4 G_2 G_7}{G_3 C_6 C_1} \right)^{1/2} (\alpha_1 \alpha_2 \alpha_3 \beta_2 \beta_3)^{\frac{1}{2}} \quad (2.38)$$

$$\frac{\omega_o}{Q_o} = \left(\frac{G_3 G_4 C_6 + G_4 G_2 C_7 (\alpha_1 \alpha_2 \alpha_3 \beta_2 \beta_3)}{G_3 C_6 C_1} \right) \quad (2.39)$$

So, the sensitivities of ω_o and ω_o/Q_o to active components are

$$S_{\alpha_1}^{\omega_o} = S_{\alpha_2}^{\omega_o} = S_{\alpha_3}^{\omega_o} = S_{\beta_2}^{\omega_o} = S_{\beta_3}^{\omega_o} = \frac{1}{2}$$

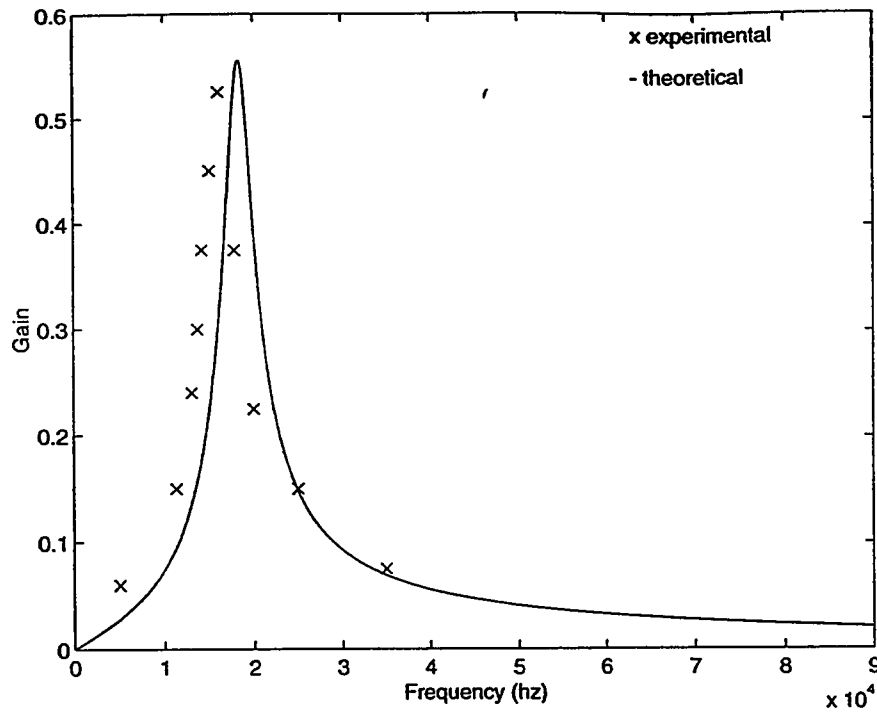
$$S_{\alpha_1}^{\frac{\omega_o}{Q_o}} = S_{\alpha_2}^{\frac{\omega_o}{Q_o}} = S_{\alpha_3}^{\frac{\omega_o}{Q_o}} = S_{\beta_2}^{\frac{\omega_o}{Q_o}} = S_{\beta_3}^{\frac{\omega_o}{Q_o}} = \frac{G_4 G_2 C_7 (\alpha_1 \alpha_2 \alpha_3 \beta_2 \beta_3)}{G_3 G_4 C_6 + G_4 G_2 C_7 (\alpha_1 \alpha_2 \alpha_3 \beta_2 \beta_3)}$$

all of which are small.

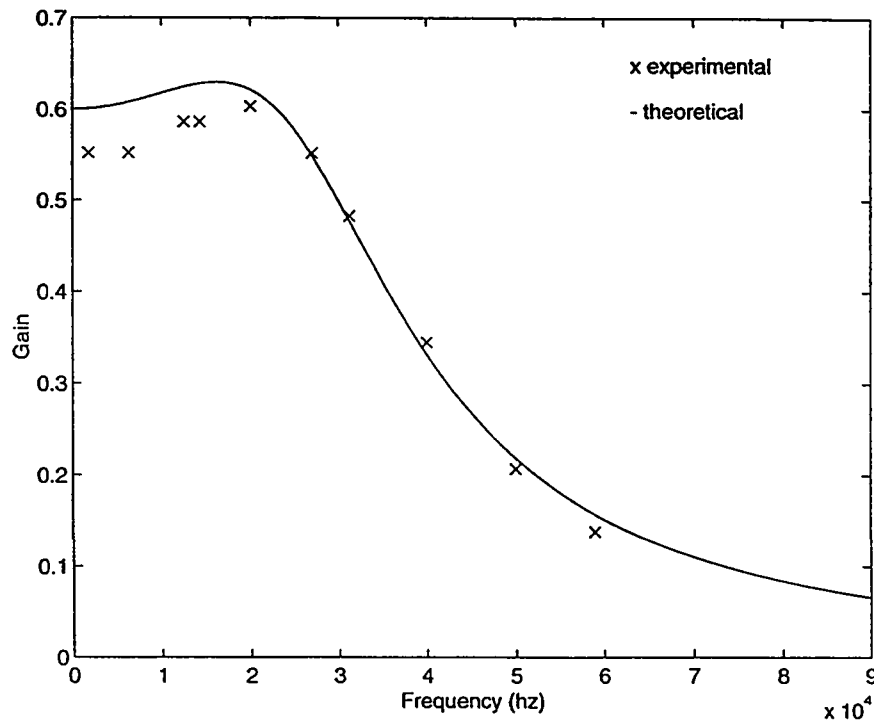
This circuit has the same advantages of the previous one. In addition, it has low sensitivities to passive and active components and less number of passive elements. Moreover, this circuit requires simpler matching conditions than the previous one.

Despite of the advantages of this circuits, the main drawback is using three CFOA rather than the two CFOAs used in the previous circuit.

To verify the theoretical analysis, the proposed universal filter of Fig.2.11 was implemented using a commercial CFOA AD844. Fig.2.12 shows comparison between the experimental and theoretical results.



(a)



(b)

Fig.2.12: Comparison between the theoretical and experimental results for the BP and LP filters

a)BP: $R_2 = R_4 = 10k\Omega$, $R_3 = 2k\Omega$, $R_5 = 3k\Omega$, $R_7 = 250\Omega$, $C_1 = 6nF$, and $C_6 = C_7 = 1nF$

b)LP: $R_3 = R_4 = 10k\Omega$, $R_5 = 3k\Omega$, $R_2 = R_7 = 1800\Omega$, and $C_1 = C_6 = C_7 = 3nF$

In conclusion, we have seen in this chapter that in some cases the experimental results deviate from the theoretical response. For example, for the BP of Fig.2.2 calculated ω_0 is equal to 16.5×10^4 rad and the measured ω_0 is equal to 17.59×10^4 rad thus the error is equal to 6.4%. Also for the BR of Fig.2.4 the calculated ω_0 is equal to 24.1×10^4 rad and the measured ω_0 is equal to 24.99×10^4 rad, thus the error is equal to 3.6%. For the BP of Fig.2.8 the calculated ω_0 is equal to 18.8×10^4 rad and the measured ω_0 is equal to 20.2×10^4 rad thus the error is equal to 7.2%. So, it is conjectured that, the nonideality of the CFOA is the main source for this deviation. To investigate this conjecture, the effect of the CFOA nonidealities will be discussed in chapter 4.

Chapter 3

Oscillators and Signal Generators

3.1 Introduction

Signals having standard waveforms are used extensively in designing and testing electronic systems. There are three basic waveforms: the sinusoidal, square wave and the ramp. Signal generator circuits built around the VOA have been used for a long time. But, due to its better performance, compared to the VOA, the CFOA has been found to be useful in various applications[1]. In this chapter the design of new CFOA based signal generators will be investigated.

New CFOA based sinusoidal oscillator circuits are presented in Sec.3.3 and in Sec.3.4 a new signal generator circuit using the CFOA is presented.

3.2 How to evaluate an oscillator?

There are many points to be taken in consideration to evaluate an oscillator.

- i) In order to control frequency of oscillation (ω_o) and condition of oscillation (C.O.) independently, there should be at least one term not common for both ω_o and C.O.
- ii) All capacitors should be grounded and minimum number of resistor's should be floating.
- iii) It will be a great advantage for the oscillator if ω_o especially and the C.O. can be controlled via grounded resistors. This situation will help to build a programmable oscillator by replacing these resistors by programmable resistors, for example a JFET transistor.
- iv) The oscillator has high efficiency from economic point of view (in terms of area and power consumption) if it has minimum numbers of active and passive components.
- v) The sensitivity of the frequency of oscillation (ω_o) to passive and active components should be as low as possible and it shouldn't exceed 1.

3.3 Sinusoidal Oscillators

Several sinusoidal oscillator circuits using CFOA have been developed recently. Shen, Chung and Dong have reported sinusoidal oscillators in [13]. The oscillation frequency and the condition of oscillation of the proposed sinusoidal oscillators can be controlled by a resistor or capacitor independently. In addition the oscillation frequency of one of the proposed sinusoidal oscillators is insensitive to the input and output voltage tracking errors of the CFOA. Moreover, one of the proposed oscillators uses grounded capacitors. Passive and active sensitivities are all low for these oscillators. In [14] three new sinusoidal oscillators using the current feedback amplifier pole are presented. Two of the proposed sinusoidal oscillators consist of CFOAs and resistors without external capacitors. Their oscillation condition and frequency can be independently controlled by two resistors. The third proposed oscillator uses the CFOA pole and one capacitor. But its oscillation frequency can not be independently controlled. Celma, Pedro and Carlosena proposed a new sinusoidal oscillator using the CFOA in [9]. This circuit enjoys independent control of the frequency of oscillation and the condition of oscillation. Unfortunately, this circuit has a floating capacitor. Also, this circuit requires matching conditions to oscillate.

3.3.1 Sinusoidal Oscillator Exploiting the Pole of the CFOA

The circuits proposed in this section exploit the internal pole of the CFOA to advantage. One of the main advantages of using CFOA's pole in designing oscillators is to reduce the requirement for physical capacitances.

A new oscillator structure using the CFOAs pole is shown in Fig.3.1[17]. The equivalent circuit of this oscillator structure is shown in Fig.3.2 where the dotted box represents a simplified equivalent circuit for the CFOA [20]. In this equivalent circuit r_i and r_o represent the output resistances of the unity-gain buffers A_1 and A_2 respectively, C_T is the internally-connected compensation capacitor [18] and R_T is the internal resistance of the gain node [19]. Assuming ideal CFOA with $r_i = r_o = 0$, routine analysis yields the characteristic equation of the circuit of Fig.3.1 which can be expressed as

$$Y_3 + Y_4 = A(s)(Y_1Y_4 - Y_2Y_3) \quad (3.1)$$

In (3.1), $A(s)$ is the transimpedance of the CFOA and can be expressed as

$$A(s) = \frac{A_o \omega_1}{s + \omega_1} \quad (3.2)$$

where A_o is the zero-frequency transimpedance and $\omega_1 = 1/R_T C_T$ is the pole of the transimpedance-frequency characteristic. Combining (3.1) and (3.2) the characteristic equation becomes

$$(s + \omega_1)(Y_3 + Y_4) = A_o \omega_1 (Y_1 Y_4 - Y_2 Y_3) \quad (3.3)$$

Using (3.3), several oscillator circuits can be derived. In deriving these oscillator circuits it must be noted that pure capacitive feedback between the output and the inverting input of the CFOA is not allowed [2]. Thus a resistive feedback path must also exist in order to ensure predictable operation of the oscillator circuit. Five possible oscillator circuits are shown in Fig.3.3. The frequency and the condition of oscillation of these five circuits are shown in Table 3.1. From Table 3.1 one can see that the frequency of oscillation of the circuit of Fig. 3.3(c) can be adjusted by tuning the capacitor C_2 without disturbing the condition of oscillation while the condition of oscillation can be adjusted by tuning the resistor R_2 without disturbing the frequency of oscillation. From Table 3.1 one can also see that the frequency of oscillation of the circuit of Fig.3.3(d) and 3.3(e) can be adjusted by tuning the resistor R_2 without disturbing the condition of oscillation, while the condition of oscillation can be adjusted by tuning the capacitor R_1 without disturbing the frequency of oscillation. Thus the circuits of Fig.3.3(c),(d) and (e) enjoy the attractive feature of independent control of the frequency and the condition of oscillation. From Table 3.1 one can also see that the frequencies of oscillation of the circuits of Fig.3.3(a) and (b) can not be

adjusted without disturbing the conditions of oscillation. These circuits are, therefore, suitable for realizing single frequency oscillators. It is also interesting to note that the circuit of Fig.3.3(a) uses grounded capacitors. This is an attractive feature for integration.

Finally, the sensitivity of the frequency of oscillation (ω_0) to the passive elements of the circuits of Table I is $\leq (1/2)$.

Thus the proposed circuits enjoy low passive sensitivities.

Taking into account the voltage and current tracking errors, Table 3.2 shows the frequency of oscillation and its sensitivities to active elements for the circuits of Fig.3.3.

Experimental Results

The proposed circuits of Fig.3.3 were experimentally tested using the AD844 CFOA. A sample of the results obtained is shown in Fig.3.4. Frequencies of oscillation up to 27.5 MHz with a peak-to-peak voltage of 2-9 V were successfully obtained with a dc supply voltage of $\pm 15V$. Fig.3.5 shows comparison between the theoretical and experimental behavior for the circuits of Fig.3.3(d) and (e).

Table 3.1 Frequency and condition of oscillation of the Circuits of Fig.3.4.

Circuit	Frequency of Oscillation ω_0^2	Condition of oscillation	Control Element of ω_0
a	$\frac{\omega_1(R_2(R_3 + R_4) + A_o R_4)}{C_3 R_2 R_3 R_4}$	$A_o \omega_1 \left(\frac{C_1}{R_4} - \frac{C_3}{R_2} \right) = \omega_1 C_3 + \frac{1}{R_3} + \frac{1}{R_4}$	-
b	$\frac{\omega_1}{(C_3 + C_4) R_3} \left(1 + \frac{A_o}{R_2} \right)$	$A_o \omega_1 \left(\frac{C_4}{R_1} - \frac{C_3}{R_2} \right) = \omega_1 (C_3 + C_4) + \frac{1}{R_3}$	-
c	$\frac{\omega_1}{C_3 R_4 (1 + A_o \omega_1 C_2)}$	$A_o \omega_1 (C_1 R_2 - C_3 R_4) = R_2 (1 + \omega_1 C_3 R_4).$	C_2
d	$\frac{\omega_1}{C_4 R_3} \left(1 + \frac{A_o}{R_2} \right)$	$A_o \omega_1 (C_4 R_3 - C_2 R_1) = R_1 (1 + \omega_1 C_4 R_3).$	R_2
e	$\frac{\omega_1}{C_4 R_3} \left(1 + \frac{A_o}{R_2} \right)$	$A_o \omega_1 \left(\frac{C_4}{R_1} \right) = \omega_1 C_4 + \frac{1}{R_3}$	R_2

Table 3.2 Frequency of oscillation and its sensitivities to active elements

Circuit	Frequency of Oscillation ω_o^2	Sensitivity of ω_o to active elements
a	$\frac{R_2(R_3 + R_4)\omega_1 + A_o\omega_1\alpha\gamma(R_3 + R_4 - \beta R_1)}{C_3R_3R_2R_4}$	$S_{\alpha}^{\omega_o} = S_{\gamma}^{\omega_o} = \frac{1}{2} \frac{A_o\alpha\gamma(R_3 + R_4 - \beta R_1)}{R_1(R_3 + R_4)\omega_1 + A_o\omega_1\alpha\gamma(R_3 + R_4 - \beta R_1)}$ $S_{\beta}^{\omega_o} = -\frac{1}{2} \frac{A_o\alpha\gamma\beta R_1}{R_1(R_3 + R_4)\omega_1 + A_o\omega_1\alpha\gamma(R_3 + R_4 - \beta R_1)}$
b	$\frac{\omega_1}{R_3(C_4 + C_3)} \left(1 + \frac{\gamma\alpha A_o}{R_2} \right)$	$S_{\alpha}^{\omega_o} = S_{\gamma}^{\omega_o} = \frac{1}{2} \frac{\alpha\gamma A_o G_2}{1 + \alpha\gamma A_o G_2}$ $S_{\beta}^{\omega_o} = 0$
c	$\frac{\omega_1(1 + \alpha\gamma A_o G_2(1 - \beta))}{R_4 C_3(1 + \alpha\gamma A_o \omega_1 C_2)}$	$S_{\alpha}^{\omega_o} = S_{\gamma}^{\omega_o} = \frac{1}{2} \frac{\alpha\gamma A_o(G_2(1 - \beta) - \omega_1 C_2)}{1 + \alpha\gamma A_o G_2(1 - \beta)}$ $S_{\beta}^{\omega_o} = -\frac{1}{2} \frac{\alpha\gamma\beta A_o G_2}{1 + \alpha\gamma A_o G_2(1 - \beta)}$
d	$\frac{\omega_1(1 + \alpha\gamma A_o G_2)}{R_3 C_4(1 + \alpha\gamma A_o \omega_1 C_2(1 - \beta))}$	$S_{\alpha}^{\omega_o} = S_{\gamma}^{\omega_o} = \frac{1}{2} \frac{\alpha\gamma A_o(G_2 - \omega_1 C_2(1 - \beta))}{1 + \alpha\gamma A_o G_2}$ $S_{\beta}^{\omega_o} = \frac{1}{2} \frac{\alpha\gamma\beta A_o \omega_1 C_2}{1 + \alpha\gamma A_o \omega_1 C_2(1 - \beta)}$
e	$\frac{\omega_1(1 + \alpha\gamma A_o G_2)}{R_3 C_4}$	$S_{\alpha}^{\omega_o} = S_{\gamma}^{\omega_o} = \frac{1}{2} \frac{\alpha\gamma A_o G_2}{1 + \alpha\gamma A_o G_2}$ $S_{\beta}^{\omega_o} = 0$

In general all the sensitivities of ω_o to active elements of all the circuits are low except for some cases. This problem can be solved by proper selection of passive element's value, for example, for circuit (a), low $S_{\beta}^{\omega_o}$ sensitivity can be realized if $R_4 \gg R_3$.

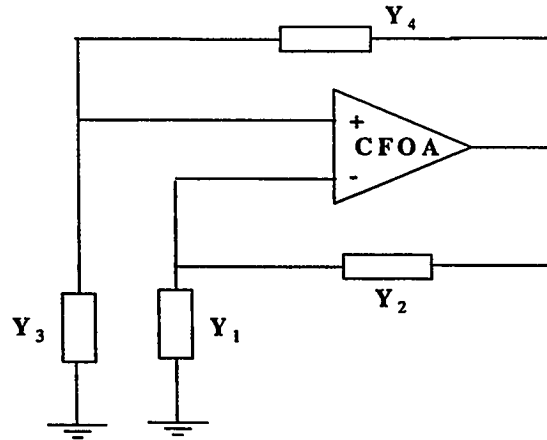


Fig.3.1 Proposed Oscillator structure

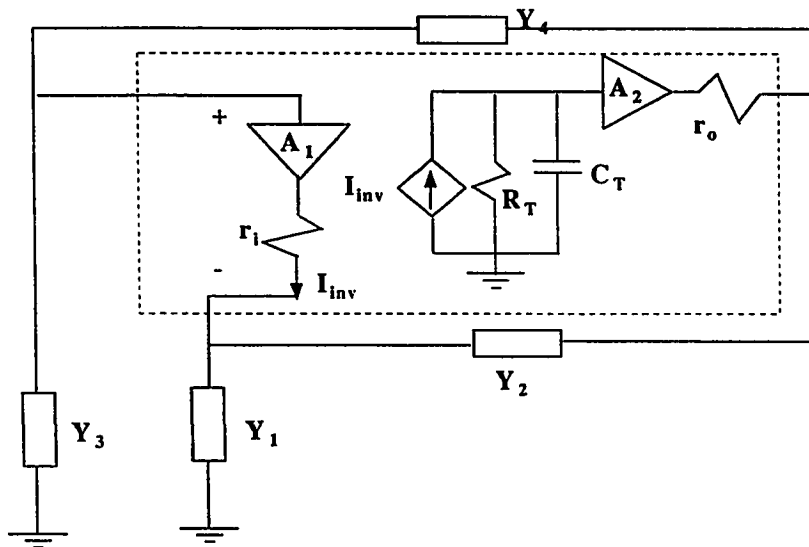


Fig.3.2 Equivalent Circuit of the Oscillator structure of Fig.3.1. The circuit inside the dotted box is a simplified equivalent circuit for the CFOA

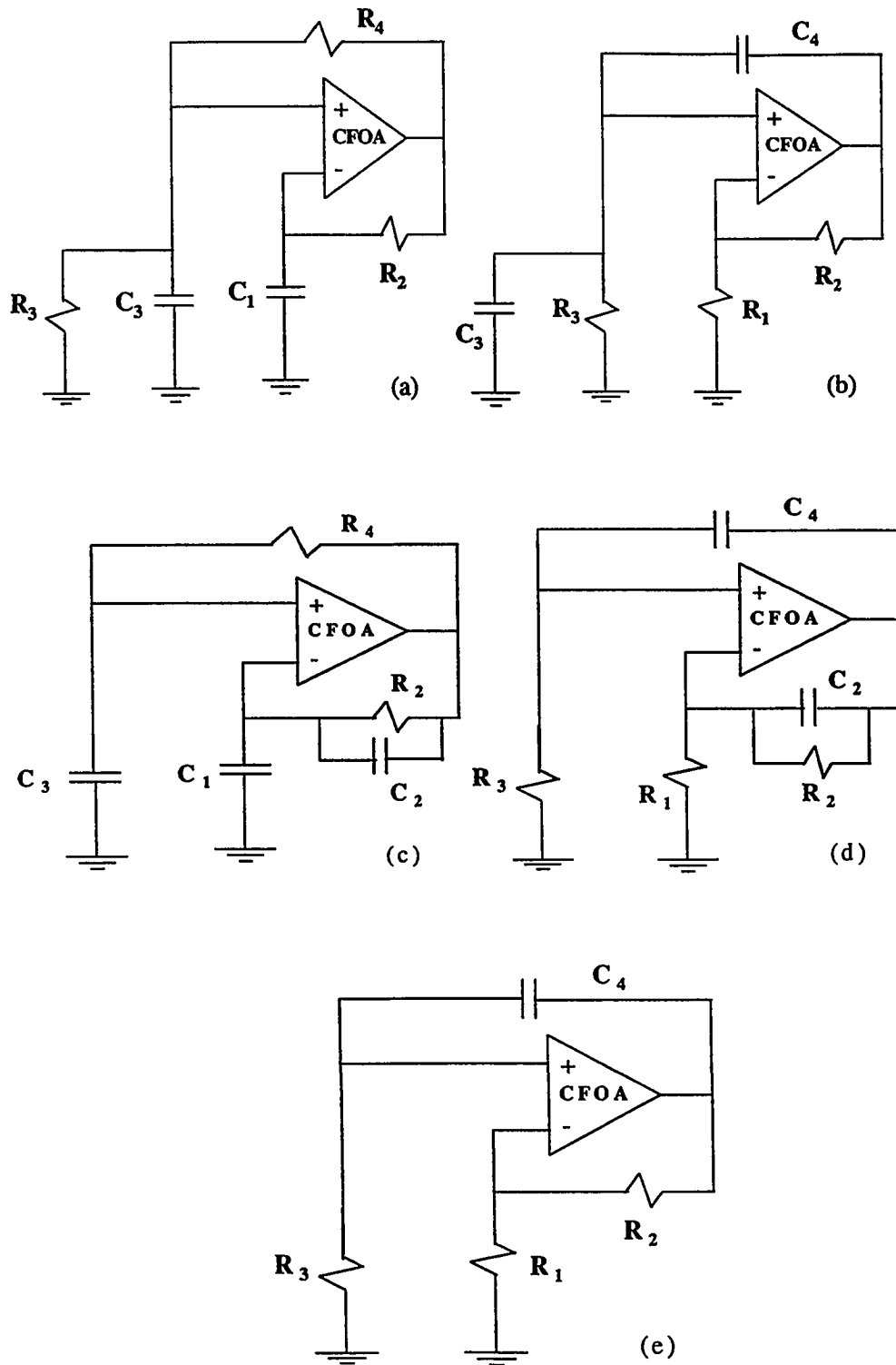


Fig.3.3 Five Oscillator Circuits derived from Fig.3.1.

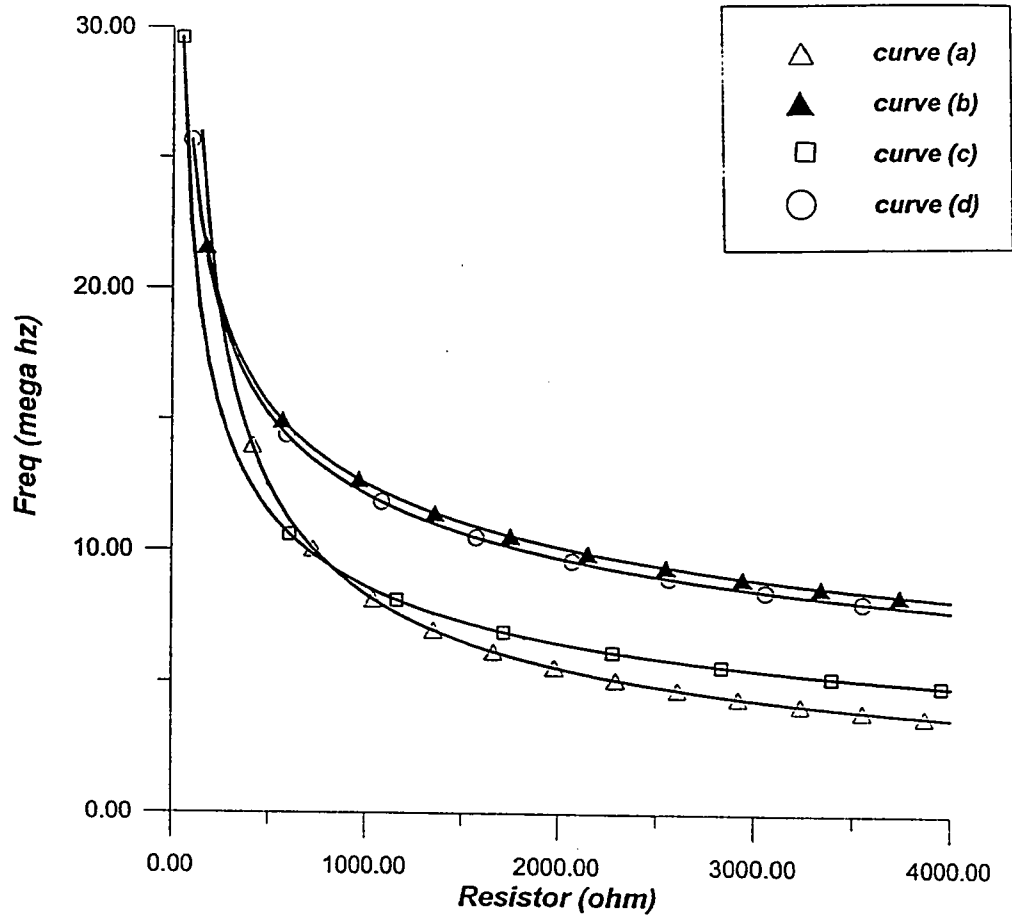
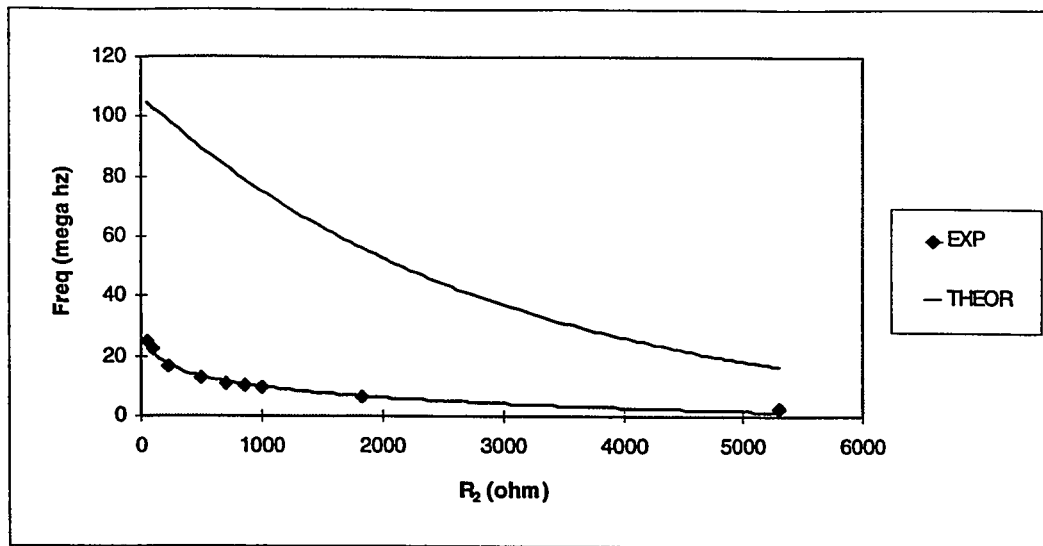
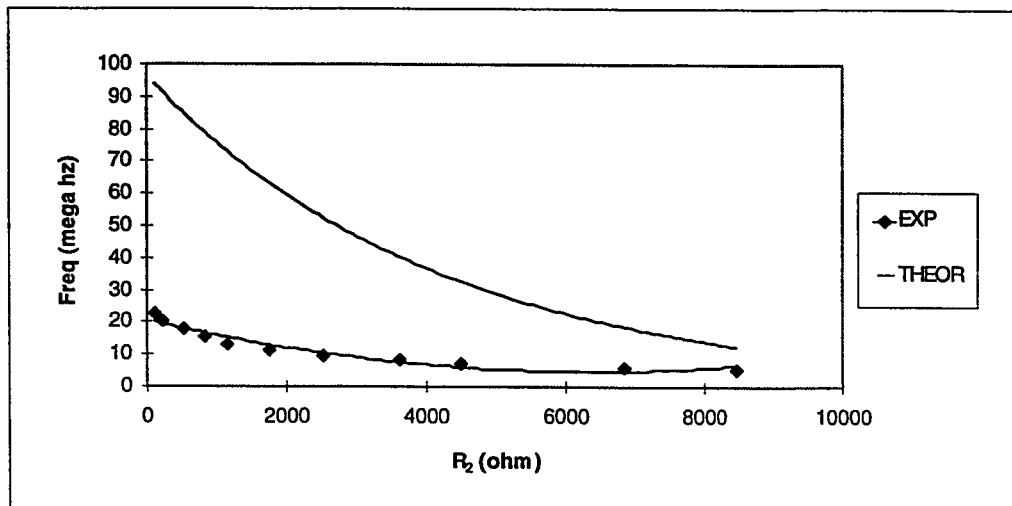


Fig.3.4 Variation of the frequency of oscillation of

- (a) . Fig.3.3(a) with resistance R_4 . $C_1 = 26.5 \text{ pF}$, $C_3 = 4.7 \text{ pF}$, $R_2 = R_3 = 100\Omega$
- (b) . Fig.3.3(b) with resistance R_2 . $C_3 = 11 \text{ pF}$, $C_4 = 22 \text{ pF}$, $R_1 = 141.2\Omega$, $R_3 = 72.7\Omega$
- (c) . Fig.3.3(d) with resistance R_2 . $C_2 = 4.7 \text{ pF}$, $C_4 = 22 \text{ pF}$, $R_3 = 97\Omega$, $R_1 = 98\Omega$
- (d) . Fig.3.3(e) with resistance R_2 . $C_4 = 22 \text{ pF}$, $R_1 = 170.6\Omega$, $R_3 = 87.8\Omega$



(a)



(b)

Fig.3.5 Comparisons between theoretical and experimental results

a) for Fig.3.3(d)

b) for Fig.3.3(e)

Although some of the five oscillator circuits of Fig.3.3 enjoy independent control of the frequency of oscillation and the condition of oscillation and some of them enjoy grounded capacitors, none of them enjoys the two features. So, our objective next is to find oscillator circuits that enjoy the two features simultaneously.

New sinusoidal oscillator circuits enjoying the above mentioned two features are shown in Figs. 3.6 and 3.7. A simple analysis of the circuit of Fig.3.6 gives the following characteristic equation

$$\begin{aligned} (sC_T + G_T)(G_2 + G_4 + G_5)(sC_3 + G_3) + (sC_T + G_T)G_4G_5 = \\ G_5G_4(sC_1 + G_1) - G_5G_2(sC_3 + G_3) \end{aligned} \quad (3.4)$$

Where $s C_T + G_T$ is the internal pole of the CFOA, as shown in Fig.3.2. Using the Barkhausen principle, by equating the real and imaginary parts to zero, the condition and frequency of oscillation of the circuit of Fig 3.6 can be expressed by

$$(G_T C_3 + G_3 C_T)(G_2 + G_4 + G_5) + G_5 G_4 C_T = G_5 G_4 C_1 - G_5 G_2 C_3 \quad (3.5)$$

and

$$\omega_o = \left(\frac{G_T G_3 (G_2 + G_4 + G_5) + G_5 G_4 G_T + G_5 G_2 G_3 - G_5 G_4 G_1}{(G_2 + G_4 + G_5) C_T C_3} \right)^{\frac{1}{2}} \quad (3.6)$$

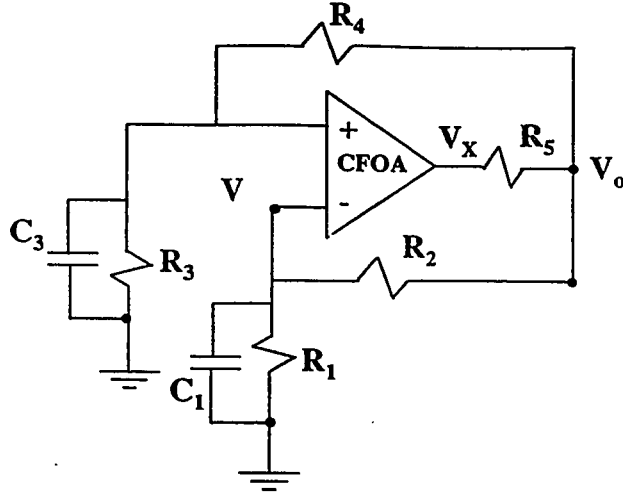


Fig.3.6: Proposed sinusoidal oscillator with single resistor control and all capacitor grounded (II).

From equation (3.6) one can see that the oscillation frequency can be controlled independently by the grounded resistor R_1 . While the oscillation condition can be independently adjusted by the grounded capacitor C_1 . The passive sensitivities of this circuit can be obtained as

$$S_{G_1}^{\omega_o} = \frac{1 - G_3 G_1 (G_2 + G_5)}{2 \Delta_1}; \quad S_{G_3}^{\omega_o} = \frac{1 G_3 (G_T - G_1) (G_2 + G_5)}{2 \Delta_1}$$

$$S_{G_2}^{\omega_o} = \frac{1 - (G_4 G_T + G_3 G_T - G_3 G_1) G_5}{2 \Delta_1}$$

$$S_{G_5}^{\omega_o} = \frac{1 - (G_4 G_T + G_3 G_T - G_3 G_1) G_2}{2 \Delta_1}$$

$$S_{G_4}^{\omega_o} = \frac{1 G_4 (G_T (G_2 + G_5) + G_5 G_2)}{2 \Delta_1}; \quad S_{G_4}^{\omega_o} = -\frac{1}{2}$$

where $\Delta_1 = (G_4 G_T + G_3 G_T - G_3 G_1)(G_2 + G_5) + G_5 G_4 G_2$

To have low sensitivities (≤ 0.5) it is required that $G_3 G_1 \gg G_4 G_2$.

Taking into account the voltage tracking error and the current tracking error the frequency of oscillation of equation (3.6) becomes

$$\omega_o = \left[\frac{G_T G_3 (G_2 + G_4 + G_5) + (G_5 + G_2) G_T G_4 - \beta G_T G_4 G_2 - \alpha \gamma \beta G_5 G_4 (G_1 + G_2) + \alpha \gamma G_5 G_2 (G_4 + G_3)}{C_T C_3 (G_5 + G_2 + G_4)} \right]^{\frac{1}{2}} \quad (3.7)$$

So, the sensitivities of ω_o to active components are

$$S_{\alpha}^{\omega_o} = S_{\gamma}^{\omega_o} = \frac{1}{2} \frac{\alpha \gamma G_5 (G_2 (G_4 + G_3) - \beta G_4 (G_1 + G_2))}{G_T G_3 (G_2 + G_4 + G_5) + (G_5 + G_2) G_T G_4 - \beta G_T G_4 G_2 + \alpha \gamma G_5 (G_2 (G_4 + G_3) - \beta G_4 (G_1 + G_2))}$$

$$S_{\beta}^{\omega_o} = -\frac{1}{2} \frac{\beta (G_T G_4 G_2 + \alpha \gamma G_5 G_4 (G_1 + G_2))}{G_T G_3 (G_2 + G_4 + G_5) + (G_5 + G_2) G_T G_4 - \beta G_T G_4 G_2 + \alpha \gamma G_5 (G_2 (G_4 + G_3) - \beta G_4 (G_1 + G_2))}$$

To have low sensitivities ($< 1/2$) $G_2 (G_4 + G_3)$, should be $\geq 2 G_4 (G_1 + G_2)$.

Fig.3.7(a) shows another sinusoidal oscillator structure with single element control using a CFOA. Routine analysis using the CFOA model of Fig 1.3 yields the characteristic equation which can be expressed by

$$\left(Y_3 Y_1 - Y_A (Y_4 + Y_3)\right) (Y_5 + Y_2) = Y_5 Y_4 Y_2 \quad (3.8)$$

where $Y_A = s C_T + G_T$ is the internal pole of the CFOA. If the admittance are $Y_1 = s C_1 + G_1$, $Y_2 = G_2$, $Y_3 = G_3$, $Y_4 = s C_4 + G_4$, and $Y_5 = G_5$, a sinusoidal oscillator, shown in Fig.3.8(b), can be obtained with

$$(G_3 C_1 - G_T C_4 - G_4 C_T - G_3 C_T) (G_2 + G_5) = G_5 G_2 C_4$$

Its oscillation frequency is

$$\omega_o = \left(\frac{(G_4 G_T + G_3 G_T - G_3 G_1) (G_2 + G_5) + G_5 G_4 G_2}{(G_2 + G_5) C_T C_4} \right)^{\frac{1}{2}} \quad (3.9)$$

and the condition of oscillation is given by

$$(G_2 + G_5) G_3 G_1 \left((G_4 + G_3) G_T (G_2 + G_5) + G_5 G_4 G_2 \right) \quad (3.10)$$

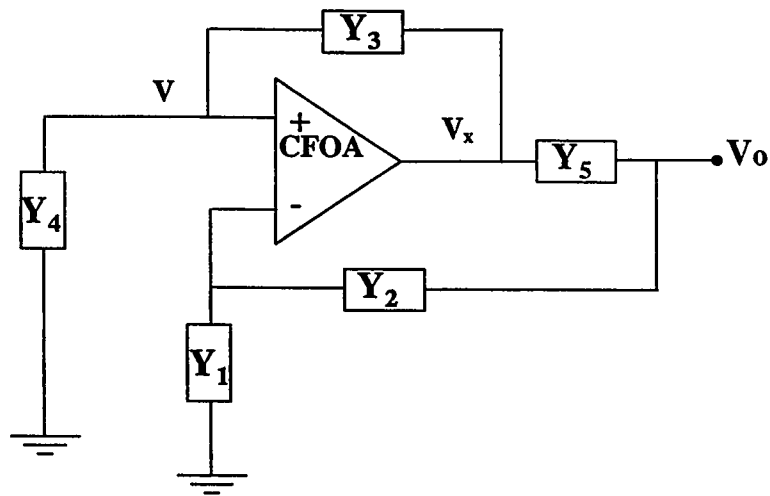


Fig.3.7(a) *Proposed Oscillator Structure (III)*

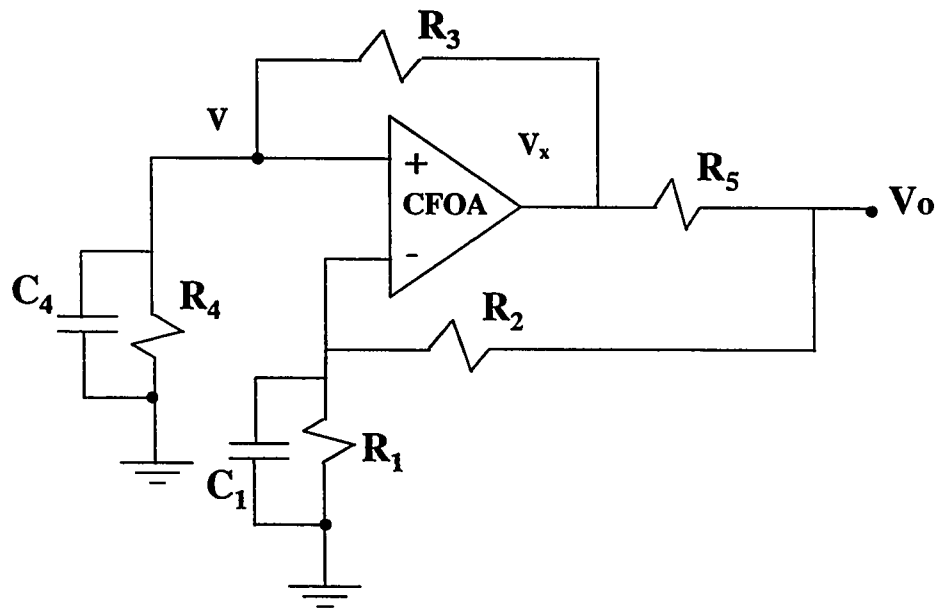


Fig.3.7(b). *Sinusoidal oscillator circuit derived from Fig.3.7(a)*

The oscillation frequency can be controlled independently by the ground resistor R_1 , while the condition of oscillation can be controlled independently by the grounded capacitor C_1 . The passive sensitivities of this circuit can be obtained as

$$S_{G_2}^{\omega_o} = S_{G_5}^{\omega_o} = \frac{1 - (G_4 G_T + G_3 G_T - G_3 G_1) G_5}{2 \Delta_1}$$

$$S_{G_4}^{\omega_o} = \frac{1}{2} \frac{G_T G_4 (G_2 + G_5) + G_5 G_4 G_2}{G_4 G_T (G_2 + G_5) + G_5 G_4 G_2 + G_3 (G_2 + G_5) (G_T - G_1)}$$

$$S_{G_3}^{\omega_o} = \frac{1}{2} \frac{(G_3 G_T - G_3 G_1) (G_2 + G_5)}{\Delta_1}$$

$$S_{G_1}^{\omega_o} = \frac{1}{2} \frac{-G_1 G_3 (G_2 + G_5)}{\Delta_1}$$

$$S_{G_4}^{\omega_o} = -\frac{1}{2}$$

Where

$$\Delta_1 = (G_4 G_T + G_3 G_T - G_3 G_1) (G_2 + G_5) + G_5 G_4 G_2$$

To have low sensitivities (≤ 0.5)

$$G_3 G_1 (G_2 + G_5) \text{ should be } \gg G_5 G_4 G_2$$

Taking into account the voltage tracking error and current tracking error the frequency of oscillation can be expressed by

$$\omega_o^2 = \frac{\alpha \gamma G_2 G_5 (G_3 + G_4) - \alpha \gamma \beta G_2 G_3 G_5 - \alpha \gamma \beta G_1 G_3 (G_5 + G_2) + G_T (G_3 + G_4) (G_5 + G_2)}{C_T C_4 (G_5 + G_2)}$$

(3.11)

So, the sensitivities of ω_o to active elements are

$$S_{\alpha}^{\omega_o} = S_{\gamma}^{\omega_o} = \frac{1}{2} \frac{\alpha\gamma (G_2G_5(G_3 + G_4) - \beta G_2G_3G_5 - \beta G_1G_3(G_5 + G_2))}{\alpha\gamma [G_2G_5(G_3 + G_4) - \beta G_2G_3G_5 - \beta G_1G_3(G_5 + G_2)] + G_T(G_3 + G_4)(G_5 + G_2)}$$

$$S_{\beta}^{\omega_o} = -\frac{1}{2} \frac{\alpha\gamma\beta (G_2G_3G_5 + G_1G_3(G_5 + G_2))}{\alpha\gamma [G_2G_5(G_3 + G_4) - \beta G_2G_3G_5 - \beta G_1G_3(G_5 + G_2)] + G_T(G_3 + G_4)(G_5 + G_2)}$$

To have low sensitivities $G_2G_4G_5$ should be $\geq G_2G_3G_5 + 2G_1G_3(G_5 + G_2)$

Both circuits of Figs.3.6 and 3.7(b) have advantages over the previous circuits. All the used capacitors are grounded. Also they enjoy independent control of the frequency of oscillation and the condition of oscillation. The control element of the frequency of oscillation is a grounded resistor.

To verify the theoretical prediction of the proposed circuits, the circuit of Fig.3.6 was examined using the CFOA AD844 with $R_2 = 377\Omega$, $R_3 = 48\Omega$, $R_4 = 107\Omega$, $R_5 = 22\Omega$, $C_1 = 26.7$ pF and $C_3 = 11$ pF. The experimental result and theoretical response are shown in Fig.3.8. Also the circuit of Fig.3.7(b) is examined using the CFOA AD844 with $R_2 = 49\Omega$, $R_3 = 481\Omega$, $R_4 = 155.1\Omega$, $R_5 = 139.6\Omega$, $C_1 = 26.7$ pF and $C_3 = 11$ pF. The experimental and theoretical response are shown in Fig.3.9.

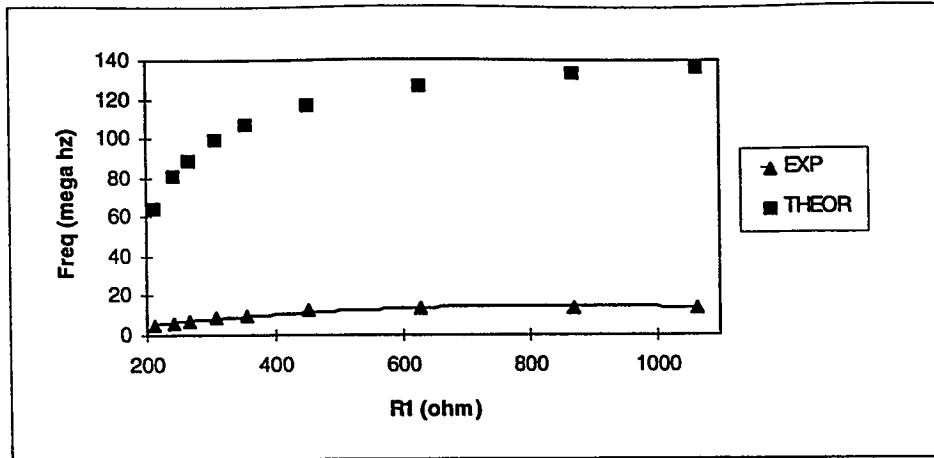


Fig.3.8 Comparisons between theoretical and experimental results of Fig.3.6.

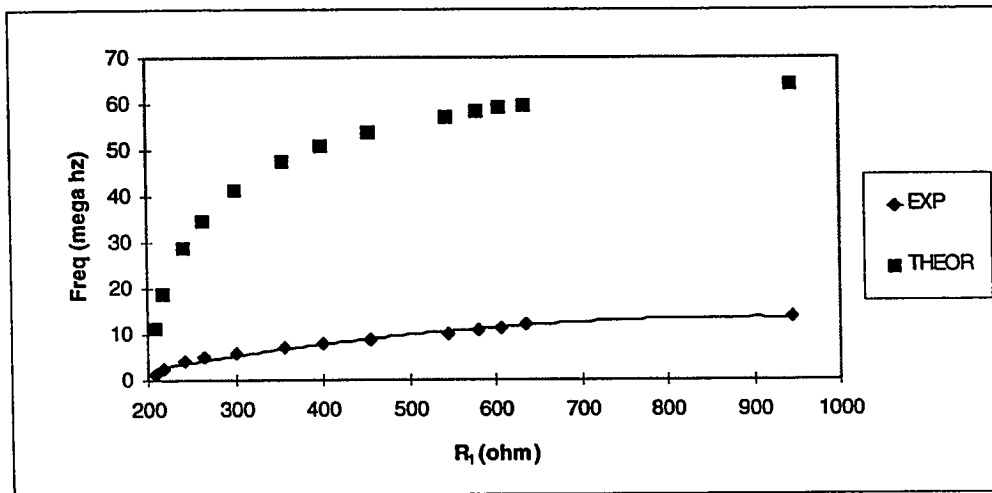


Fig.3.9 Comparisons between theoretical and experimental results of Fig.3.7.

In conclusion, seven new RC oscillator circuits have been presented in this section. Three of the proposed circuits (Figs 3.3(c), (d) and (e)) enjoy independent control of the frequency of oscillation and the condition of oscillation and, therefore, can be used for realizing single-element controlled oscillators. Also two of the proposed circuits (Figs 3.6 and 3.7(b)) enjoy independent control of the frequency of oscillation and the condition of oscillation and uses grounded capacitors. Using commercially available CFOA oscillation frequencies up to 27.5 MHz were successfully obtained.

3.3.2 Sinusoidal Oscillator Based on Ideal CFOA

The CFOA-based oscillator circuits in this section are designed assuming that the CFOA does not have a pole.

A new configuration for realizing sinusoidal oscillator is shown in Fig.3.10. Its characteristic can be expressed by

$$Y_2 Y_5 Y_1 = Y_3 Y_5 Y_1 + Y_3 Y_4 Y_1 + 2Y_3 Y_4 Y_2 \quad (3.12)$$

If the admittance are $Y_1 = G_1$, $Y_2 = SC_2$, $Y_3 = G_3$, $Y_4 = SC_4$ and $Y_5 = G_5$, a sinusoidal oscillator, shown in Fig.3.11, can be obtained with $C_2 G_5 = C_4 G_3$. Its oscillation frequency is independently controlled by grounded resistor R_1 and can be given by

$$\omega_o = \left[\frac{G_1 G_5}{2C_4 C_2} \right]^{1/2} \quad (3.13)$$

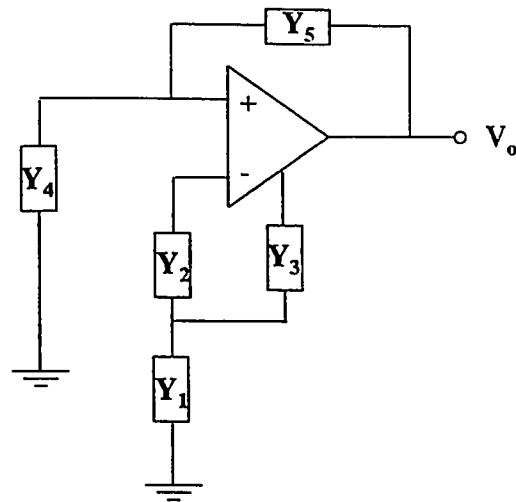


Fig.3.10: Configuration for synthesizing sinusoidal oscillators using a CFOA (IV)

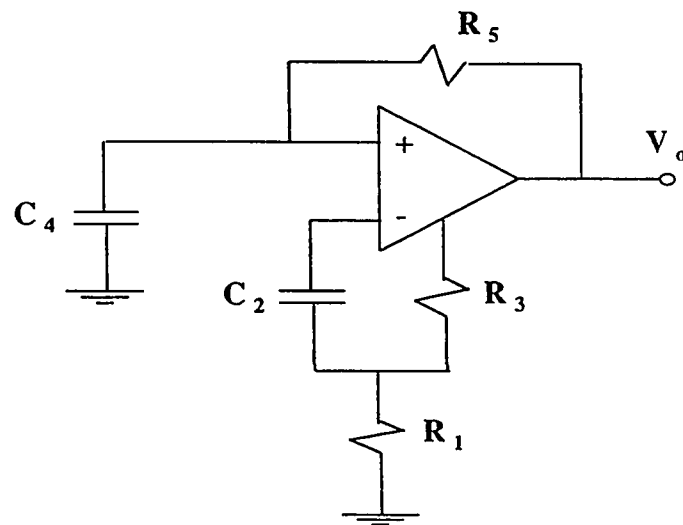


Fig.3.11: Proposed sinusoidal oscillator driven from Fig.3.10.

The passive sensitivities of this sinusoidal oscillator can be obtained as

$$S_{G_1}^{\omega_o} = S_{G_5}^{\omega_o} = -S_{C_4}^{\omega_o} = -S_{C_2}^{\omega_o} = \frac{1}{2}$$

The calculated passive sensitivities are all low.

The remaining oscillators derived from Fig.3.10 are summarized in Table 3.3.

Taking into account the voltage tracking error and current tracking error of the CFOA, the frequency of oscillation can be expressed by

$$\omega_o = \left[\frac{G_1 G_5}{C_2 C_4 (1 + \alpha)} \right]^{\frac{1}{2}} \quad (3.14)$$

So, the sensitivities of ω_o to active components are

$$S_{\alpha}^{\omega_o} = -\frac{1}{2} \frac{\alpha}{1 + \alpha}$$

$$S_{\gamma}^{\omega_o} = S_{\beta}^{\omega_o} = 0$$

all of which are small.

Table 3.3 Remaining Sinusoidal Oscillators derived from Fig.3.10.

Admittance					Frequency Oscillation (ω_o^2)	Condition of Oscillation
Y1	Y2	Y3	Y4	Y5		
SC_1	G_2	G_3	$SC_4 + G_4$	G_5	$\frac{2G_2 G_4}{C_1 C_4}$	$G_2 G_5 C_1 = G_3 (G_5 C_1 + G_4 C_1 + 2G_2 C_4)$
SC_1	G_2	G_3	G_4	$SC_5 + G_5$	$\frac{2G_3 G_4 G_2}{(G_2 - G_3) C_1 C_5}$	$G_2 G_5 = G_3 (G_4 + G_5)$ $G_2 > G_3$

Although one of the three oscillator circuits enjoys independent control of the frequency of oscillation and the condition of oscillation and one uses grounded capacitors, none of them enjoys the two features simultaneously. So, our objective next is to find an oscillator circuit that enjoys the two features.

A new sinusoidal oscillator configuration using a CFOA is shown in Fig.3.12. Its characteristic equation can be expressed by

$$Y_4(Y_2 + Y_3) = Y_2Y_1 \quad (3.15)$$

Two new oscillator circuits can be driven from this configuration by proper selection for the components Y_1 , Y_2 , Y_3 and Y_4 . One of them enjoys the tow features. If the admittances are $Y_1 = SC_1 + G_1$, $Y_2 = SC_2$, $Y_3 = G_3$ and $Y_4 = SC_4 + G_4$ the first sinusoidal oscillator, shown in Fig.3.13, can be obtained with $G_3C_4 + G_4C_2 = G_1C_2$. Its oscillation frequency is

$$\omega_o = \left(\frac{G_4G_3}{C_2(C_4 - C_1)} \right)^{1/2} \quad \text{for } C_4 > C_1 \quad (3.16)$$

The oscillation condition can be independently adjusted by the grounded resistor R_1 . The oscillation frequency can be independently controlled by the grounded capacitor C_1 . The passive sensitivities of this sinusoidal oscillator can be obtained as

$$S_{G_4}^{\omega_o} = S_{G_3}^{\omega_o} = -S_{C_2}^{\omega_o} = \frac{1}{2}, S_{C_1}^{\omega_o} = \frac{1}{2} \frac{C_1}{C_4 - C_1}, S_{C_4}^{\omega_o} = -\frac{1}{2} \frac{C_4}{C_4 - C_1}$$

The calculated passive sensitivities are all low except for C_1 and C_4 where the sensitivities can reach high value. To avoid high sensitivities $2C_1$ should be $\leq C_4$.

Taking into account the voltage tracking error and current tracking error of the CFOA the frequency of oscillation can be expressed by

$$\omega_o^2 = \frac{G_3 G_4}{C_2 \left(C_4 - \frac{C_1 \beta}{\alpha \gamma} \right)} \quad (3.17)$$

So, the sensitivities of ω_o to the active components are

$$S_{\alpha}^{\omega_o} = S_{\gamma}^{\omega_o} = S_{\beta}^{\omega_o} = -\frac{1}{2} \frac{\beta C_1}{\alpha \gamma C_4 - \beta C_1}$$

To have low sensitivities $\alpha \gamma C_4$ should be $\geq 2\beta C_1$.

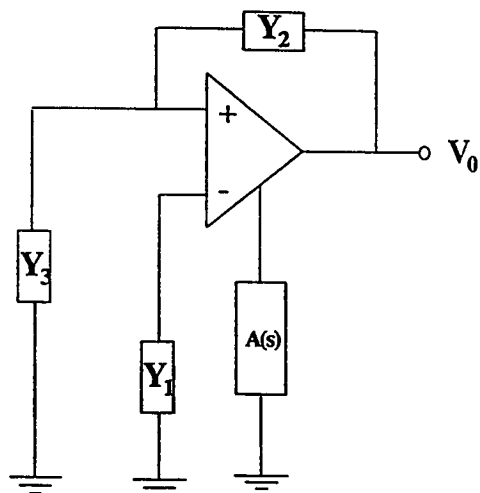


Fig.3.12: Configuration for synthesizing sinusoidal oscillators using a CFOA (V)

Fig.3.14 shows another sinusoidal oscillator derived from Fig.3.12. Routine analysis using the CFOA model of Fig.1.3 yields the following condition of oscillation

$$G_2 C_4 + G_4 C_3 = G_2 C_1 \quad (3.18)$$

and the following oscillation frequency

$$\omega_o = \left(\frac{G_2 (G_4 - G_1)}{C_3 C_4} \right)^{\frac{1}{2}} \quad \text{for } G_1 < G_4 \quad (3.19)$$

From equations (3.18) and (3.19) one can see that the frequency of oscillation can be adjusted by changing the grounded resistor R_1 without disturbing the condition of oscillation which can be adjusted by changing a grounded capacitor C_1 without disturbing the frequency of oscillation

The passive sensitivities of this oscillator can be obtained as

$$S_{G_2}^{\omega_o} = -S_{C_3}^{\omega_o} = -S_{C_4}^{\omega_o} = \frac{1}{2}, \quad S_{G_4}^{\omega_o} = \frac{1}{2} \frac{G_2 G_4}{G_2(G_4 - G_1)}, \quad S_{G_1}^{\omega_o} = -\frac{1}{2} \frac{G_2 G_1}{G_2(G_4 - G_1)}.$$

To have low sensitivities G_4 should be $\geq 2G_1$.

Taking into account the voltage tracking error and current tracking error the frequency of oscillation can be expressed by

$$\omega_o = \left(\frac{G_2 \left(\frac{G_4}{\alpha\gamma} - G_1 \right)}{C_3 C_4} \right)^{\frac{1}{2}} \quad (3.20)$$

So, the sensitivities of ω_o to the active components are

$$S_{\alpha}^{\omega_o} = S_{\gamma}^{\omega_o} = -\frac{1}{2} \frac{G_4}{G_4 - \alpha\gamma G_1}$$

$$S_{\beta}^{\omega_o} = 0$$

To have low sensitivities G_4 should be $\geq 2G_1$.

This oscillator can generate low oscillation frequency without using large-valued capacitors, whereas high frequency without low-valued capacitors can be generated by the circuit of Fig.3.13.

To verify the theoretical analysis, the proposed oscillators of Fig.3.11 and Fig.3.14 were implemented using a commercial CFOA (AD844). Fig.3.15 shows the experimental results obtained from the sinusoidal oscillator of Fig.3.11 with $C_4 = C_2 = 200$ pF, $R_5 = 521 \Omega$ and $R_3 = 644 \Omega$. Fig.3.16 shows the experimental results obtained from the sinusoidal oscillator of Fig.3.14 with $C_1 = 150$ pF, $C_3 = 200$ pF, $C_4 = 100$ pF, $R_2 = 295 \Omega$, $R_4 = 1436 \Omega$.

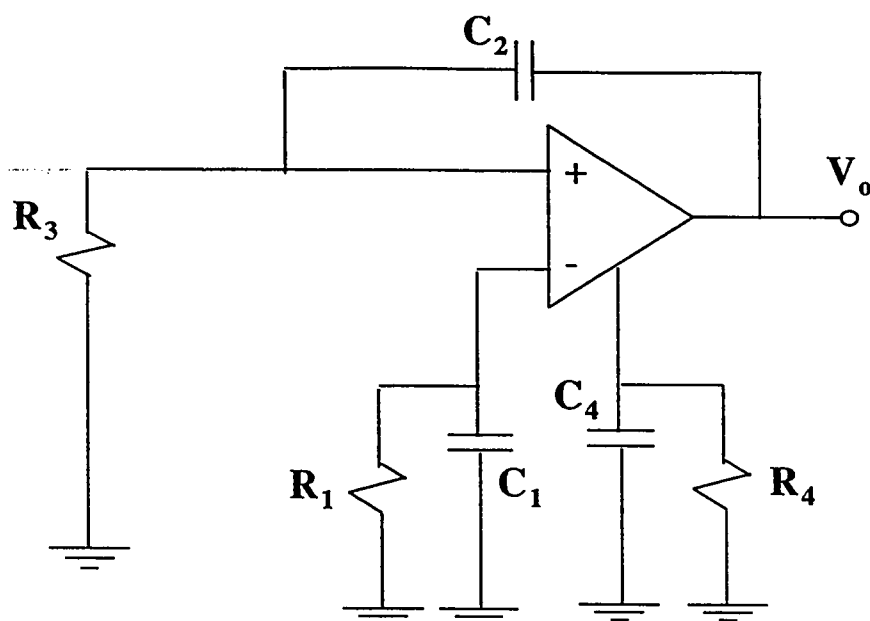


Fig.3.13: Proposed sinusoidal oscillator derived from Fig.3.12.

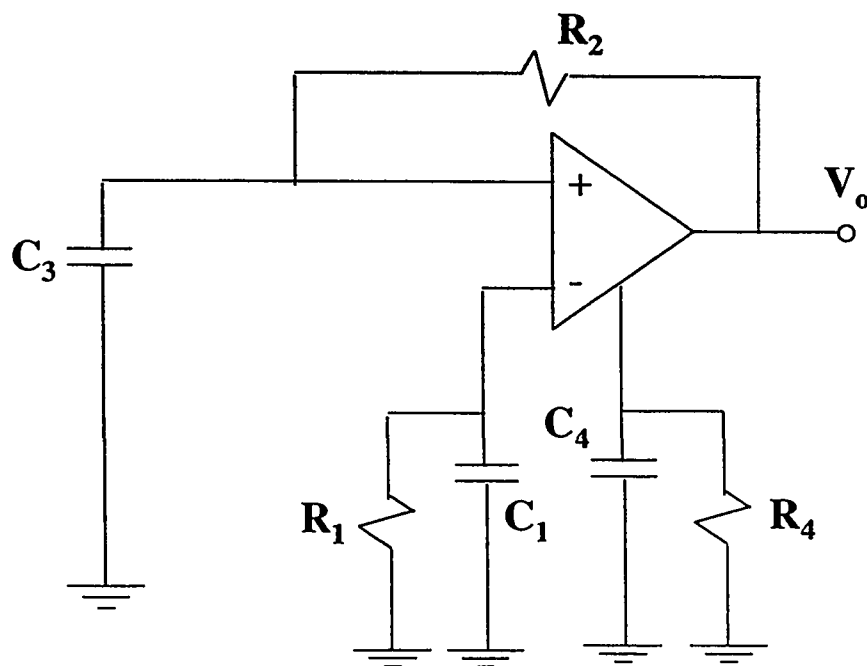


Fig.3.14: Proposed sinusoidal oscillator with single resistor control and all capacitors grounded

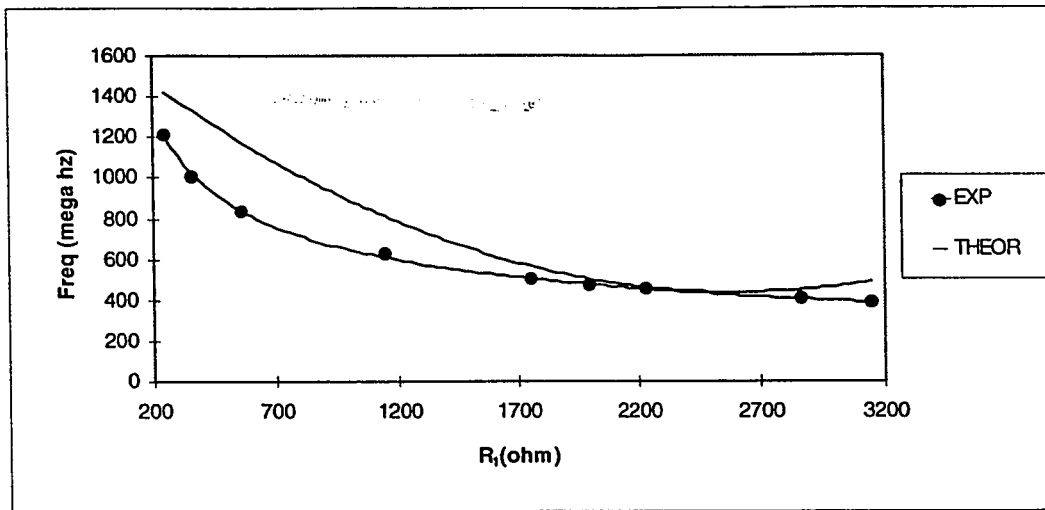


Fig.3.15 Comparisons between theoretical and experimental results of Fig.3.11

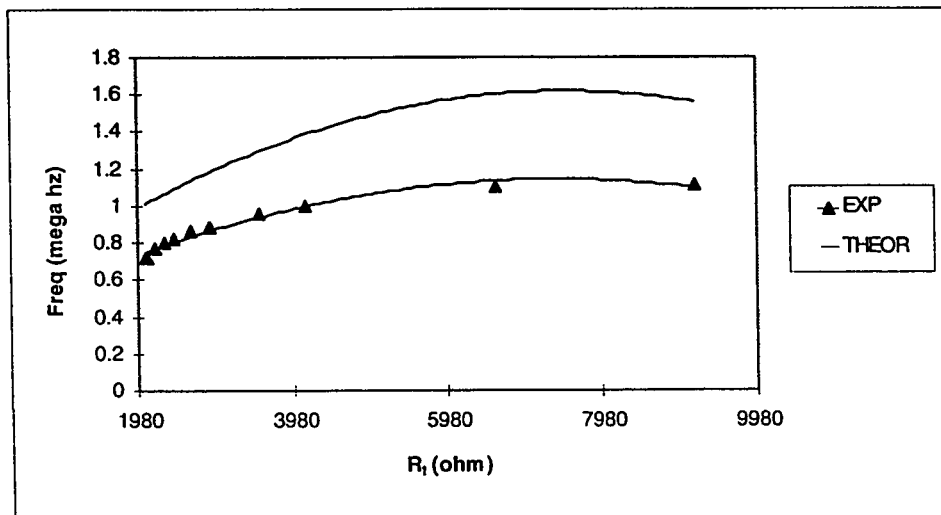


Fig.3.16 Comparisons between theoretical and experimental results of Fig.3.14

In conclusion, five new RC oscillator circuits have been presented in this section using the ideal CFOA. Two of them enjoy independent control of the frequency of oscillation and condition of oscillation. And one of them enjoys independent control of the frequency of oscillation and condition of oscillation and uses grounded capacitors.

3.4 Square, Triangular and Ramp Waveforms Generator

In the design of electronic system the need frequently arises for signals having standard waveforms, for example, square, triangular, pulse and so on. Circuits that generate these waveforms are called nonlinear oscillators or signal generators. There are many circuits that realize square, triangular and pulse waveforms using VOA or transconductance amplifier. In order to get benefit of the good performance of the CFOA new signal generator using the CFOA are presented in this section.

To the best of my knowledge such research has not been published in the open literature. Fig 3.17 shows a new signal generator where a triangular waveform is generated at point A and square waveform is generated at point B. The triangular waveform is generated by linear charging and discharging the capacitor C_1 .

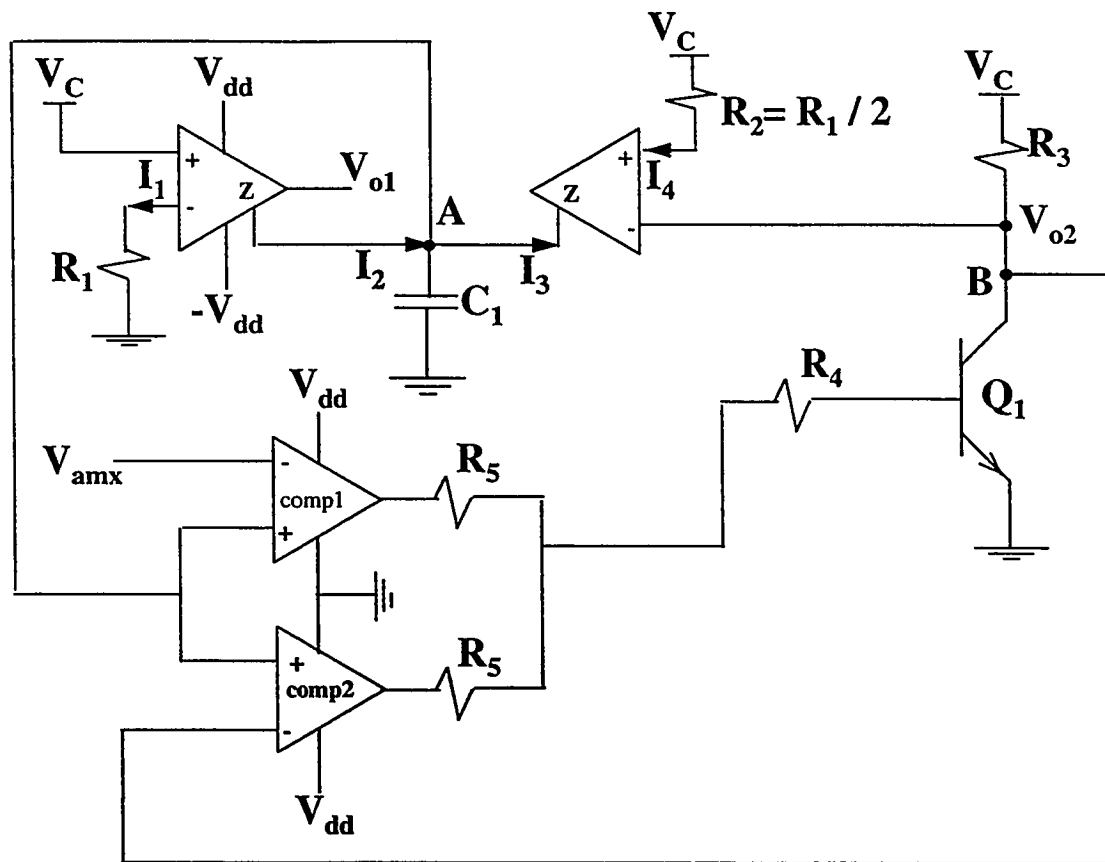


Fig.3.17: Proposed signal waveform generator

Circuit description

To see how this circuit operates assume that initially V_A is equal to zero volt, transistor Q_1 is off so V_B is equal to the control voltage V_C . Assume also that V_{max} is less than V_C and greater than V_A . From the above conditions the outputs of the comparators 1 and 2 are low level, for example zero. And since I_3 is given by

$$I_3 = I_4 = \frac{V_C - V_B}{R_1/2} \quad (3.21)$$

then with $V_B = V_C$ we get $I_3 = 0$.

The capacitor C_1 will start changing from zero volt linearly by a constant current I_2 which is given by

$$I_2 = I_1 = \frac{V_C}{R_1} \quad (3.22)$$

Thus the voltage V_{o1} is

$$V_{o1} = V_A = \frac{1}{C_1} \int I_2 dt \quad (3.23)$$

or

$$V_{o1} = \frac{I_2 t}{C_1} = \frac{V_C t}{R_1 C_1} \quad (3.24)$$

when V_A reaches, and begins to exceed, V_{max} the output of comparator 1 goes high, turning on transistor Q_1 . Transistor Q_1 will be saturated, and thus V_B will be close to 0 V, resulting in high level at the output of comparator 2. From equation (3.21) I_3 is equal to $\frac{2V_C}{R_1}$. Thus C_1 begins to discharge by $I_3 - I_2$. The voltage V_A decreases linearly toward 0

V. When V_A reaches V_{max} , the output of comparator 1 goes low. Since the output of comparator 2 is high, the transistor Q_1 will not change its state. The voltage V_A continues in decreasing until it reaches V_B . At this instant of time, the transistor Q_1 is turned off. The voltage V_B goes high, resulting in $I_3 = 0$ and the cycle continues producing triangular waveform at the output V_{o1} .

From the above description we can also see that the transistor Q_1 oscillates between on and off states producing a square waveform at the output V_{o2} . The frequency of oscillation can be determined as follows. Reference to Fig.3.18 indicates that during the charging time V_{o1} rises from V_{CEsat} to V_{max} . Substituting $V_{o1} = V_{max}$ in equation (3.24) result in

$$T_{ch} = \frac{V_{max} R_1 C_1}{V_C} \quad (3.25)$$

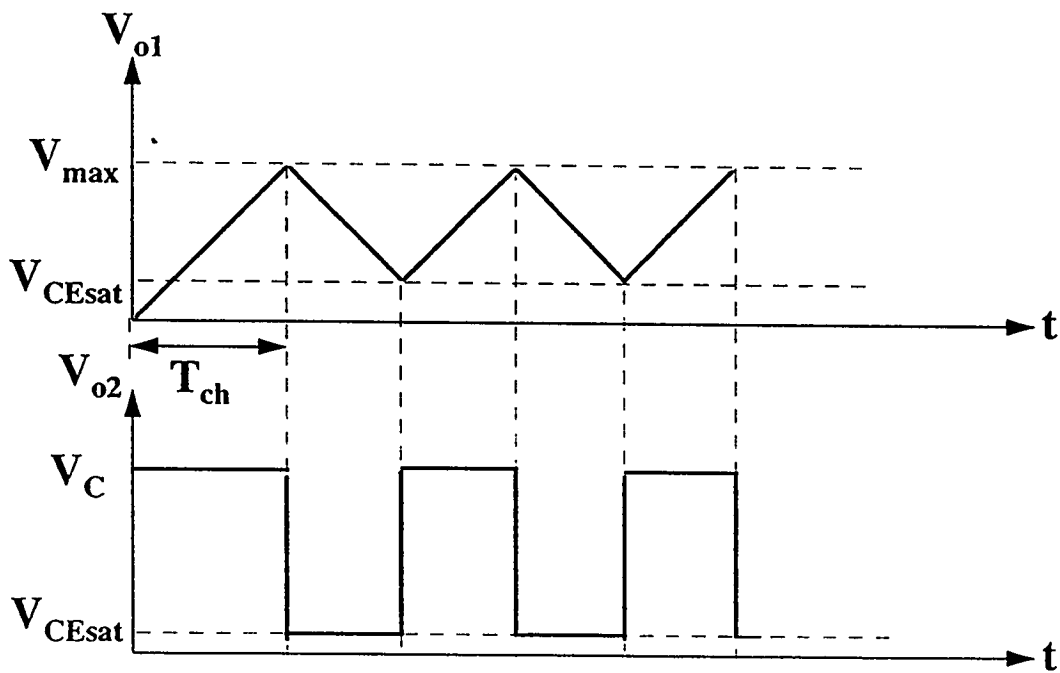


Fig.3.18: The outputs waveforms of the proposed circuit

Since the capacitor C_1 is charged and discharged by an equal amount of current, charging and discharging time is equal. The period T of the outputs square and triangular waves can be expressed as

$$T = \frac{2V_{\max} R_1 C_1}{V_C} \quad (3.26)$$

and the frequency f is

$$f = \frac{1}{T} = \frac{V_C}{2V_{\max} R_1 C_1} \quad (3.27)$$

The ramp waveform is a special case of the triangular waveform where the discharging time is very small compared to the charging time. To generate a ramp signal from the proposed circuit the discharging time should be minimized. This can be done easily by increasing I_3 .

This circuit has many advantages. Equation (3.27) indicates that the frequency can be controlled via R_1 , C_1 , V_C or V_{\max} . In fact, the amplitude of the square waveform can be controlled via V_C also. By changing V_{\max} we can control the amplitude of the triangular waveform. Also the duty cycle of the output signals can be controlled by R_2 . In contrast with the 555 timer-based square-wave generators where only square waveform is generated, the proposed circuit can generate three different waveforms.

To demonstrate the practical behavior of the proposed circuit, the circuit of Fig.3.17 was tested using the CFOA AD844 with $R_1 = 2R_2 = 30 \text{ k}\Omega$ $R_3 = 5 \text{ k}\Omega$ and $C_1 = 1 \text{ nF}$. The experimental result and theoretical response are shown in Fig.3.19.

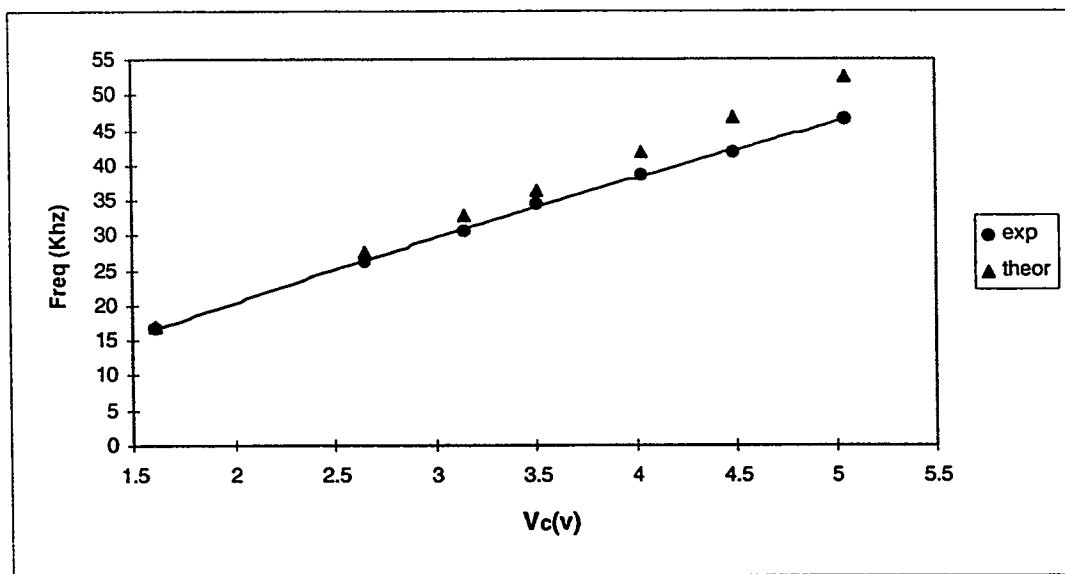


Fig.3.19 Comparisons between theoretical and experimental results of Fig.3.17

The schmitt trigger is a circuit used to obtain a free-running square-wave generator. It is used extensively in both analog and digital areas. For a long time, VOA has been used to realize the schmitt trigger circuit. Recently, a schmitt-trigger circuit using the current conveyor is presented in [21].

A CFOA-based schmitt trigger is shown in Fig.3.20 where r_x represents the output resistance of the input buffer. In fact, this circuit will operate only in two stable states. To see how bistability is obtained, consider the case when the output voltage decreases. The decrease in the output voltage will cause a decrease in the V_y and consequently an increase in I_x . Since I_z is proportional to I_x , I_z will increase by the same amount as I_x resulting in an increase in V_z . From the above and since the output voltage of the CFOA is limited by the power supply, the output voltage of this circuit will be either equal to V_{satH} or V_{satL} .

A square waveform can be generated by connecting the bistable circuit with an RC circuit in a feedback loop as shown in Fig.3.21. To see how this circuit operates assume that initially V_o is in one of the two possible levels, say V_{satH} , and thus $V_y = V_{satH} R_2 / (R_1 + R_2)$. The capacitor will start charging from zero volt linearly towards $V_y - I_1 R_x$ by a constant current I_1 which is given by

$$I_1 = V_{satH} / R_3 \quad (3.28)$$

Thus the voltage V_c is

$$V_c = \frac{1}{C} \int I_1 dt = \frac{I_1 t}{C} = \frac{V_{satH} t}{CR_3} \quad (3.29)$$

The output voltage will remain in the positive level V_{satH} until V_A reaches V_y , and begins to exceed it, I_1 direction will be reversed and thus the output voltage V_o goes negative to V_{satL} . The voltage divider in turn causes V_y to go negative and the capacitor C starts discharging towards $V_y + I_2 R_3$ by a constant current I_2 which is given by

$$I_1 = V_{\text{satL}} / R_3 \quad (3.30)$$

The output voltage will remain in the negative level until V_A goes negative to the point that it equals $V_y = V_{\text{satL}} R_2 / (R_1 + R_2)$. As V_A goes below this value, I_2 direction will be reversed and thus the output voltage goes positive V_{satH} and the cycle repeats itself.

From equations (3.28) and (3.30) one can see that for equal magnitude of the positive level V_{satH} and the negative level V_{satL} the capacitor C will charge and discharge by an equal amount of current and thus equal charging and discharging time.

The maximum value can V_c reach is given by

$$V_{C_{\text{max}}} = V_{\text{satH}} \left(\frac{R_1}{R_1 R_2} - \frac{R_x}{R_3} \right) \quad (3.31)$$

The time needed for the capacitor voltage V_c to reach the maximum value is given by

$$t = CR_3 \left(\frac{R_1}{R_1 R_2} - \frac{R_x}{R_3} \right) \quad (3.32)$$

Thus the period T of the output square wave can be expressed by

$$T = 2CR_3 \left(\frac{R_1}{R_1 R_2} - \frac{R_x}{R_3} \right) \quad (3.33)$$

and the frequency f is given by

$$f = \frac{1}{2CR_3 \left(\frac{R_1}{R_1 R_2} - \frac{R_x}{R_3} \right)} \quad (3.34)$$

To demonstrate the practical behavior of the proposed circuit, the circuit of Fig.3.21 was tested using the CFOA AD844. The experimental results and theoretical response are shown in Fig.3.22.

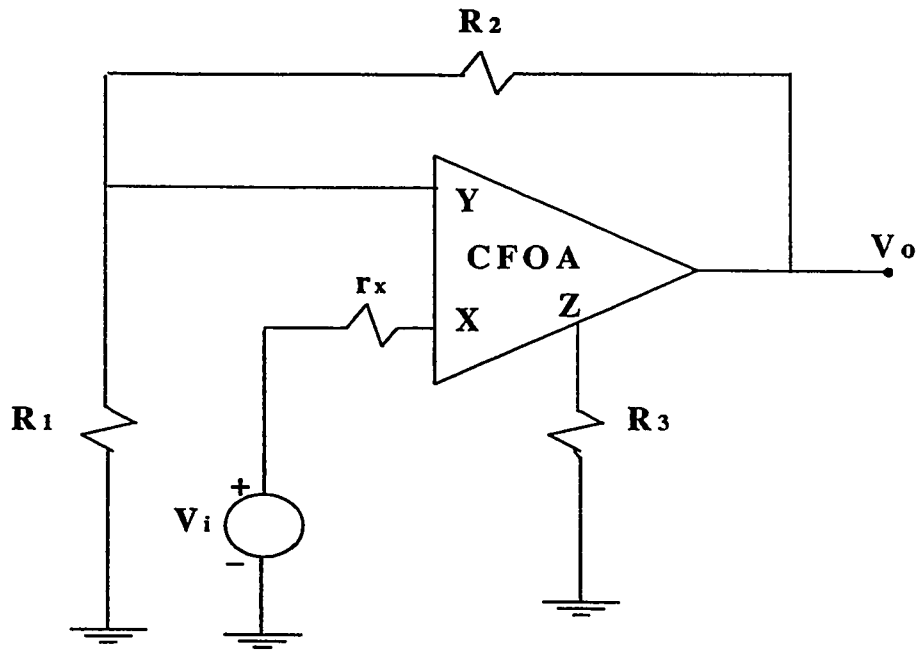


Fig.3.20: Schmitt trigger with a CFOA

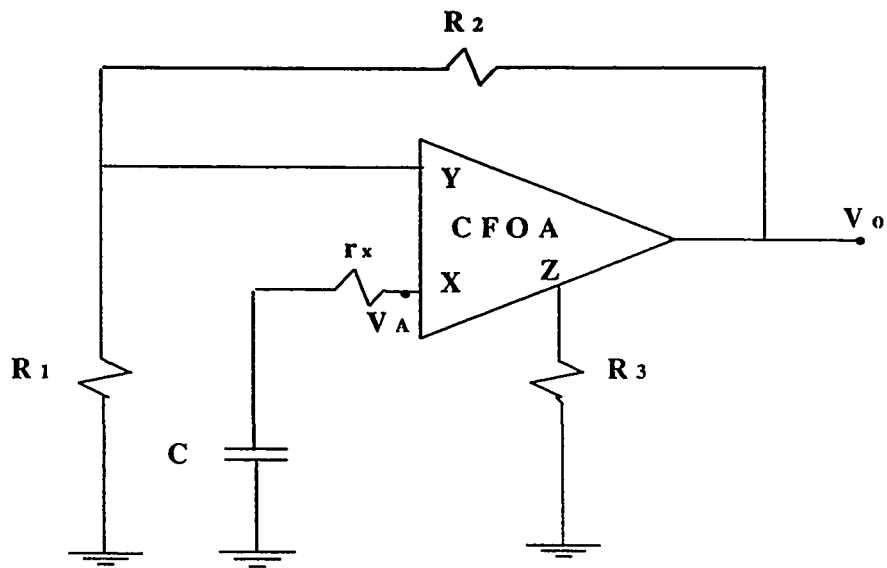
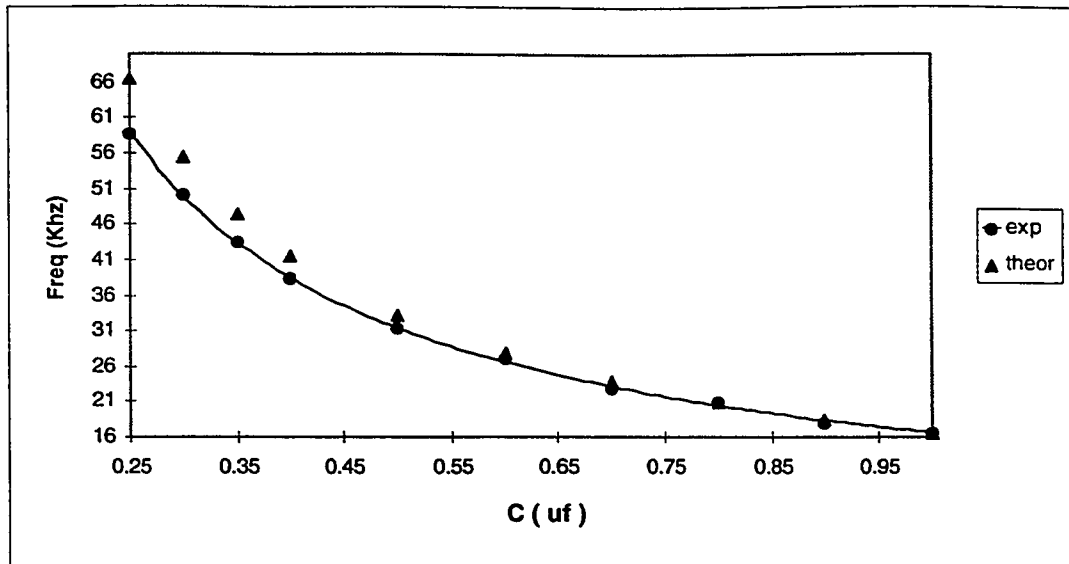
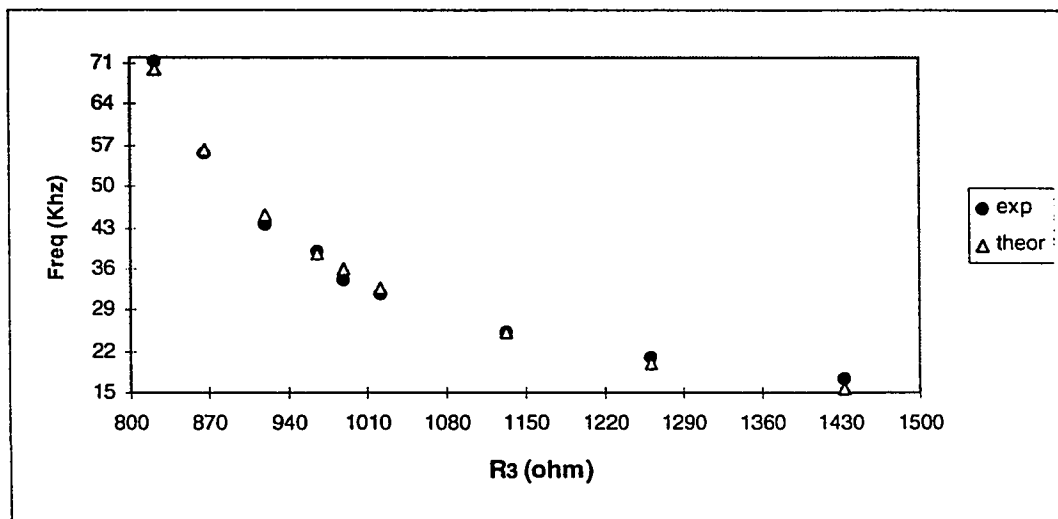


Fig.3.21: Proposed square waveform generator



a)



b)

Fig.3.22 Comparisons between theoretical and experimental results of Fig.3.21

a) $R_1 = 276\Omega$, $R_2 = 3120\Omega$ and $R_3 = 1017\Omega$

b) $R_1 = 276\Omega$, $R_2 = 3120\Omega$ and $C = .5\mu\text{f}$

In this chapter we have seen that some of the experimental results deviate from the theoretical responses. For example, for the oscillator circuit of Fig.3.3(d) the calculated ω_0 is equal to 13.8×10^7 rad and the measured ω_0 is equal to 22.4×10^6 (see Fig.3.5) rad thus the error is equal to 83%. Also for, the oscillator of Fig.3.14, the calculated ω_0 is equal to 9.98×10^6 rad and the measured ω_0 is equal to 6.98×10^6 rad thus the error is equal to 30%. For the oscillator of Fig.3.11 the calculated ω_0 is equal to 2.76×10^6 rad and the measured ω_0 is equal to 2.42×10^6 rad thus the error is equal to 12.5%. It is conjectured that, the nonideality of the CFOA is the main source for this deviation. To investigate this conjecture, the nonideality effect of the CFOA will be discussed in chapter 4.

Chapter 4

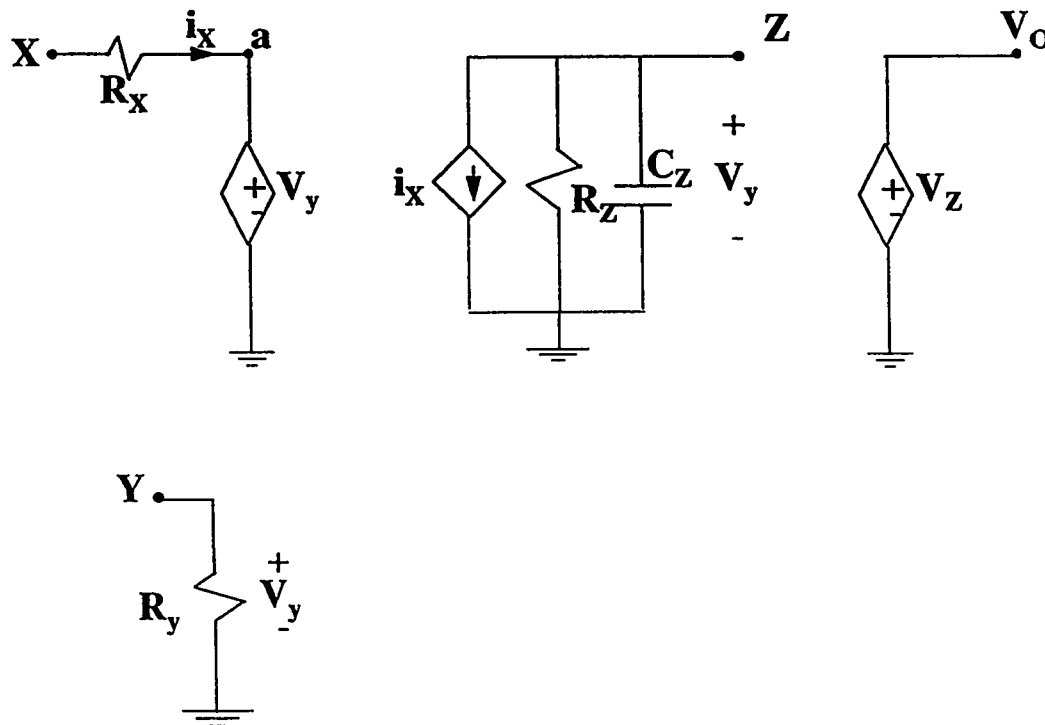
Effect of CFOA Non-idealities

4.1 Introduction

Universal active filters and oscillators circuits were proposed in the last two chapters. It could be noticed that all these circuits required at least one active element (CFOA), in addition to four or more passive components. In addition, all the circuits were analysed assuming the active devices as ideal except for the analysis considering the current and voltage tracking errors. In this chapter we will study indepth the effect of non-idealities due to the current and voltage tracking errors, finite input /output impedance of the input and output buffers, finite pole of the input and output buffers and finite gains pole on the operation and performance of these proposed circuits.

To study the non-ideality affect on the proposed circuits three non-ideal models for the CFOA (AD844) are used here. The first non-ideal model is Svoboda model [22]. It is a simple model, as shown in Fig.4.1, that includes input and output impedances and

a gain having one pole . The second non-ideal model (Bruun model) is shown in Fig. 4.2 [18]. This model takes into consideration the effects of the gain's pole and the input stages capacitances. The third one is the modified Bruun model where the effect of the output stages capacitances is taken in consideration as well. Fig.4.3 shows the third model. This model gave good result at high frequency. Although analysing these circuits using non-ideal model is a very tedious procedure, we will use the first model to analyse one or more of the circuits proposed in chapter 2 and 3. The rest will be analysed using Spice program.



$$R_X = 50 \Omega, R_Y = 10 \text{ M}\Omega, R_Z = 3 \text{ M}\Omega, C_Z = 4.5 \text{ pF}$$

Fig.4.1: Svoboda model of non-ideal CFOA (AD844) [22]

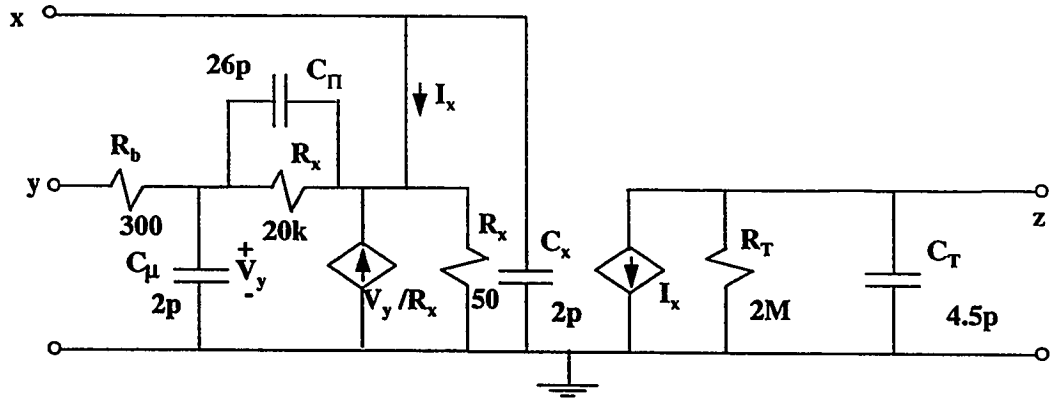


Fig.4.2: Bruun-model of non-ideal CFOA (AD844) [18]

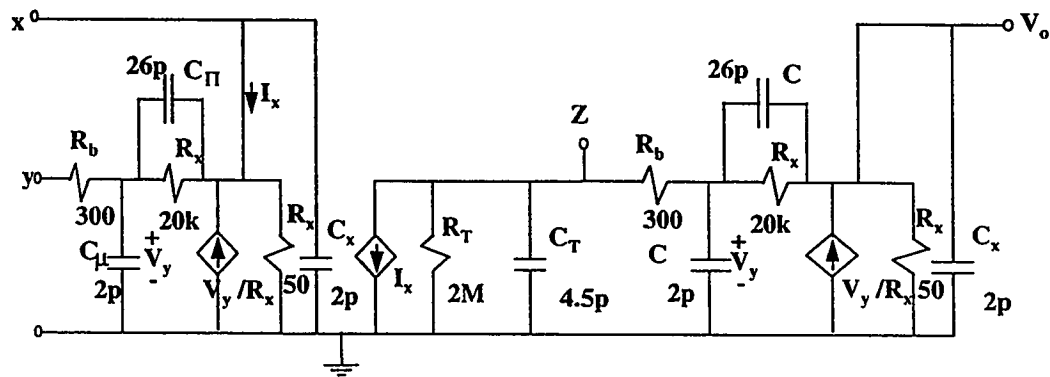


Fig.4.3: Modified Bruun-model of non-ideal CFOA (AD844)

4.2 Effect of the non-idealities on the active filter circuits

Consider, for example, the active filter circuit of Fig.2.1 discussed in chapter 2 and redrawn in Fig. 4.4. Fig.4.5 shows equivalent circuit of the active filter of Fig.4.4 using Svoboda-model.

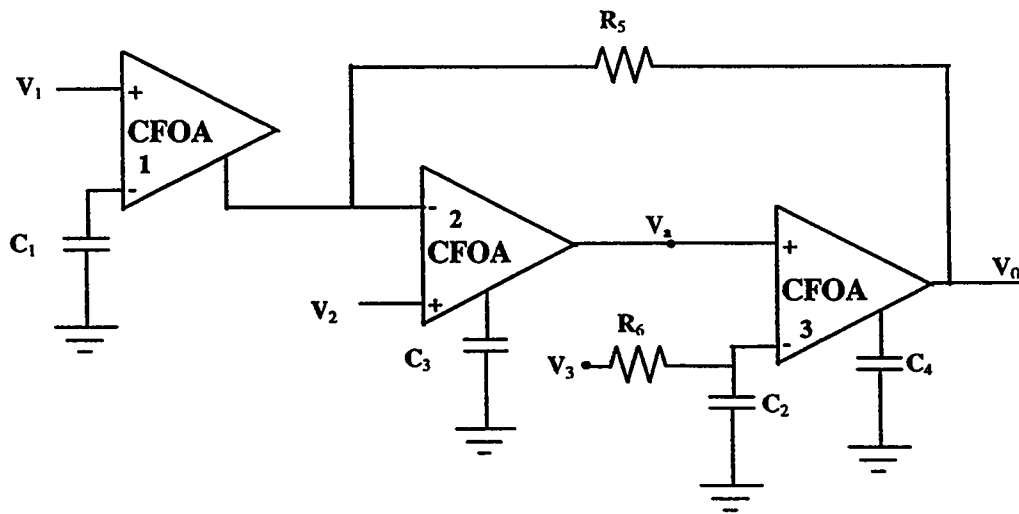


Fig.4.4: *The proposed universal voltage-mode filter of Fig.2.1*

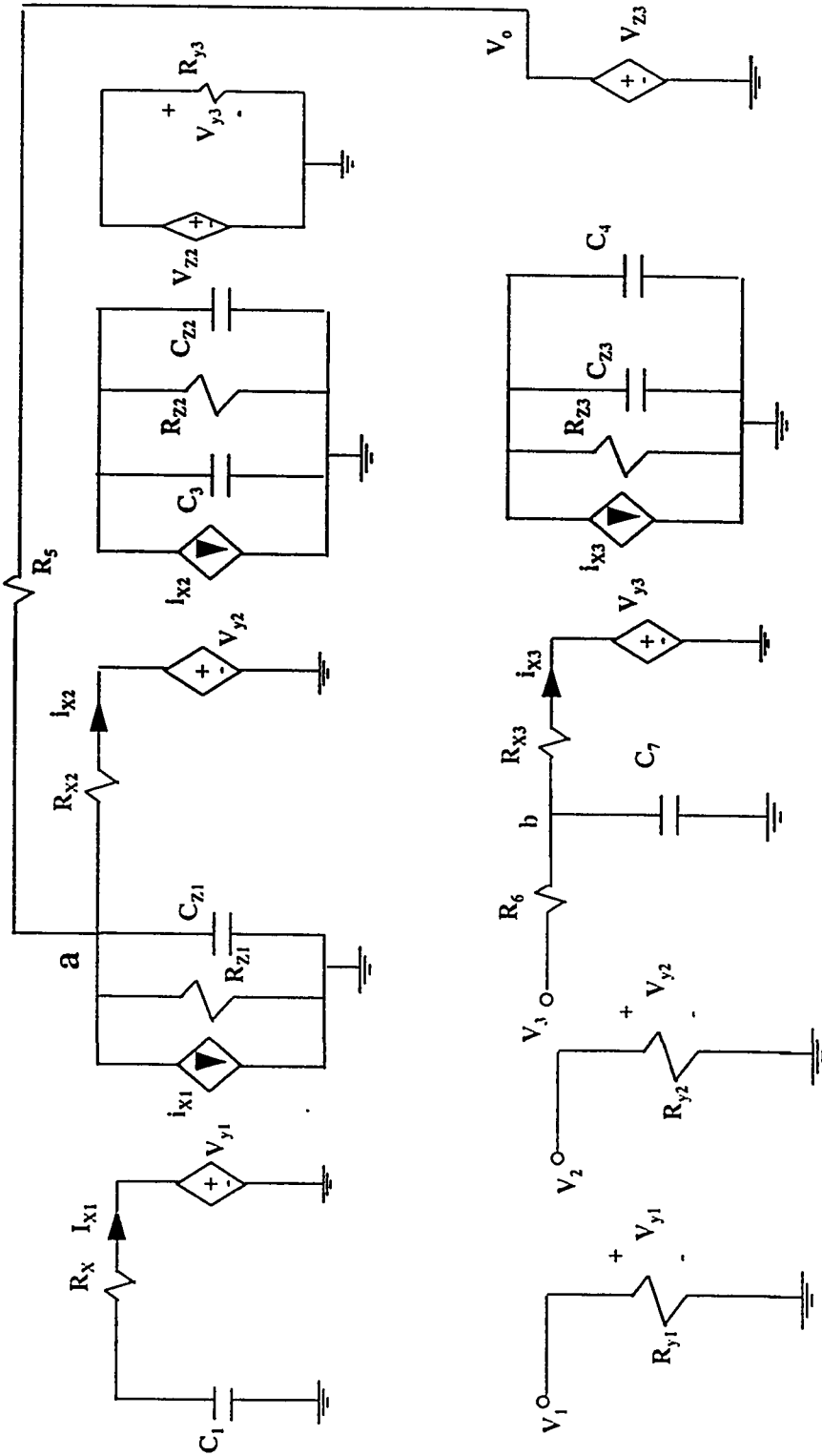


Fig.4.5 Equivalent circuit of the active filter of Fig.4.4 using Svoboda model

Analysing the circuit shown in Fig.4.5, yields ,(for more detail see Appendix A)

$$V_o = \frac{T_1 T_2 T_3 V_3 + T_4 V_2 + T_5 V_1}{T_6 T_2 T_7 + T_8} \quad (4.1)$$

where

$$T_1 = -R_x s(C_z + C_3) - R_x G_z$$

$$T_2 = sC_z + G_z + G_x + G_5$$

$$T_3 = \frac{G_6}{sC_7 + G_6}$$

$$T_4 = sC_z + G_z + G_5$$

$$T_5 = \frac{-sC_1}{1 + R_x sC_1}$$

$$T_6 = R_x s(C_z + C_3) + R_x G_z$$

$$T_7 = \frac{s(C_z + C_4) + G_z}{sC_7 + G_6} + R_x s(C_z + C_4)$$

and

$$T_8 = G_5$$

Further simplification yields

$$V_o \approx \frac{-G_6(G_z + sC_3 + R_x s^2 C_1 C_3)V_3 + (sG_5 C_7 + G_5 G_6)V_2 - (s^2 C_1 C_7 + sC_1 C_6)V_1}{s^2 C_3 C_4 + G_5 G_6 + sG_5 C_7}$$

(4.2)

The effect of the nonideality can be seen by comparing equation (4.2) with Equation (2.6). It can be noticed that the nonideality introduces new terms (sC_3 and $s^2R_xC_1C_3$) in numerator of equation (4.2). Figs. 4.6 and 4.7 show comparisons between the experimental results and the calculated values using ideal, Svoboda and Bruun models for the active filter circuits of Figs.2.1 and 2.7 respectively.

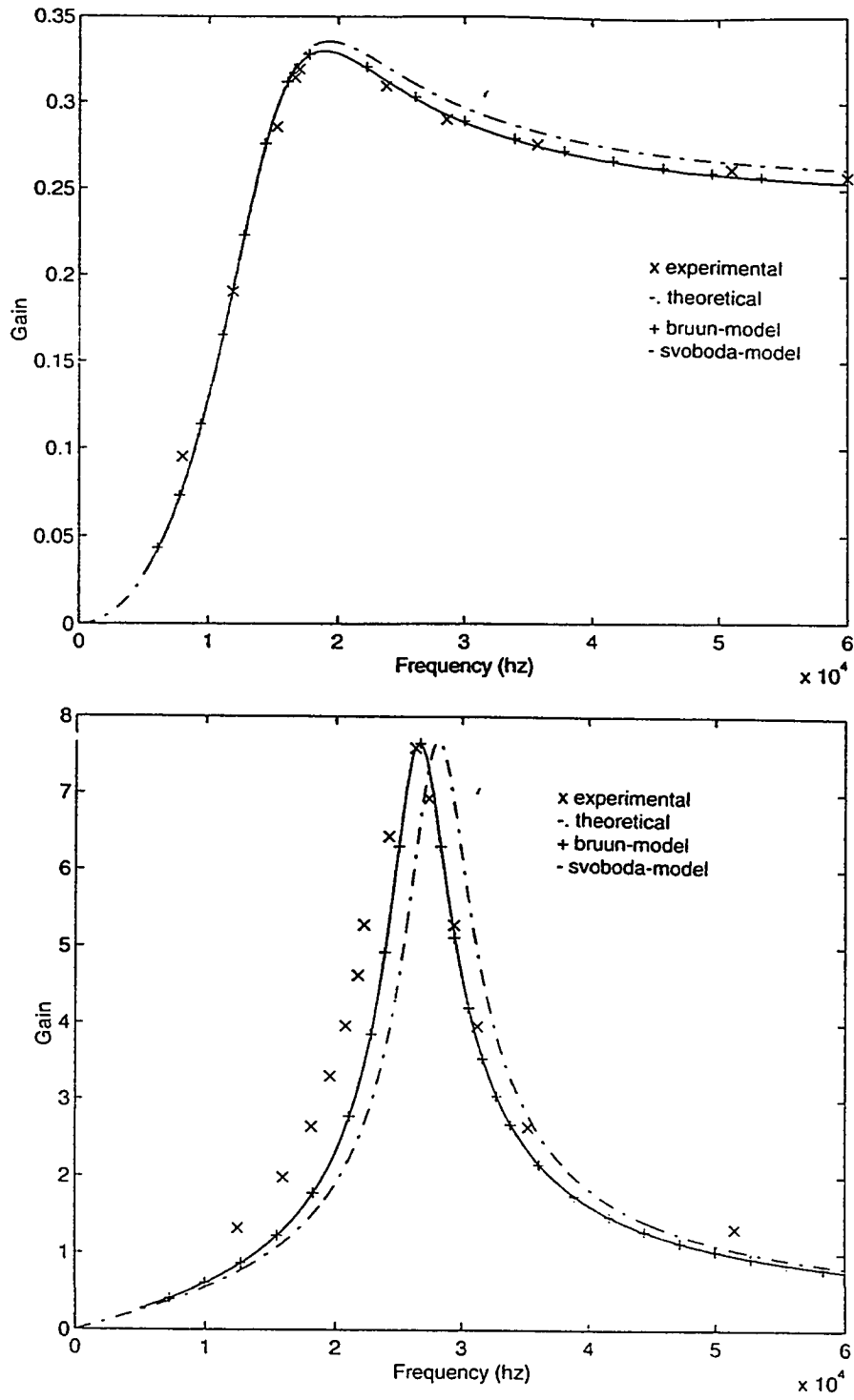


Fig.4.6: Comparison between experimental and calculated results for the BP and HP filters of the universal active filter shown in Fig.4.4.

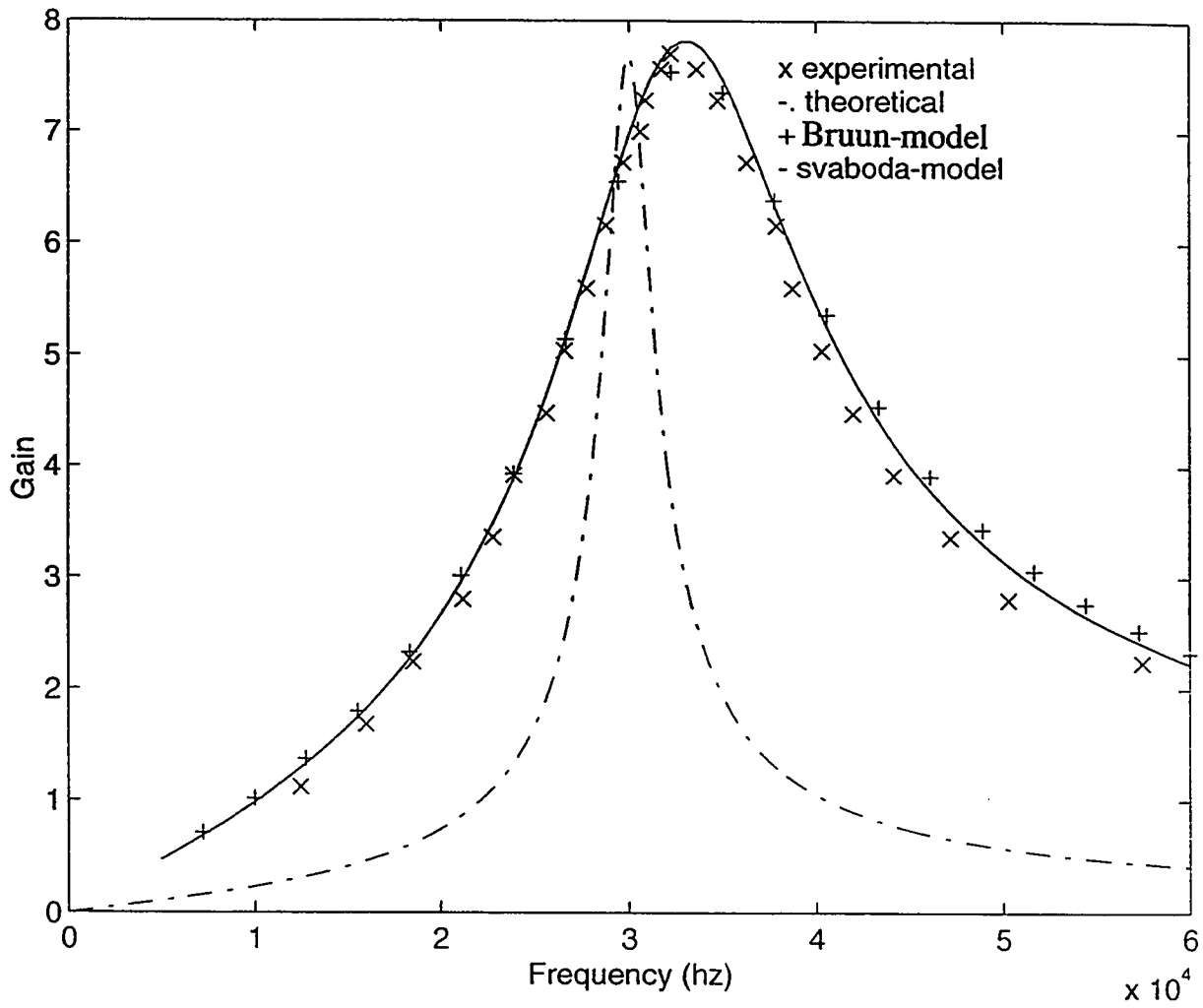


Fig.4.7: Comparison between experimental and calculated results for the BP filter of the universal filter shown in Fig.2.7.

Consider, for example, the active filter circuit of Fig.2.4 discussed in chapter 2 and redrawn in Fig.4.8 to investigate the effect of the voltage and the current tracking errors in more detailed manner. Fig.4.9 shows the equivalent circuits of this filter using Svoboda model where $\alpha_1, \alpha_2, \beta_1, \beta_2, \beta_3$ represent the current and voltage tracking errors.

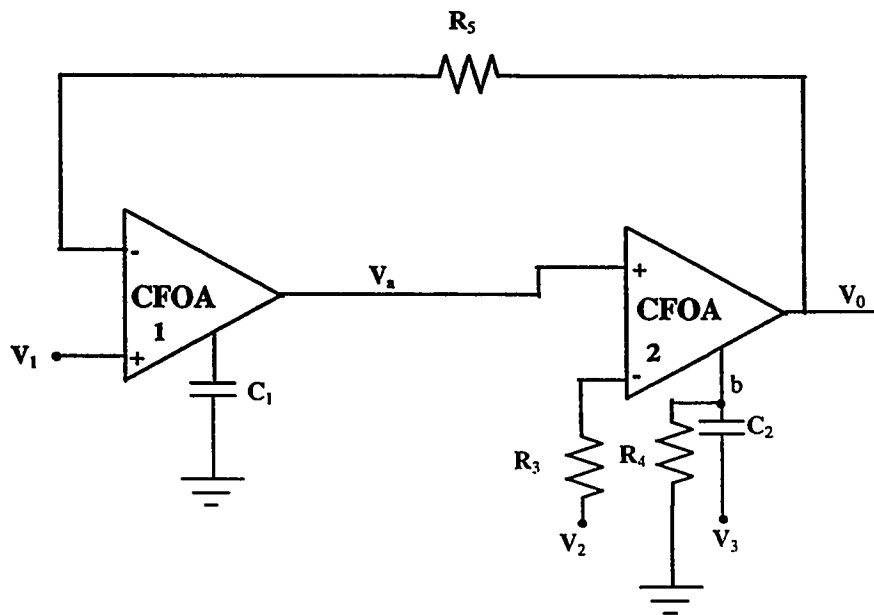


Fig.4.8: *The proposed universal voltage-mode filter of Fig.2.4*

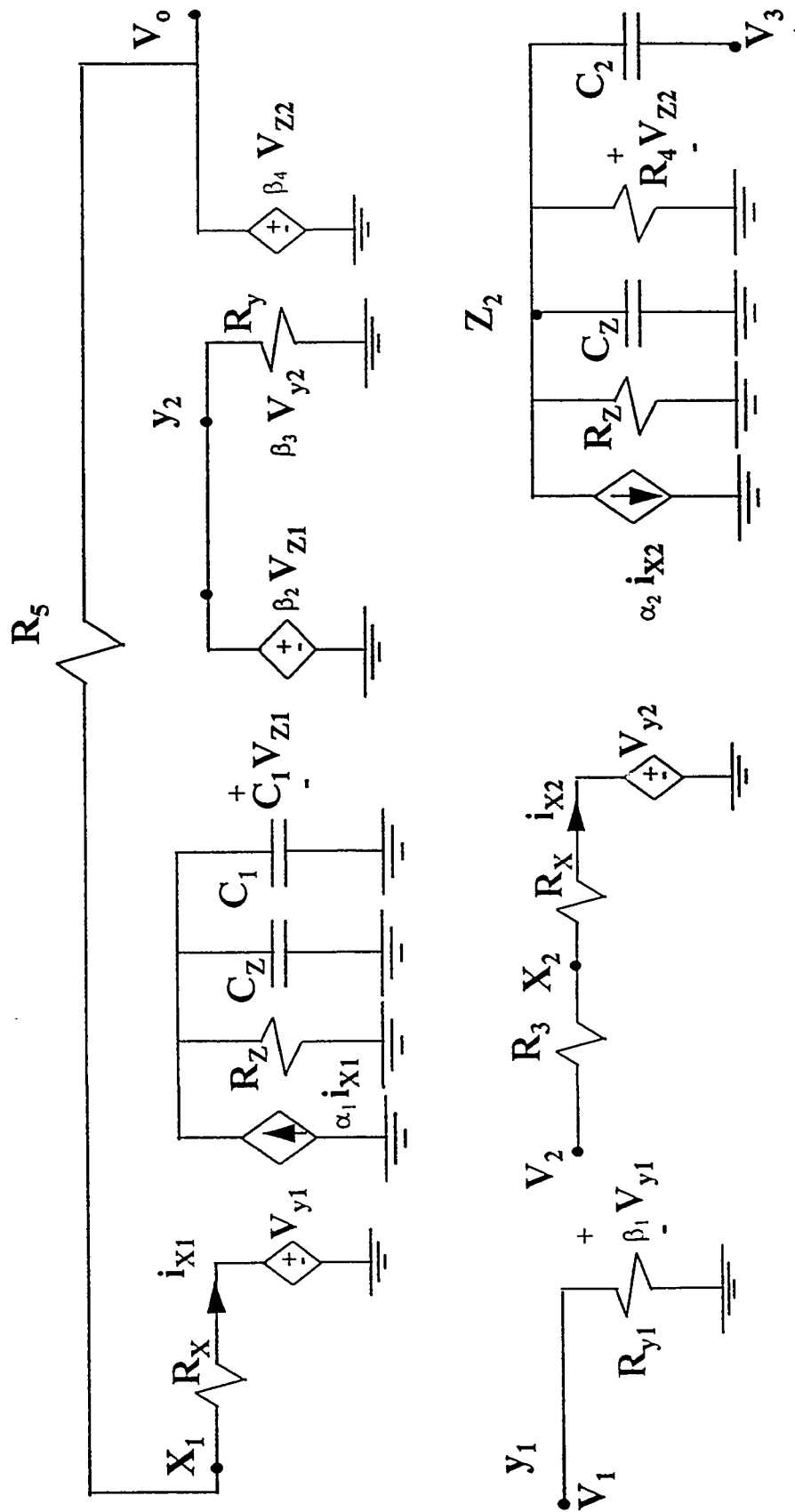


Fig.4.9: Equivalent circuit of the active filter of fig.4.8 using Svoboda model

Analysing the circuit shown in Fig.4.9, yields ,(for more detail see Appendix B)

$$\begin{aligned} V_o \left[1 + \frac{\beta_4 \alpha_2}{G_4 + sC_2} \frac{1}{(R_3 + R_x)} \left(\frac{R_z}{1 + R_z sC_1} \right) \frac{\beta_2 \alpha_1}{\beta_3 (R_5 + R_x)} \right] = \\ \beta_4 \frac{sC_2}{G_4 + sC_2} - \frac{\beta_4 \alpha_2}{G_4 + sC_2} \left[\frac{V_2}{R_3 + R_x} - \frac{1}{R_3 + R_x} \left[\frac{\beta_2}{\beta_3} \alpha_1 \frac{R_z}{1 + R_z sC_1} \frac{1}{R_5 + R_x} \frac{V_1}{\beta_1} \right] \right] \end{aligned} \quad (4.3)$$

$$V_o = \frac{T_1 V_1 + T_2 V_2 + T_3 V_3}{T_4} \quad (4.4)$$

where

$$T_1 = \frac{\beta_4 \alpha_2}{G_4 + sC_2} \frac{1}{(R_3 + R_x)} \left(\frac{\beta_2}{\beta_1 \beta_3} \alpha_1 \frac{R_z}{(1 + R_z sC_1)(R_5 + R_x)} \right)$$

$$T_2 = -\frac{\beta_4 \alpha_2}{(G_4 + sC_2)(R_3 + R_x)}$$

$$T_3 = \frac{\beta_4 sC_2}{(G_4 + sC_2)}$$

$$T_4 = 1 + \frac{\beta_4 \alpha_2}{(G_4 + sC_2)(R_3 + R_x)} \left(\frac{R_z}{(1 + R_z sC_1)} \right) \frac{\beta_2 \alpha_1}{\beta_3 (R_5 + R_x)}$$

The effect of the nonideality can be seen by comparing equation (4.4) with equation (2.12). Fig.4.10 shows comparisons between the experimental results and the calculated values using ideal, Svoboda and Bruun models for the active filter circuit of Fig.4.8.

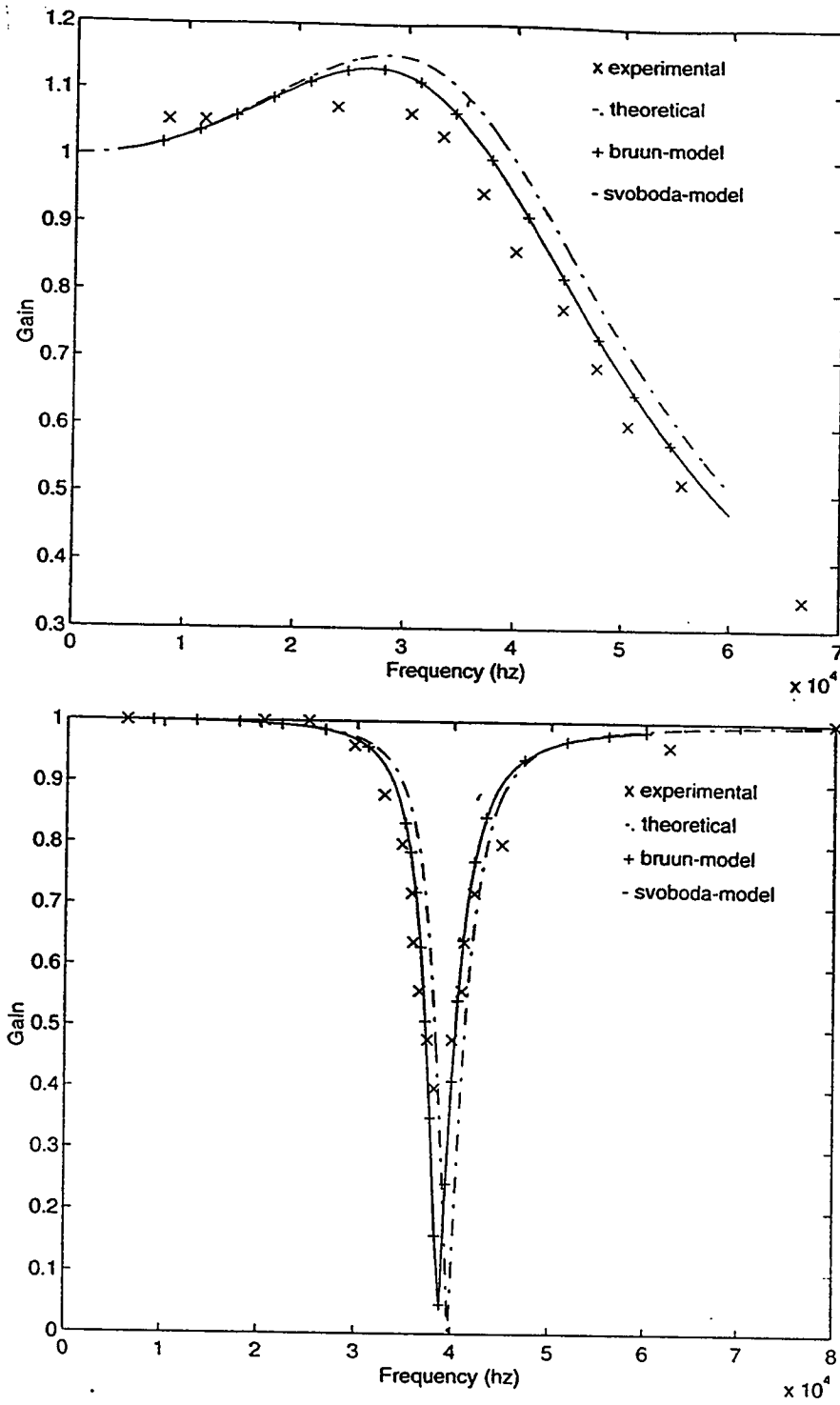


Fig.4.10: Comparison between experimental and calculated results for the BR and LP filters of the universal active filter shown in Fig.4.8.

4.3 Effect of the non-idealities on the Oscillator Circuits

Consider, for example, the oscillator circuit of Fig.3.14 discussed in chapter 3 and redrawn in Fig.4.11. The equivalent circuit of this oscillator using Svoboda-model is shown in Fig.4.12.

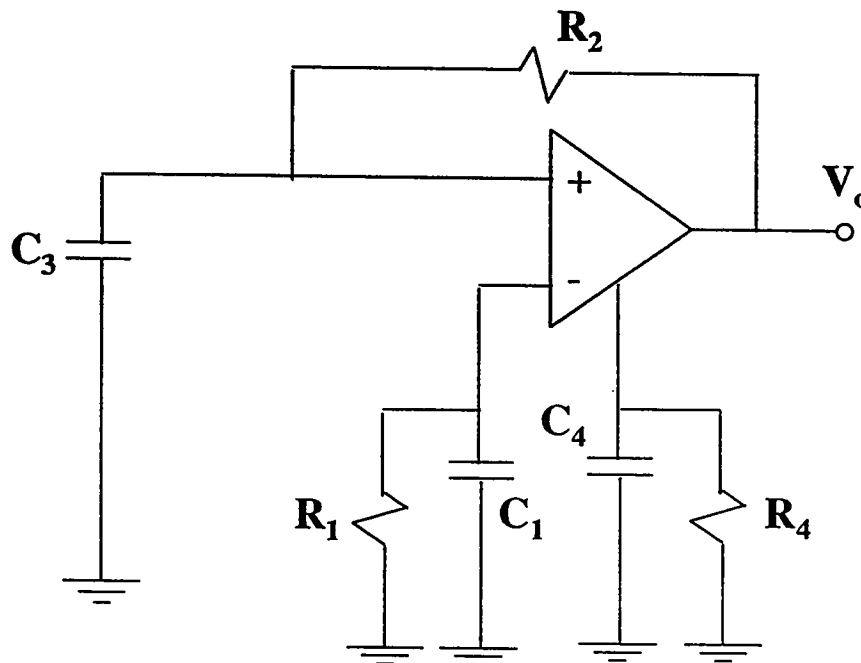


Fig.4.11: *The proposed oscillator circuit of Fig.3.14*

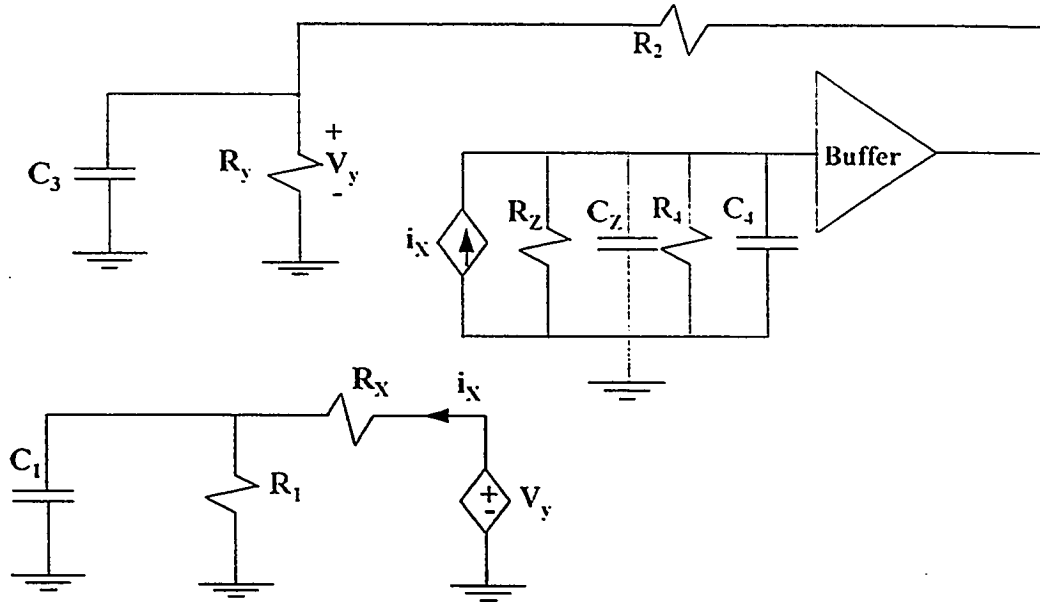


Fig.4.12.Equivalent circuit of the oscillator circuit of Fig.4.8 using Svoboda model

Analysing the circuit shown in Fig.4.12, yields the frequency of oscillation as (for more detail see Appendix C)

$$\omega_o^2 = \frac{(R_y + R_2)(R_1 + R_x) - R_1 R_y}{R_4 R_y R_1 C_B (R_x C_1 + R_2 C_3) + R_4 C_B R_2 R_x (R_1 C_1 + R_y C_3) + R_2 R_y R_x R_1 C_3 C_1} \quad (4.5)$$

where

$$C_B = C_4 + C_z$$

and the condition of oscillation as

$$\begin{aligned} (R_4 R_2 R_y R_x R_1 C_B C_3 C_1) (R_y + R_2) (R_1 + R_x) - R_4 R_y = \\ (R_4 R_y R_1 C_B (R_x C_1 + R_2 C_3) + R_4 C_B R_2 R_x (R_1 C_1 + R_y C_3) + R_2 R_y R_x R_1 C_3 C_1) \\ (R_y R_1 (R_x C_1 + R_2 C_3) + R_2 R_x (R_1 C_1 + R_y C_3) + R_y C_B (R_y + R_2) (R_1 + R_x) - R_4 R_y R_1 C_1) \end{aligned} \quad (4.6)$$

The effect of the nonideality can be seen by comparing equation (3.21) with equation (4.5). Table 4.1 shows the experimental results and the calculated one using Equations (3.20) and (4.5) as a function of R_1 . The same data in addition to the calculated one using Bruun model and improved Bruun model is depicted in the form of a graph, shown in Fig.4.13.

Table 4.1: Comparison of measured and calculated values of the frequency of oscillation of Fig.4.11.

R1 (ohm)	Experimental (mega hz)	Theoretical (mega hz)	Sva-model (mega hz)
9190	1.111	1.588	1.349
6610	1.0526	1.529	1.3089
4130	1	1.3964	1.1918
3540	0.95238	1.333	1.14
2910	0.909909	1.2306	1.0515
2673	0.869565	1.176	1.009
2445	0.83333	1.1107	0.9532
2332	0.8	1.0717	0.9183
2206	0.76923	1.0215	0.88
2114	0.74074	0.9792	0.846
2067	0.714285	0.95534	0.831

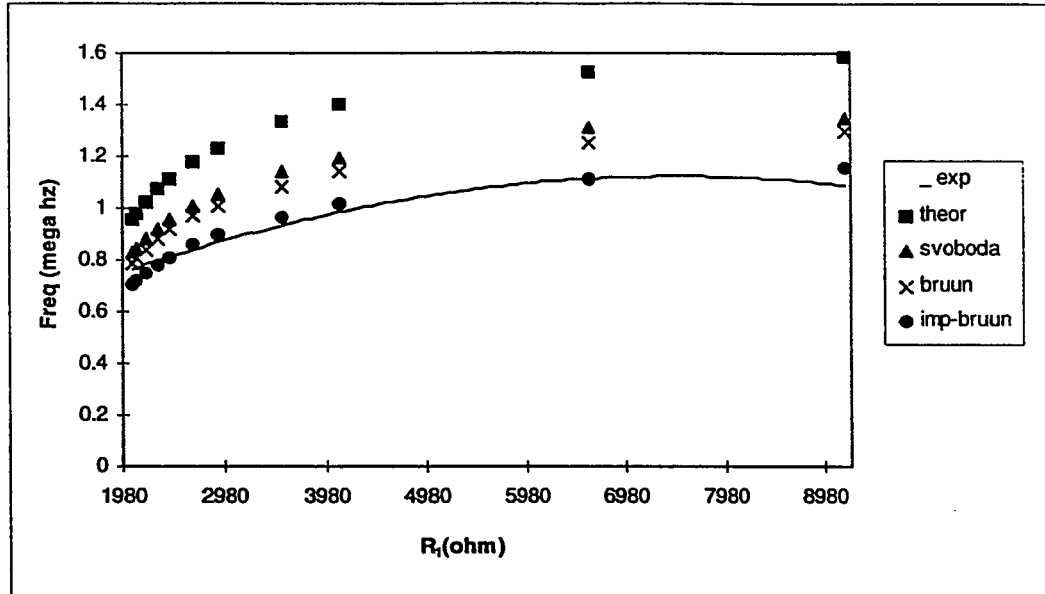


Fig.4.13: Comparison between experimental and calculated results for the frequency of oscillation of Fig.4.11.

Figs. 4.14, 4.15 and 4.16 show comparisons between the experimental results and the calculated one using ideal and modified Bruun models for two of the proposed circuits in chapter 3 (Figs.3.3(d),(e) and 3.6).

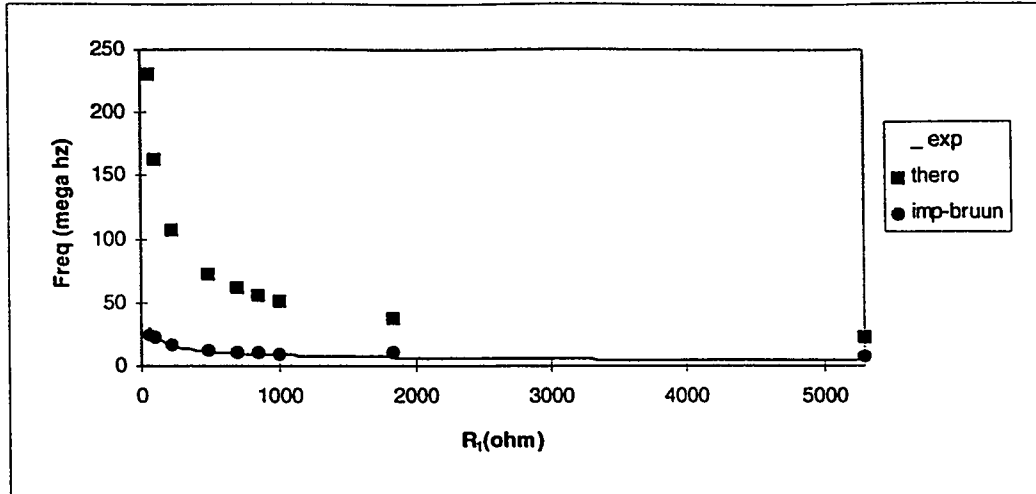


Fig.4.14: Comparison between the experimental and calculated results for the oscillator circuit shown in Fig.3.3(d)

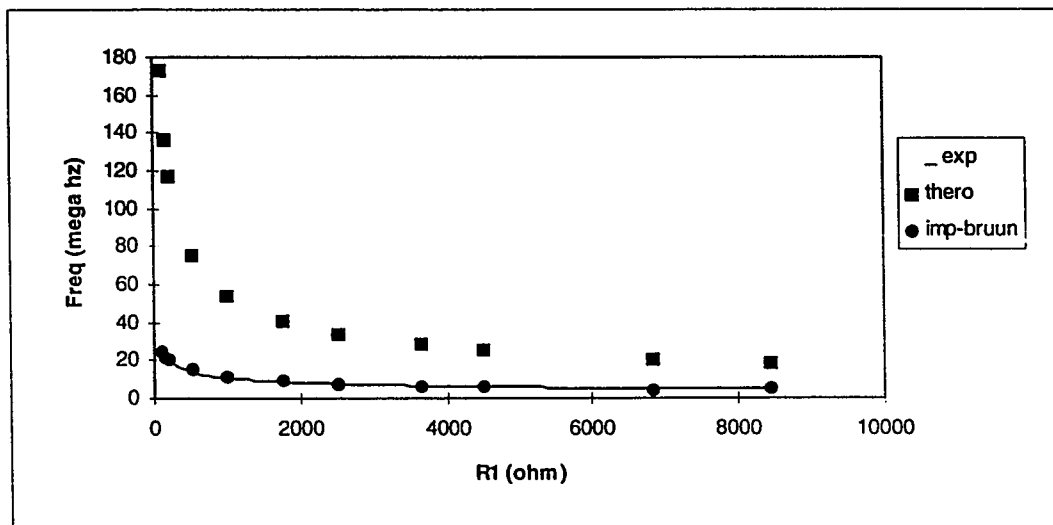


Fig.4.15: Comparison between the experimental and calculated results for the oscillator circuit shown in Fig.3.3(e)

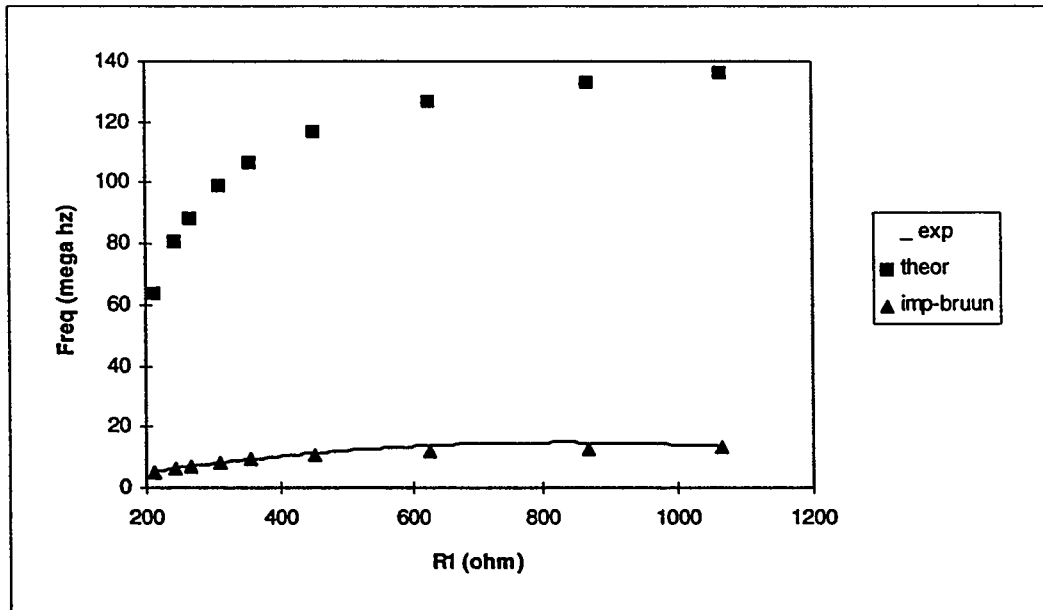


Fig.4.16: Comparison between the experimental and calculated results for the oscillator circuit shown in Fig.3.6.

In conclusion, it appears that the deviation between the experimental and the calculated result is decreased when the nonideal model of the CFOA is used. This prove that the non idealities of the CFOA are the main sources of the errors observed in Figs.(2.2, 2.4, 2.8, 2.10, 3.5, 3.8, 3.9, 3.15 and 3.16)shown in chapters 2 and 3 where the errors were relatively large.

Chapter 5

Conclusion and Future Work

5.1 Introduction

In this thesis, we have investigated the use of Current feedback operational amplifiers in designing universal active filters. In this regard, five new universal active filters were presented. Also, a number of oscillator and signal generator circuits were presented using the CFOA. In this chapter, we will draw some conclusions regarding this work. Then, some important extensions that can be considered for further research in this area are proposed.

5.2 Conclusions

Current feedback operational amplifier have proved to be functionally flexible and versatile. From this fact the current feedback operational amplifier have been used in some areas such as active filters and oscillators.

In this thesis, the current feedback operational amplifier has been used in three areas: active filters, oscillators and signal generators. In active filter area three voltage-mode and two current-mode active filters were presented. A comparison between the most recently published circuit and the proposed circuits has been done. The comparison shows that the proposed active filters have some advantages over the published one.

In oscillators, a number of CFOA-based oscillator circuits were presented. Most of them use grounded capacitors and enjoy both independent control of frequency and condition of oscillation.

A new CFOA-based signal generator was presented, where three different signals can be generated from this signal generator. Also a square waveform generator using CFOA was presented.

Many points have been taken into consideration to evaluate these circuits. Then this evaluation was used to find optimum circuits wherever possible.

The effect of current and voltage tracking errors of the CFOA were taken into account in the proposed circuits of filters and oscillators. Active and passive sensitivities of the ω_0 and Q in filters and of ω_0 in oscillators were calculated and found to be small.

These circuits were practically implemented to verify the theory. The measured and calculated results are in good agreement in most of the cases. In some cases the experimental results deviate appreciably from the theoretical response. For example, for the BP of Fig.2.1 calculated ω_0 is equal to 16.5×10^4 rad and the measured ω_0 is equal to 17.59×10^4 rad thus the error is equal to 6.4%. Also for the BP of Fig.2.7 the calculated ω_0 is equal to 18.8×10^4 rad and the measured ω_0 is equal to 20.2×10^4 rad thus the error is equal to 7.2%. For the oscillator circuit of Fig.3.3(d) calculated ω_0 is equal to 13.8×10^7 rad and the measured ω_0 is equal to 22.4×10^6 rad thus the error is equal to 83%. Also for, the oscillator of Fig.3.14, the calculated ω_0 is equal to 9.98×10^6 rad and the measured ω_0 is equal to 6.98×10^6 rad thus the error is equal to 30%. To investigate the possible reasons behind these differences many proposed circuits were either reanalyzed using Svoboda model or simulated by PSPICE using Bruun and modified Bruun models of the CFOA. The agreement between the experimental and the improved analysis and / or simulation appears to be good.

To conclude, one can say that the CFOA-based filters, oscillators and signal generators circuits presented in this thesis have attractive features compared to the related existing circuits.

5.3 Directions for Future Work

Since nothing is perfect and complete in this life, this work can be improved and extended in many directions.

- Finding universal filter circuits which have advantages over the proposed circuits in terms of grounded capacitors, independent control of ω_0 , ω_0/Q_0 , minimum number of passive and active components and no requirement for matching conditions simultaneously.
- Realizing universal current-mode single input multiple outputs filters using the CFOA.
- Introducing the CFOA into the signal generator area. For example, in chapter 3 we have proposed a signal generator circuit. One way to improve this circuit is to replace the voltage mode comparators by CFOA-based comparators.

APPENDIX

Appendix A

Analyzing the circuit shown in Fig.4.5, we have,

$$i_{x_1} = -V_1 \frac{sC_1}{1 + R_x sC_1} \quad (\text{A.1})$$

$$i_{x_2} = -\frac{R_z s(C_z + C_3) + 1}{R_z} V_{y_3} \quad (\text{A.2})$$

$$i_{x_3} = -\frac{R_z s(C_z + C_4) + 1}{R_z} V_o \quad (\text{A.3})$$

Applying KCL at node a yields,

$$V_a \left(\frac{R_z sC_z + 1}{R_z} + G_x + G_5 \right) + i_{x_1} - V_o G_5 - V_2 G_x = 0 \quad (\text{A.4})$$

Applying KCL at node b yields,

$$V_b (sC_7 + G_6) - V_3 G_6 + i_{x_3} = 0 \quad (\text{A.5})$$

Substituting equation (A.3) in Equation (A.5), we get,

$$V_b = \left(V_3 G_6 + \frac{R_z s(C_z + C_4) + 1}{R_z} V_o \right) \left(\frac{1}{sC_7 + G_6} \right) \quad (A.6)$$

Now

$$i_{x_3} = (V_b - V_{y_3}) G_x \quad (A.7)$$

Substituting Equations (A.3) and (A.6) in (A.7), we get,

$$V_{y_3} = V_3 \left(\frac{G_6}{sC_7 + G_6} \right) + V_o \left(\frac{R_z s(C_z + C_4) + 1}{R_z (sC_7 + G_6)} + \frac{R_z s(C_z + C_4) + 1}{R_z G_x} \right) \quad (A.8)$$

Putting V_{y_3} from equation (A.8) in equation (A.2) gives,

$$i_{x_2} = -\frac{R_z s(C_z + C_3) + 1}{R_z} \left(V_3 \frac{G_6}{sC_7 + G_6} + V_o \left(\frac{R_z s(C_z + C_4) + 1}{R_z (sC_7 + G_6)} + \frac{R_z s(C_z + C_4) + 1}{R_z G_x} \right) \right) \quad (A.9)$$

At node a,

$$V_a = i_{x_2} R_x + V_2 \quad (A.10)$$

Substituting equation (A.9) in Equation (A.10), we get,

$$V_a = -\frac{R_x R_z s(C_2 + C_3) + R_x}{R_z} \left(V_3 \frac{G_6}{sC_7 + G_6} + V_o \left(\frac{R_z s(C_2 + C_4) + 1}{R_z (sC_7 + G_6)} + \frac{R_z s(C_2 + C_4) + 1}{R_z G_x} \right) \right) + V_2 \quad (\text{A.11})$$

Equations (A.1), (A.4) and (A.11) gives

$$V_o = \frac{T_1 T_2 T_3 V_3 + T_4 V_2 + T_5 V_1}{T_6 T_2 T_7 + T_8} \quad (\text{A.12})$$

where

$$T_1 = -R_x s(C_2 + C_3) - R_x G_z$$

$$T_2 = sC_2 + G_z + G_x + G_5$$

$$T_3 = \frac{G_6}{sC_7 + G_6}$$

$$T_4 = sC_2 + G_z + G_5$$

$$T_5 = \frac{-sC_1}{1 + R_x sC_1}$$

$$T_6 = R_x s(C_2 + C_3) + R_x G_z$$

$$T_7 = \frac{s(C_2 + C_4) + G_z}{sC_7 + G_6} + R_x s(C_2 + C_4)$$

and

$$T_8 = G_5$$

Further simplification yields

$$V_o \approx \frac{-G_6(G_Z + sC_3 + R_x s^2 C_1 C_3)V_3 + (sG_5 C_7 + G_5 G_6)V_2 - (s^2 C_1 C_7 + sC_1 C_6)V_3}{s^2 C_3 C_4 + G_5 G_6 + sG_5 C_7}$$

(A.13)

Appendix B

Analyzing the circuit shown in Fig.4.9, we have,

$$i_{x_1} = \frac{V_o - V_{y_1}}{R_5 + R_x} \quad (\text{B.1})$$

$$V_1 = \beta_1 V_{y_1} \quad (\text{B.2})$$

Substituting equation (B.1) in equation (B.2), we get

$$i_{x_1} = \frac{V_o - (V_1/\beta_1)}{R_5 + R_x} \quad (\text{B.3})$$

$$V_{z_1} = \alpha_1 i_x \frac{\frac{1}{R_z s(C_z + C_1)}}{R_z + \frac{1}{s(C_z + C_1)}} = \alpha_1 i_x \frac{R_z}{1 + R_z s(C_z + C_1)} \quad (\text{B.4})$$

Substituting Equation (B.3) in equation (B.4), we get

$$V_{z_1} = \alpha_1 \left(\frac{V_o - (V_1/\beta_1)}{R_5 + R_x} \right) \frac{R_z}{1 + R_z s(C_z + C_1)} \quad (\text{B.5})$$

$$V_{y_2} = \frac{\beta_2}{\beta_3} V_{z_1} \quad (\text{B.6})$$

Putting V_{z_1} from equation (B.5) in equation (B.6) gives

$$V_{y_2} = \frac{\beta_2}{\beta_3} \alpha_1 \left(\frac{V_o - (V_1/\beta_1)}{R_5 + R_x} \right) \frac{R_z}{1 + R_z s(C_z + C_1)} \quad (\text{B.7})$$

Applying kcl at node X_2 yields,

$$i_{x_2} = \frac{V_2 - V_{y_2}}{R_3 + R_x} = \frac{V_2}{R_3 + R_x} - \frac{1}{R_3 + R_x} \left[\frac{\beta_2 \alpha_1 \left(\frac{V_o - (V_1/\beta_1)}{R_5 + R_x} \right) \frac{R_z}{1 + R_z s(C_2 + C_1)}}{\beta_3} \right] \quad (\text{B.8})$$

$$.V_{z_2} \left[\frac{1}{R_4} + sC_2 + \frac{1}{R_z} + sC_2 \right] - V_3 sC_2 + \alpha_2 i_{x_2} = 0 \quad (\text{B.9})$$

Applying kcl at node Z_2 yields,

$$.V_{z_2} = \frac{sC_2}{G_4 + sC_2 + G_z + sC_2} V_3 - \frac{\alpha_2}{G_4 + sC_2 + G_z + sC_2} i_{x_2} \quad (\text{B.10})$$

$$.V_o = \beta_4 V_{z_2} \quad (\text{B.11})$$

Substituting Equations (B.8) and (B.10) in equation (B.11), we get,

$$.V_o = \beta_4 \frac{sC_2}{G_4 + sC_2 + G_z + sC_2} V_3 - \frac{\beta_4 \alpha_2}{G_4 + sC_2 + G_z + sC_2} \left[\frac{V_2}{R_3 + R_x} - \frac{1}{R_3 + R_x} \left[\frac{\beta_2 \alpha_1 \left(\frac{V_o - (V_1/\beta_1)}{R_5 + R_x} \right) \frac{R_z}{1 + R_z s(C_2 + C_1)}}{\beta_3} \right] \right] \quad (\text{B.12})$$

or

$$.V_o \left[1 + \frac{\beta_4 \alpha_2 \frac{1}{R_3 + R_x} \left(\frac{R_z}{1 + R_z s(C_2 + C_1)} \right) \frac{\beta_2 \alpha_1}{\beta_3}}{G_4 + sC_2 + G_z + sC_2} \right] = \beta_4 \frac{sC_2}{G_4 + sC_2 + G_z + sC_2} V_3 - \frac{\beta_4 \alpha_2}{G_4 + sC_2 + G_z + sC_2} \left[\frac{V_2}{R_3 + R_x} - \frac{1}{R_3 + R_x} \left[\frac{\beta_2 \alpha_1 \frac{R_z}{1 + R_z s(C_2 + C_1)} \frac{1}{R_5 + R_x} \frac{V_1}{\beta_1}}{\beta_3} \right] \right] \quad (\text{B.13})$$

Since

$$C_z \ll C_2$$

$$C_z \ll C_1$$

$$G_z \ll G_4$$

We can simplify equation (B.13)

$$\begin{aligned}
 \cdot V_o \left[1 + \frac{\beta_4 \alpha_2}{G_4 + sC_2} \frac{1}{(R_3 + R_x)} \left(\frac{R_z}{1 + R_z sC_1} \right) \frac{\beta_2 \alpha_1}{\beta_3 (R_5 + R_x)} \right] = \\
 \cdot \beta_4 \frac{sC_2}{G_4 + sC_2} - \frac{\beta_4 \alpha_2}{G_4 + sC_2} \left[\frac{V_2}{R_3 + R_x} - \frac{1}{R_3 + R_x} \left[\frac{\beta_2 \alpha_1}{\beta_3} \frac{R_z}{1 + R_z sC_1} \frac{1}{R_5 + R_x} \frac{V_1}{\beta_1} \right] \right]
 \end{aligned}
 \tag{B.14}$$

or

$$\cdot V_o = \frac{T_1 V_1 + T_2 V_2 + T_3 V_3}{T_4} \tag{B.15}$$

where

$$\cdot T_1 = \frac{\beta_4 \alpha_2}{G_4 + sC_2} \frac{1}{(R_3 + R_x)} \left(\frac{\beta_2 \alpha_1}{\beta_1 \beta_3} \frac{R_z}{(1 + R_z sC_1)(R_5 + R_x)} \right)$$

$$\cdot T_2 = - \frac{\beta_4 \alpha_2}{(G_4 + sC_2)(R_3 + R_x)}$$

$$\cdot T_3 = \frac{\beta_4 sC_2}{(G_4 + sC_2)}$$

$$\cdot T_4 = 1 + \frac{\beta_4 \alpha_2}{(G_4 + sC_2)(R_3 + R_x)} \left(\frac{R_z}{(1 + R_z sC_1)} \right) \frac{\beta_2 \alpha_1}{\beta_3 (R_5 + R_x)}$$

Appendix C

Analyzing the circuit shown in Fig.4.12, we have,

$$V_y = V_z \left(\frac{R_y}{R_y + R_2(1 + R_2 s C_3)} \right) \quad (C.1)$$

$$i_x = V_y \left(\frac{1 + R_1 s C_1}{R_1 + R_x(1 + R_1 s C_1)} \right) \quad (C.2)$$

also

$$i_x = V_z \left(\frac{1 + R_4 s(C_4 + C_z)}{R_4} \right) \quad (C.3)$$

Combining equations (C.2) and (C.3) yields,

$$V_y \left(\frac{1 + R_1 s C_1}{R_1 + R_x(1 + R_1 s C_1)} \right) = V_z \left(\frac{1 + R_4 s(C_4 + C_z)}{R_4} \right) \quad (C.4)$$

By substituting equation (C.1) in equation (C.4), we get,

$$\left(\frac{R_y}{R_y + R_2(1 + R_2sC_3)} \right) \left(\frac{1 + R_1sC_1}{R_1 + R_x(1 + R_1sC_1)} \right) = \left(\frac{1 + R_4s(C_4 + C_z)}{R_4} \right) \quad (C.5)$$

Simplifying equation (C.5) we get the characteristic equation of the circuit as,

$$\begin{aligned} R_y R_4 (1 + R_1 s C_1) &= (1 + R_4 s (C_4 + C_z)) \\ (R_y R_1 + R_y R_x (1 + R_1 s C_1) + R_1 R_2 (1 + R_y s C_3) + R_2 (1 + R_y s C_3) R_x (1 + R_1 s C_1)) & \end{aligned} \quad (C.6)$$

Now, comparison of real quantities on both sides of equations (C.6) and simplification gives

$$\begin{aligned} (R_4 C_B R_y R_1 (R_x C_1 + R_2 C_3) + R_4 C_B R_2 R_x (R_1 C_1 + R_y C_3) + R_2 R_y R_x R_1 C_3 C_1) \omega^2 &= \\ . R_y (R_1 + R_x) + R_2 (R_1 + R_x) - R_4 R_y & \end{aligned} \quad (C.7)$$

where

$$C_B = C_4 + C_z$$

Similarly, comparing imaginary quantities on both sides of equations (C.6) and simplifying, we get,

$$\begin{aligned} (R_4 R_2 R_y R_x R_1 C_B C_3 C_1) \omega^2 = \\ .R_y R_1 (R_x C_1 + R_2 C_3) + R_2 R_x (R_1 C_1 + R_y C_3) + R_y C_B (R_y + R_2) (R_1 + R_x) - R_4 R_y R_1 C_1 \end{aligned} \quad (C.8)$$

From the last two equations we can obtain the frequency of oscillation as

$$\omega_o^2 = \frac{(R_y + R_2)(R_1 + R_x) - R_4 R_y}{R_4 R_y R_1 C_B (R_x C_1 + R_2 C_3) + R_4 C_B R_2 R_x (R_1 C_1 + R_y C_3) + R_2 R_y R_x R_1 C_3 C_1} \quad (C.9)$$

and the condition of oscillation as

$$\begin{aligned} (R_4 R_2 R_y R_x R_1 C_B C_3 C_1) (R_y + R_2) (R_1 + R_x) - R_4 R_y = \\ (R_4 R_y R_1 C_B (R_x C_1 + R_2 C_3) + R_4 C_B R_2 R_x (R_1 C_1 + R_y C_3) + R_2 R_y R_x R_1 C_3 C_1) \\ (R_y R_1 (R_x C_1 + R_2 C_3) + R_2 R_x (R_1 C_1 + R_y C_3) + R_y C_B (R_y + R_2) (R_1 + R_x) - R_4 R_y R_1 C_1) \end{aligned} \quad (C.10)$$

References

[1] D. Nelson and S. Evans, "A new approach to opamp design". *Application Note 300-1, March 1985, 1991 Data Book, Comlinear Corp, Fort Collins, CO 80525, USA.*

[2] C. Toumazou and T.Sverre. "Current-feedback opamps: A blessing in disguise" . *IEEE Circuits and Devices Magazine*, pages 34-37, January 1994.

[3] Sergio Franco. "Analytical foundations of current-feedback amplifiers". *International symposium on circuit and systems*, 2:1050-1053, 1993.

[4] F. Derek. "The so-called current-feedback operational amplifier technological breakthrough or engineering curiosity?". *International Symposium on circuit and systems*, 2:1054-1057, 1993.

[5] O. Steven. "The good, the bad and the ugly: Current feedback-technical contribution and limitations". *International Symposium on Circuit and Systems*, 2:1058-1061, 1993.

[6] A. Fabre. "Insensitive voltage-mode and current mode filters from commercially available transimpedance opamps". *IEE Proceedings G*, 140(5), October 1993.

- [7] S.I. Liu and Y.S. Hwang. "Realization of r-l and c-d impedance's using current feed back amplifier". *Electronics Letters*, 30(5):380-381, March 1994.
- [8] A. Fabre. "Gyrator implementation from commercially available transimpedance operational amplifiers". *Electronics Letters*, 28(3), January 1992.
- [9] S. Celma, A.Pedro and A.Carlosena. "Current feedback amplifiers based sinusoidal oscillators". *IEE Transactions Circuits and System*; 41(12):906-2, December 1994.
- [10] D. Wu, S.Liu, Y.Hwang and Y.Wu. "Multiphase sinusoidal oscillator using the CFOA pole". *IEE Proc. - Circuits Devices Syst.*, 142(1):37-40 February 1995.
- [11] C.S. Chang, C.M. Hwang and S.H. Tu. "Voltage-mode notch, lowpass and bandpass filter using current-feedback amplifiers". *Electronics Letters*, 30(24):2022-2023, November 1994.
- [12] S. Liu and J.Chen. "Realisation of analogue divider using current feedback amplifiers". *IEE Proc.-Circuits Devices Syst.*, 42(1):45-47, February 1995.

- [13] L. Shen, S.Chung and W.Dong “Sinusoidal oscillators with single element control using a current-feedback amplifier”. *Int. J. Electronics*, 77(6):1007-1013, 1994.
- [14] L. Shen, C. Chien and W. Dong. “Active-R sinusoidal oscillators using the CFA pole”. *Int. J. Electronics*, 77(6): 1035-1042, 1994.
- [15] WU. Dong, L. Hot-san, H. Yuh-shyan and WU. Yan. “CFA - based universal filter deduced from a Mason graph”. *Int. J. Electronics*, 77(6):1059-1065, 1994.
- [16] B. Wilson.”Recent developments in current conveyors and current-mode circuits”,*Proc.IEE*, 137,pt G, :63-70, 1990.
- [17] M. Abuelma’atti, A.Aamir and S. Alshahrani. “Novel RC Oscillators Using the Current-Feedback Operational Amplifier”. Submitted to *Electronics Letters*.
- [18] E. Bruun. “A dual current feedback OpAmp in CMOS technology, Analog Integrated Circuits and Signal Processing.” Vol.5,pp.213-217,1994.
- [19] B. Harvey. “Current opamp limitations: A state-of-the-art review.” *International Symposium on Circuits and Systems*, pp.1066-1069,1993.

[20] A. Payne and C.Toumazou. "High frequency self-compensation of current-feedback devices". *International Symposium on Circuits and Systems*, pp.1376-1379, 1992.

[21] G. Dicataldo, G.Palumbo and S.Pennid. "A schmitt trigger by means of a CCII+". *Int.J.Circuit Theory and Applications*, 23:161-165, 1995.

[22] J. Svaboda. "Comparison of RC op.-amp. and RC current conveyor filters". *Int. J. Electronics*, 76(4): 615-626, 1993.

Vita

- **Saad Mohammad Al-Shahrani.**
- **Born in Riyadh, Saudi Arabia.**
- **Received Bachelor's degree in Electrical Engineering from King Fahd University of Petroleum and Minerals, Dhahran, Saudi Arabia in 1992.**
- **Completed Master's degree requirements at King Fahd University of Petroleum and Minerals, Dhahran, Saudi Arabia in October, 1995.**